THE UNIVERSITY OF OKLAHOMA

GRADUATE COLLEGE

CATALYTIC REACTIONS FOR UPGRADING BIO-OILS AND PETROLEUM FUELS

A DISSERTATION

SUBMITTED TO THE GRADUATE FACULTY

in partial fulfillment of the requirement for the

Degree of

DOCTOR OF PHILOSOPHY

By

PHUONG THI MAI DO
Norman, Oklahoma
2010

CATALYTIC REACTIONS FOR UPGRADING BIO-OILS AND PETROLEUM FUELS

A DISSERTATION APPROVED FOR THE

SCHOOL OF CHEMICAL, BIOLOGICAL AND MATERIALS ENGINEERING

BY

Dr. Daniel Resasco, chair

Dr. Richard Mallinson

Dr. Lance Lobban

Dr. Rolf Jentoft

Dr. Kenneth Nicholas

© Copyright by PHUONG THI MAI DO 2010
All Rights Reserved.

ACKNOWLEDGEMENTS

First of all, I would like to thank Prof. Daniel Resasco, who has given me the opportunity to work in this project and great professional instructions during many years I have been here and many years to come. I also want to give special thanks to Dr. Lobban, Dr. Mallinson, and Dr. Rolf Jentoft, who have assisted me in this project in many ways, and Dr. Nicholas for being in the committee. I have been received a lot of helps from colleagues in the lab. They have assisted me with the experiments and instrumental operations. They have also given me a lot of useful advice. I have also enjoyed working with many co-workers in both bio-fuel and nanotube groups in the diesel groups. The research discussions I had with them have made me excited and deeply interested. Involvement in many extra activities outside research with them has made me relaxed and filled with energy. I deeply appreciate. I also want to thank the school of chemical, material and biological engineering for the graduate assistantship. The department staff also assists me in ordering chemicals, equipment and filing paperwork. In term of financial supports, I would like to thank ConocoPhillips Petroleum Company for the fellowship, Oklahoma Center for Advancement of Science and Technology (OCAST), the Secretary of Energy for the State of Oklahoma, and the Oklahoma Bionenergy Center for the research funding. Last but not least, I am very grateful to my husband, children, family and friends. I see myself lucky to be surrounded by their love, support and understanding. I feel strongly motivated in my professional work when they are around me.

TABLE OF CONTENTS

LIST OF TABLES

LIST OF FIGURES

ABSTRACT

The increasing consumption and phase-out of conventional fuels has derived the tremendous interest of our society in making uses of renewable energy resources such as biomass. In response to this interest, bio-oil produced from biomass feed stocks has been gradually making its contribution as a part of normal fuels. However, since the bio-oil is not stable due to its high oxygen content, upgrading is necessary to improve its performance. In parallel to the need for sustainable fuel sources, a huge desire in creating more environmentally friendly fuels is generated. For instance, lowering emission for conventional diesel and gasoline fuels has been considered one of the actions to reduce the negative impacts of fuel combustion on human health. From point of view of upgrading petroleum fuels, this could partially mean reduction in aromatic content in both diesel and gasoline. In the scope of this dissertation, the author will present two catalytic strategies to improve the performances of bio-oils and conventional diesel and gasoline fuels. Since the high oxygen content of bio-oils has limited its storage ability and lower its heating content, in some cases, removing oxygen or deoxygenating bio-oil molecules has been proposed as a recommended catalytic reaction. In the first part of the dissertation, the author will focus on the deoxygenation reaction of methyl esters and triglycerides, which can be derived from biomass feed stocks and contain the ester functional group (-COO-) relevant to bio-oil molecules. Hydrocarbons are the desired products from the deoxygenation reactions. The first step in optimizing the yield and selectivity of the hydrocarbons is to establish the reaction mechanisms with all possible reaction pathways leading to formation of hydrocarbons. In addition, the effects of various parameters on the deoxygenation reactions have been examined. The important

parameters include pressure, temperature, hydrogen partial pressure, and reactor configuration. Certainly, one cannot exclude the important role of catalysts. The catalysts implemented in these reactions were supported noble-metal-based catalysts such as Pt and Pd. The variation of these parameters will be used in the reactions of several representative molecules such as methyl hexanoate, methyl octanoate, methyl dodecanone, and triacetin. A number of interesting findings on reaction mechanism, catalyst deactivation, and the role of active sites have been drawn from these studies. The second part of this work has touched on the upgrading reactions of aromatics in petroleum fuel. Hydrogenation of the aromatic rings followed by selective ring opening of the corresponding naphthenic compounds has been proposed as one of the strategies to improve the cetane number and other fuel properties. In this work, the ring opening reactions of various naphthenic compounds on different modified Iridium catalysts have been studied. The supported Iridium catalysts are not only active for ring opening reaction but also selective for certain positions of C-C cleavage when supports and additive modifications are applied. Although the two parts of this dissertation deal with different feed molecules, they all bring the common understandings on how to modify the reaction variables to optimize the selective production of hydrocarbon fuels.

PART A: REACTIONS OF METHYL ESTERS AND TRIGLYCERIDES ON SUPPORTED PLATINUM CATALYSTS

CHAPTER I: INTRODUCTION AND LITERATURE REVIEW

1. Introduction

As fossil fuels are becoming less abundant, and the need for greenhouse gas neutral fuels has been accepted, tremendous attention has turned to maximizing the use of renewable energy resources such as biomass, vegetable oils, animal fat, and algae.[1-3] For instance, the U.S. Department of Energy has established very specific targets to replace 30% of the liquid petroleum transportation fuel with biofuels and to replace 25% of industrial organic chemicals with biomass-derived chemicals by 2025. [4] Although those sustainable materials are composed of a variety of structural building blocks at different compositions, alkyl esters, along with others such as furans, phenols, aldehydes/alcohols, carboxylic acids, appear as commonly derived components from those blocks. [5 - 6] Particularly, the sugars from the biorefinery process can be converted into various building-block components. The major chemical products include ethanol, C_3 to C_6 carboxylic acids, and alcohols. [7]Another example is vegetable oils, which contain mostly triglycerides of fatty acids. Biodiesel or fatty acid methyl esters, which are obtained through transesterification of the triglycerides with methanol, are widely used as renewable fuels. However, there are several main issues with biodiesel. They have low stability and are not fungible. Their instabilities are oxidative and thermal. Both of these types of instability are associated with the amount and configuration of the olefinic unsaturation of the fatty acid chains. [8] Hydrogenation of double bonds in biodiesel molecules is one of the proposed solutions to improve their stability. Besides, due to the presence of oxygen in biodiesel molecules, their heat contents are 9-13 % lower than that of conventional diesel fuels on a mass basis.[9] Catalytic deoxygenation of biodiesel could

remove the ester functional groups and resolve all of the fungibility issues.[10] The chemistry of ester functional group not only has been applied to biodiesel, but also is extremely important to bio-oil upgrading since alkyl esters of short carboxylic acids are present in bio-oil obtained from fast biomass pyrolysis. In fact, these molecules have low commercial values and are reactive, therefore, many researchers have proposed coupling or condensing these molecules to form higher molecular weight compounds, which helps to reduce the oxygen content and create higher valued chemical products.[11-13].

The objective of this dissertation is to study the reaction chemistry of methyl esters and triglycerides and optimize the transformation of these feeds into valuable chemicals and fuel compounds. These desirable products, in fact, are hydrocarbons, which can be obtained through deoxygenation reactions of the feeds. In order to optimize the yield and selectivity of the hydrocarbons, the first step is to establish and verify the reaction mechanisms, in which all possible reaction pathways leading to formation of major hydrocarbon products and side products are identified. Second, the effects of various parameters on the deoxygenation reactions also need to be examined. The important parameters include pressure, temperature, hydrogen partial pressure, and reactor configuration. Certainly, catalysts should also be considered as the most crucial parameter. The variation of these parameter will be implemented in the reactions used several probe molecules such as methyl hexanoate, methyl octanoate, methyl dodecanone, and triacetin. Throughout this work, the operating pressure and temperature will vary from 0.1 to 3.4MPa and from 573 to 673 K, respectively. Since the hydrogen concentration strongly affects the product distribution and catalyst deactivation, a wide range of concentration from zero to 100% will be screened. The changes in hydrogen

concentrations will happen in two reactor configurations: plug flow and trickle bed. Through the testing of these variables, more knowledge on how to optimize the production of desirable products via manipulating the operating parameters will be gained. Another important piece of information will be obtained by varying the catalyst active elements and compositions, which includes different metals, molar ratios, and supports. Metals from group VIII (i.e. Pt and Pd) and IB (i.e. Cu) will be exploited in this work because of their effectiveness previously shown in the similar reactions. The supports will be altered among alumina, titania, silica, and metal foam. The performances of different catalysts will be characterized using a number of techniques such as: temperature-programmed reduction, temperature-programmed oxidation, X-ray photo spectroscopy, transmission electron spectroscopy, BET, and carbon monoxide chemisorption. All of this information will be gathered and processed to provide the complete strategy to optimize the production of desirable hydrocarbons from methyl ester and triglyceride feed stocks.

2. Literature Review

For many years, researchers have proposed a number of groups of studied reactions involving alkyl esters and carboxylic acids. The catalysts used also vary accordingly. Important reactions include decarboxylation / decarbonylation, hydro-deoxygenation, and coupling (i.e. ketonization). The studies have been examined both theoretically and experimentally. The catalysts vary from single crystals to powder catalysts. The active components range from metals, oxides and combination of metals and oxides. Before introducing the experimental data, it is useful to review works on the

related feeds (i.e. alkyl esters, carboxylic acids, and even vegetable oils) and provide background information on the chemistry of each listed reaction.

2.1 Deoxygenation of oxygenate compounds

Although the focus of this work is alkyl esters, particularly methyl esters, the reactions of alkyl esters form various oxygenate and hydrocarbon products, which simultaneously generate a network of side reactions. Therefore, the study on related oxygenates (i.e. alcohol, aldehyde, ketone, and triglycerides) and hydrocarbons (i.e. alkanes and alkenes) will be reviewed in order to provide additional information on the reaction of alkyl esters. The review not only centers on the vapor and liquid phase reactions but also focus on another reactor configuration: trickle bed with monolith catalyst.

2.1.1 Reactions of alcohols, aldehyde, and ketones

2.1.1.1 Surface study of oxygenates on metal catalysts

For many years, alcohols, aldehydes, and ketones have been the topics of numerous surface reactivity and experimental studies. The majority of surface studies focus on the decomposition mechanisms of these molecules on transition metals of group VIII and IB. The reaction pathways of alcohols, aldehydes, and ketones on transition metals are dependent on the identity of the metal and the molecular structures of the reactants. For instance, the reaction sequence of alcohol decomposition on Pt-group metals includes several steps: (1) formation of an alkoxide intermediate via hydroxyl-hydrogen elimination (2) α-hydrogen abstraction leading to an aldehyde species bonded with the surface via carbon and oxygen of the carbonyl group (designated as η^2configuration) or via only oxygen atom (noted as η^1 configuration). [14] The former route

can proceed via acyl intermediate followed by CO elimination and hydrocarbon fragment. Besides these common species, other researchers also proposed formation of oxametallacycles from ethanol on Rh (111) to explain some of the results. [15] The surface species alkoxides, η^1, η^2, acyls, and oxametallacycles are shown in figure A-1.1. In fact, the dissociation of O-H bond of alcohols is known to occur at low temperatures to form stable alkoxide intermediates. [16] The required temperatures for group VIII metals are between 100 K and 200 K. The temperature required for Cu and Ag is usually higher.

Carbonyl-containing compounds adsorb on metal surfaces via two alternatives: η^1 and η^2 modes. In the case of η^1 mode, bonding is established through donation of oxygen lone pair orbital to the metal atom. Meanwhile, in η^2 mode, the bonding of carbonyl molecules occurs via carbonyl π orbital with back-donation from the metal to the adsorbate through the carbonyl π^* orbital.[17] Different metals and surface modifiers will certainly affect the statistic of these two species on the surface.[14] For instance, the presence of electronegative surface modifiers such as oxygen and sulfur will decrease the electron density of the metal; consequently decrease the back-donation to the carbonyl group. In that case, η^1 mode is preferred. In the same fashion, this mode has been detected exclusively in the adsorption of carbonyl groups on Group IB metal surfaces, which is probably due to the high affinity for oxygen of these metals. Regarding Group VIII metals, both η^1 and η^2 modes have been reported. Particularly with clean Ru and Rh surfaces, Anton et al.,[17] Henderson et al.,[18] and Barteau et al.,[14] have spotted η^1 mode as the favorable bonding configuration of aldehydes and ketones.

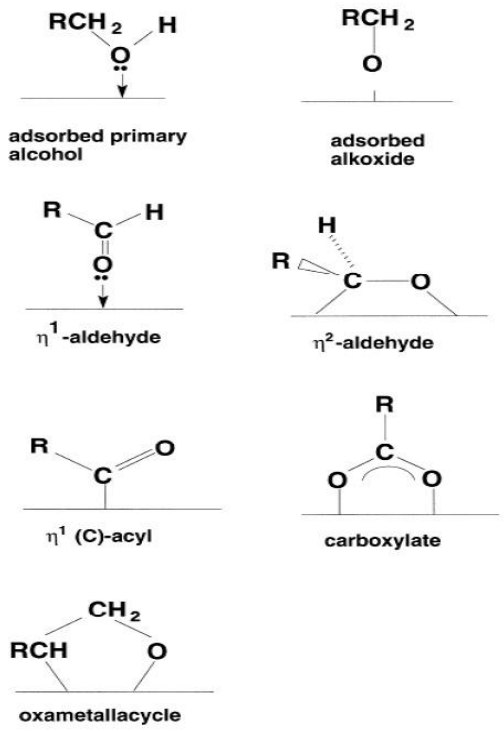

Figure A-1.1: Various surface species of adsorbed oxygenates on metal surfaces. Cited from reference 14.

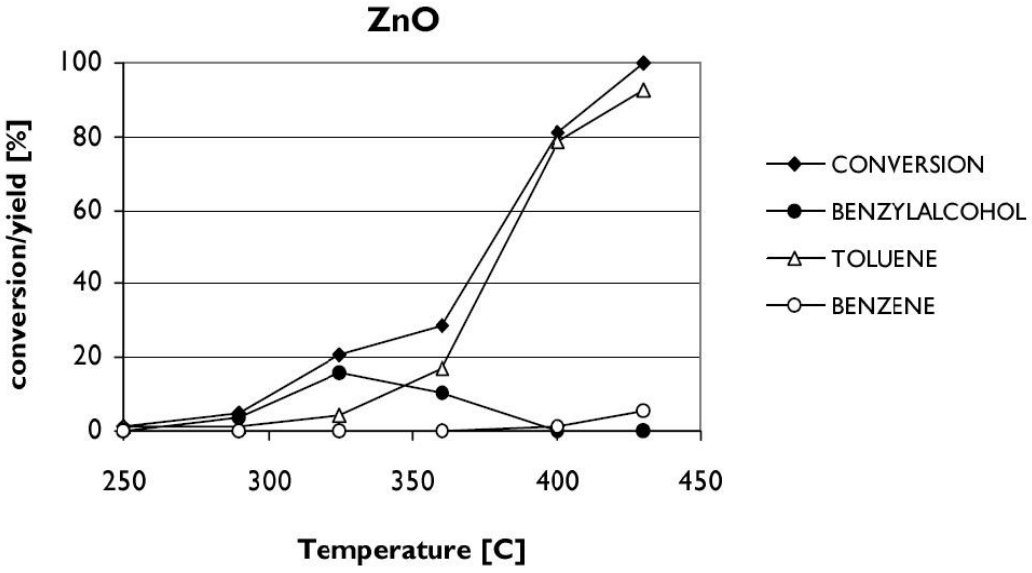

Figure A-1.2: Hydrogenation of benzaldehyde on ZnO as a function of temperature. Cited from reference 27.

Regarding platinum metal, the adsorption of acetone on clean Pt (111) occurs via both η^1 and η^2 configurations. A DFT study from Baiker et al. has showed that for acetone the η^1 mode is about 3.0 kcal/mol more stable than the η^2 mode.[19] η^1-Adsorbed species are favored by the co-adsorption of electronegative atoms, such as oxygen and sulfur that increase the work function of the metal. Meanwhile, the presence of some co-adsorbed species, such as potassium ion, causes a decrease in metal surface work function; therefore favors the η^2 mode. In the same line, the adsorption of hydrogen on Pt (111) has been proposed to reduce the work function, which leads to an increasing η^2/η^1 ratio. Ponec et al. also reported that it seems that the presence of steps suppresses the population of the η^1-species and promotes the presence of the η^2-species. [20]These two bonding configurations are found directly associated with their thermal stability. One would expect that η^2 with bonding of two carbonyl atoms with metal surface might be more stable than η^1, in which only oxygen atom participates in bonding. Consequently, the latter would desorb at lower temperatures. Often, η^1 mode is found to desorb molecularly. Meanwhile η^2 mode reacts further. For instance, Hughes et al. has spotted that decomposition of alcohol on Pt (111) follows the sequence: alcohol → alkoxide → η^2 aldehyde → acyl → CO.[21] The acyl intermediate decomposition liberates CO in the gas phase and leaves hydrocarbon fragments on the surface. The rate limiting step for this part of the sequence greatly depends on the type of metal and adsorbed molecules. For alcohol decomposition, some researchers claim that C–H, not C–C scission is the rate-determining step in acetyl decomposition. The formed ketene species will undergo rapid C-C bond rupture to release CO and hydrocarbon fractions on the surface. For acetone

decarbonylation, Anton et al. has proposed that acyl transformation invokes first C-C bond cleavage, as a rate-limiting step on Ru (001) surface. [17]

2.1.1.2 Reactions of alcohol, aldehydes, and ketones on metal and metal oxide catalysts

In addition to theoretical study, the reaction of alcohols, aldehydes and ketones have been experimentally investigated using a variety of catalysts. In details, the deoxygenation reactions of ketones were tested over supported noble metal catalysts. The decomposition reactions of alcohols and aldehydes were carried on reducible metal oxide catalysts.

In fact, the deoxygenation reactions of ketones are associated with hydro-deoxygenation (HDO) reactions of oxygen-containing compounds. The HDO reactions can occur either on hydrotreating catalysts or supported noble metal catalysts. Recently, the focus has been shifted to HDO of renewable bio-oil compounds. A great deal of work have centered on the HDO of ketones and alcohols on transition metal catalysts such as Ni/Al_2O_3 [22] or sulfidied Ni-Mo or Co-Mo catalysts. [23-25]According to Cejka et al. and others, noble metal (i.e. Pd) supported on activated carbon and zeolite were also found to be very active for HDO of benzophenone and acetophenone.[26] The conversion of a ketone to corresponding hydrocarbons in a hydrogenative environment can proceed via several mechanisms. The first mechanism is operative on bifunctional catalysts with acidic support and a metal component. The carbonyl group can be first hydrogenated to alcohol on metal function. The acid component is responsible for the dehydration of the alcohol to form the C=C bond. The double bond then gets hydrogenated to the desirable

hydrocarbons in the final step. It could be also possible that in the second mechanism the alcohol undergoes C-O hydrogenolysis on metal catalyst to form the hydrocarbons.

The deoxygenation of alcohols and aldehydes can occur on the reducible oxides such as ZnO or ZrO_2 catalysts.[27] Under the reductive conditions and at elevated temperatures, the surface of ZnO gets reduced followed by desorption of water and the formation of oxygen vacancies. In fact, on ZnO surface, the dissociation of strong H-H bond is believed to be promoted by the presence of surface defects.[28] The hydrogen activation is easier on ZnO than that on ZrO_2 catalyst because of the difference on metal-oxygen bond strength.[29] The hydrogen adsorption capabilities of metal oxides could be significantly promoted by the presence of a metal. Hydrogen is then dissociated on the metal and migrates or spills over to the oxide part of the catalyst.[30]Even the metal surface that is fully covered by the carboxylate adsorbates is still able to adsorb hydrogen and pass it to the oxide.[31]Consequently, oxygen vacancies are much more abundant when the oxide is in a close contact with a metal (i.e. Pt and Pd). Figure A-1.2 shows that ZnO is an active catalyst for deoxygenation of benzaldehyde to toluene. It could be possible that the benzaldehyde is hydrogenated to alcohol on ZnO surface and the alcohol reacts with oxygen vacancy to form toluene at elevated temperature.

2.1.2 Reactions of carboxylic acids and alkyl esters

2.1.2.1 Surface reactions of carboxylic acids

The dissociative adsorption of carboxylic acids and esters on both metal and oxide surfaces yields carboxylate species. Barteau et al. has detected acetate species when adsorbing acetate on Pd (111) surface.[32]

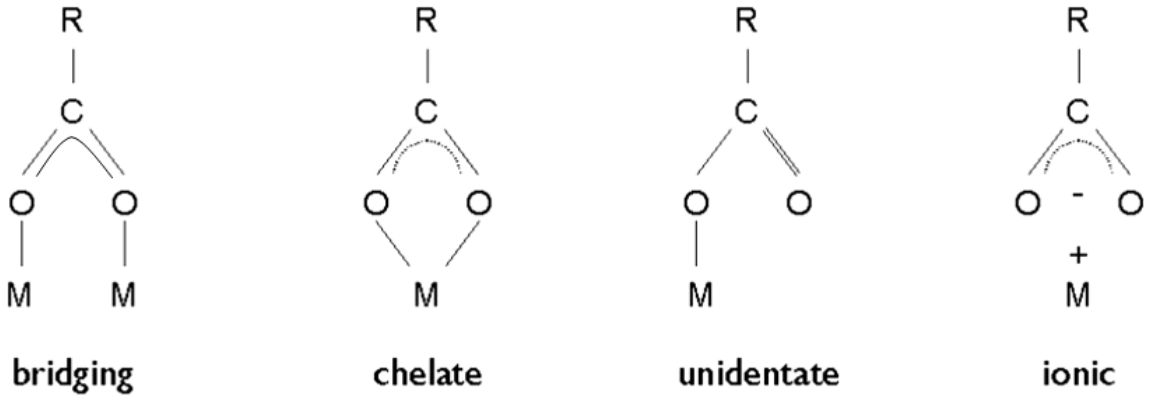

Figure A-1.3: Metal carboxylate configurations. Cited from reference 27.

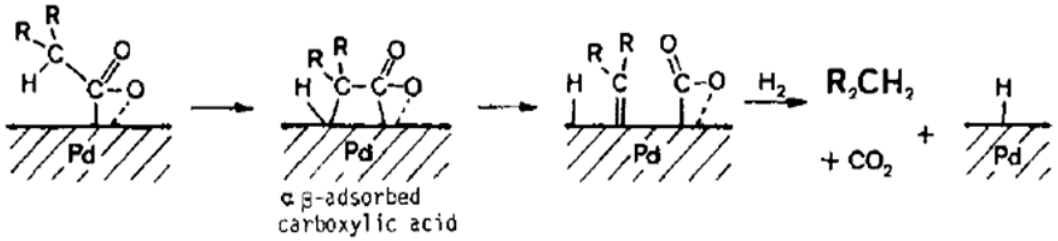

Figure A-1.4: Reaction scheme of deoxygenation reaction of carboxylic acids on Pd surface. Cited from reference 38.

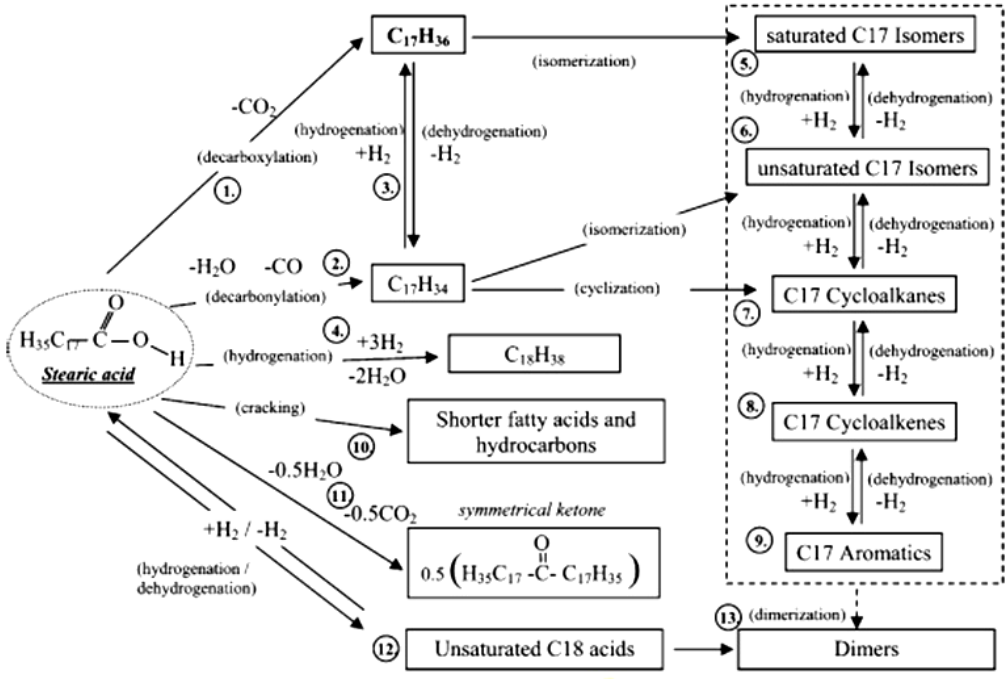

Figure A-1.5: Reaction network of stearic acid over supported metal catalysts. Cited from reference 39.

A long time before this finding, Strojny et al. had reported that both benzoic acid and methyl benzoate form benzoate intermediates on metal oxide surfaces. [33] Benzoic acid dissociates into H^+ and RCOO group, whereas, the ester dissociation occurs at the acyl C-O bond.[34] Carboxylates can appear as counter ions in a salt. This species is commonly seen with alkali metals, not with transition metals. Other structural carboxylates include bridging, chelating, and unidentate. The most common coordination mode of carboxylates is bidentate bridging mode.[27] Figure A-1.3 shows the configurations of four possible carboxylate species. These species are generally stable at low temperatures. However, upon heating to high temperatures, the carboxylates decompose molecularly or bimolecularly. The molecular decomposition yields product with one carbon less than the original acid. Reactions involving two carboxylate species are namely ketonization and transesterification.

Although surface reaction studies of esters are very limited, there are several adsorption studies of carboxylic acids on single crystals. Barteau and co-workers have studied the adsorption of different carboxylic acids on metal surfaces. In fact, the adsorption of formic acid, acetic acid, and propanoic acid on the oxygen-dosed Pd (111) yields the adsorbed carboxylate species.[35-36] There are two main decomposition pathways of carboxylates on metal surfaces without hydrogen: decarboxylation and decarbonylation. For example, in the decarboxylation reaction of acetate, the α C–H bond of the methyl group on acetate is activated, following by the C–C bond cleavage to release CO_2. The α C–H bond activation of acetate is speculated to be rate-limiting step. Under hydrogen atmosphere, the resulting methylene fragment that forms is hydrogenated to methane. However, the decarbonylation of acetic acid proceeds via

acetyl formation, resulting from C-O bond cleavage of the carboxylates. Shekhar et al. has proposed that the acetyl species undergoes C–C bond scission to liberate CO and methyl surface fragments similarly to decomposition of aldehyde. [37] The selectivity of these pathways is dependent on the metal-oxygen bond strength. Group VIII metals such as Pt and Pd, which possess weak metal-oxygen bonds, consequently exhibits low activity for C-O bond rupture. Conversely, metals such as Cu, Rh, Ru, and Fe show a great tendency for C-O bond cleavage of the carboxylates.

2.1.2.2 Decarboxylation / decarbonylation reactions of carboxylic acids and esters

In the 80s, Maier et al. first showed the gas phase decarboxylation of carboxylic acids on metal supported catalysts. [38]Initially he found that Ni on alumina is an effective catalyst for decarboxylation of a variety of substituted admantanes. Later, Pd/SiO_2 catalyst at 603 K under hydrogen was discovered to be more effective in decarboxylating the alphatic acids, heptanoic and octanoic acids, than Ni/Al_2O_3 catalyst. Figure A-1.4 shows the proposed reaction scheme of deoxygenation of carboxylic acid on Pd surface. Since the olefins were detected as the primary products, the authors claimed that the catalyst attack at the α-position to the carboxyl group. Interestingly, he also found that hydrogen is not needed for the decarboxylation reaction, but it promotes the desorption of the organic substrates from the active catalytic sites.

In the same fashion, Murzin's group has applied the use of metal catalysts in deoxygenation of renewable fatty acids and fatty acid alkyl esters to produce chemicals and fuel compounds. [39]They screened a number of catalysts and reported that both Pt/C and Pd/C are the most active catalysts for decarboxylation / decarbonylation of stearic

acid and ethyl stearate. The reactions were carried out in liquid phase at mildly elevated pressures. Figure A-1.5 depicts the reaction network of stearic acid over supported metal catalysts. The desirable products here are C_{17} and C_{18} hydrocarbons. However, C_{17}s are the dominant products since the catalysts are highly selective in decarboxylating the original feeds. In the same line with what has been reported by Maier et al., Murzin also reported that the decarboxylation reaction still occur without hydrogen. The decarboxylation reaction of ethyl stearate proceeds via stearic acid intermediate, which decomposes to form unsaturated C_{17} hydrocarbons. In fact, the selectivity toward unsaturated C_{17} hydrocarbons is highest when no hydrogen is present since the alkene-to-alkane hydrogenation reactions are limited. Conversely, under hydrogen atmosphere, only trace amount of unsaturated C_{17} hydrocarbons are detected. From the analysis of the gas products, Murzin claimed that the dominating process over palladium catalyst was stearic acid decarboxylation, whereas over platinum, the decarbonylation reaction was more profound. In fact, the CO_2/CO ratio over the former catalyst was >17, whereas for the latter catalyst it was <1.[40] However, this author has not taken into account other reactions that could alter the original CO_2/CO such as water-gas-shift reactions. In the following sections, more detailed analysis of the gas products from conversion of vegetable oils over hydrotreating catalysts will be reviewed.

Although the decarboxylation/decarbonylation reactions of carboxylic acids and esters are reported to happen mostly on supported metal catalysts, there are some studies on the conversion of these compounds over zeolites such as HZSM-5. [41] Since the target of this work is on biomass derived compounds, the carbon chain lengths of the acids are relatively short. Figure A-1.6 displays the proposed reaction pathway for conversion of

acids and esters on HZSM-5. Two major reaction routes are apparent here. The first route involves decarboxylation of short acids/esters via cracking to hydrocarbon gases and CO_2. The second route includes deoxygenation of acids/esters to corresponding aldehydes and water. The Aldol condensation reaction catalyzed by the zeolite acidic sites produces adehydes and ketones containing larger alkyl groups. Since the alkyl groups are olefinic, they are responsible for aromatization reactions, leading to benzene-derived products.

2.2 Hydro-deoxygenation reactions of carboxylic acids and alkyl esters

The apparent difference between hydro-deoxygenation and decarboxylation/decarbonylation reactions of acids/esters is that corresponding products from the former reactions keep the same carbon chain length as in the feeds, whereas the latter reactions result in products with 1-carbon shorter chain length. While decarboxylation/decarbonylation reactions are known to be operative regardless of hydrogen, hydro-deoxygenation reactions require the presence of hydrogen. In fact, hydrogen participates in the reactions and activates the catalysts. The hydro-deoxygenation reactions of acids/esters have been reported over both metal catalysts and bifunctional catalysts of metal and oxide. The desirable products of these reactions are the corresponding alcohols and aldehydes as valuable chemicals from carboxylic acids and esters.

For many years, the production of fatty alcohols from the hydrogenolysis of fatty methyl esters is a step to manufacture detergents from natural feed stocks.[42] Supported copper catalysts are used mostly because they are selective for hydrogenation of C-O bonds, not C-C bond hydrogenolysis. [43] The conventional catalyst is copper chromite, which is prone to deactivation. [44-45]

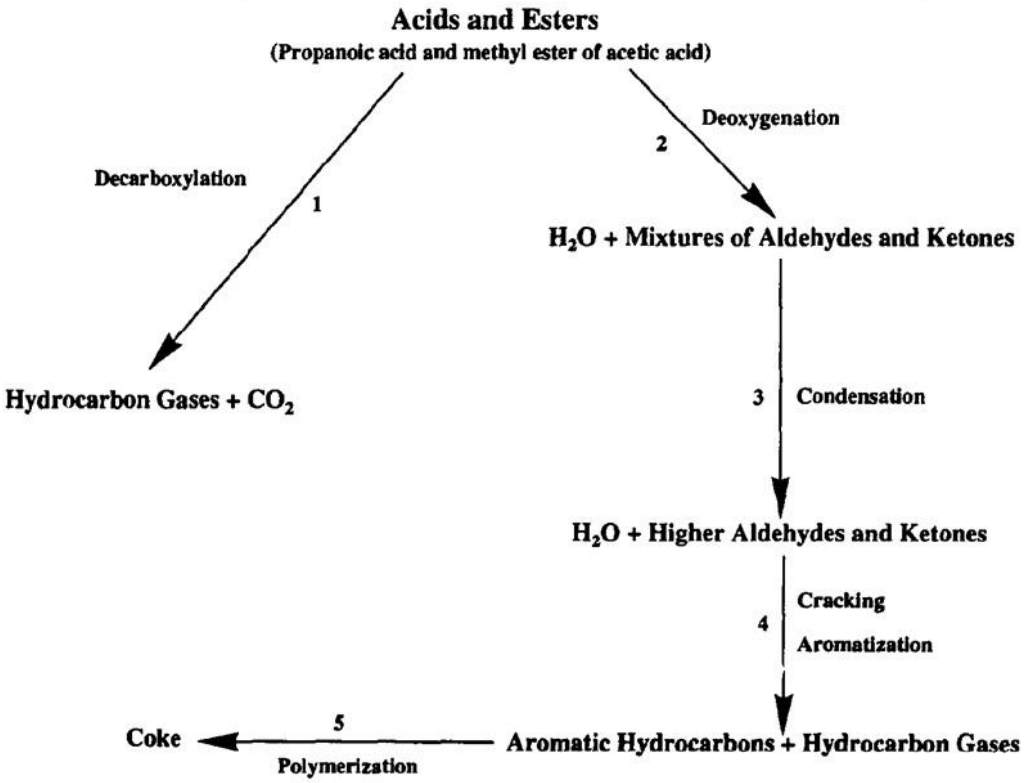

Figure A- 1.6: Reaction pathways for conversion of acids and esters on HZSM-5 catalyst. Cited from reference 41.

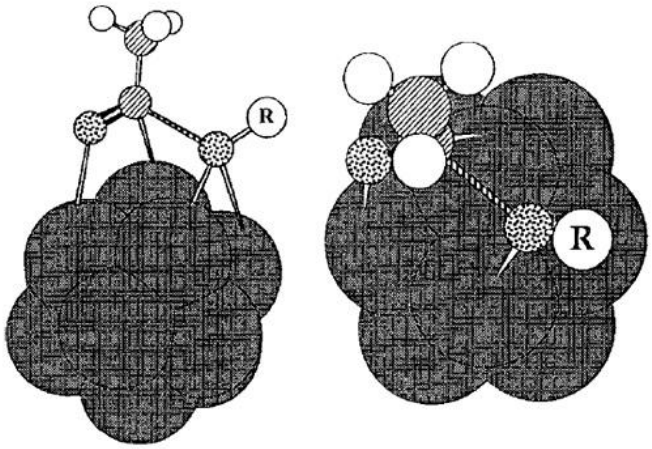

	E_a, [kJ/mol]
CH_3COOH	90–100
CH_3COOCH_3	70–80
$CH_3COOC_2H_5$	50–60
CH_3CHO	40–50

Figure A-1.7: Transition states and activation energies for dissociative adsorption of various carbonyl-containing organic molecules on copper. Cited from reference 47.

Consequently, copper on silica is used to avoid this problem. However, pure copper catalyst is not active and shows lower mechanical stability during industrial operation. Doping copper with other promoters has been proven to improve the performance of the catalysts. In addition to experimental studies of catalytic reduction of carboxylic acids and alkyl esters on supported Cu catalysts, other work also dedicates to the theoretical aspects of these reactions. Cant et al. suggested that the hydrogenation of ethyl acetate over copper-based catalysts proceeds via dissociative adsorption of the reagent into CH_3C^*O and $C_2H_5O^*$ species, where * represents a surface site, leading to two alcohol products.[46] Dumesic et al. has reported the similar finding in which the high initial heats observed from microcalorimetric studies of methyl acetate and ethyl acetate adsorption on silica-supported copper at 300 K prove that these probe molecules adsorb dissociatively on copper. [47] For instance, the dissociation of ethyl acetate on copper surface yields acyl and alkoxy species. By using DFT calculation, he also found that the activation energy for dissociative adsorption increases from ethyl acetate to methyl acetate to acetic acid (as seen in figure A-1.7). In fact, the rate of dissociation of these molecules on copper is limited by carbonyl-adjacent C-O bond cleavage. The C-O bond strength, in turn, is affected by the ability of donating electron from alkyl or hydrogen group. The kinetic study showed that both C-O dissociation and hydrogenation of acyl species to alcohol are critical for the overall reduction reaction of esters. In the mean time, formation of alcohol from alkoxy species is rapid.

Another theoretical study of hydrogenolysis of acetic acid was done by Neurock et al.[48] In the postulated mechanism, acetic acid readily dissociates to form acetate on the Pd (111) surface. The acetate species is also energetically favored compared to

adsorption mode of acetic acid via η^1 geometry, in which the oxygen of the carbonyl group is bound to the surface. However, at high coverage, the η^1 species might be preferred due to low repulsive interaction. Consequently, surface acetic acid dissociates to form an acetyl surface intermediate. The acetyl intermediate is then subsequently hydrogenated to ethanol via the formation of an acetaldehyde surface intermediate. The detailed reaction network of acetic acid hydrogenolysis on Pd (111) is depicted in figure A-1.8. Based on the DFT calculation, it is shown that the dissociation of acetic acid to acetyl is likely the rate-controlling step in acetic acid hydrogenolysis over Pd (111). Since Pd is a hydrogenation catalyst, the activation energy for hydrogenation of acetyl species is relatively low. According to DFT calculations, C–OH activation, a precursor for acetyl specie formation, is favored on metals to the left in the periodic table such as Re (0001). However, pure Re leads to decarboxylation/decarbonylation of acetic acid because C–H bond-breaking reactions are generally more favored on Re or Rh surfaces, in which the d-band of the metal is more prone to back-donate to the antibonding C-H.[49] Therefore, a bimetallic Pd–Re catalyst, atomically dispersed Re ensembles on Pd, is a suitable catalyst for acetic acid hydrogenolysis reaction. Others have also proposed that Rh-Sn system is an effective catalyst for hydrogenolysis reaction.[50]

Besides theoretical studies, many works have been dedicated to the reactions of acetic acid over supported catalysts. For example, Cressely et al. studied acetic acid hydrogenation over three silica-supported Cu, Fe, or Co catalysts.[51] While, Cu/SiO_2 catalyst was active for the formation of ethanol, acetaldehyde, and ethyl acetate; acetone is the only product over Fe/SiO_2 catalyst. On supported Co catalyst, only gases (CH_4 and CO_2) and surface carbons were detected.

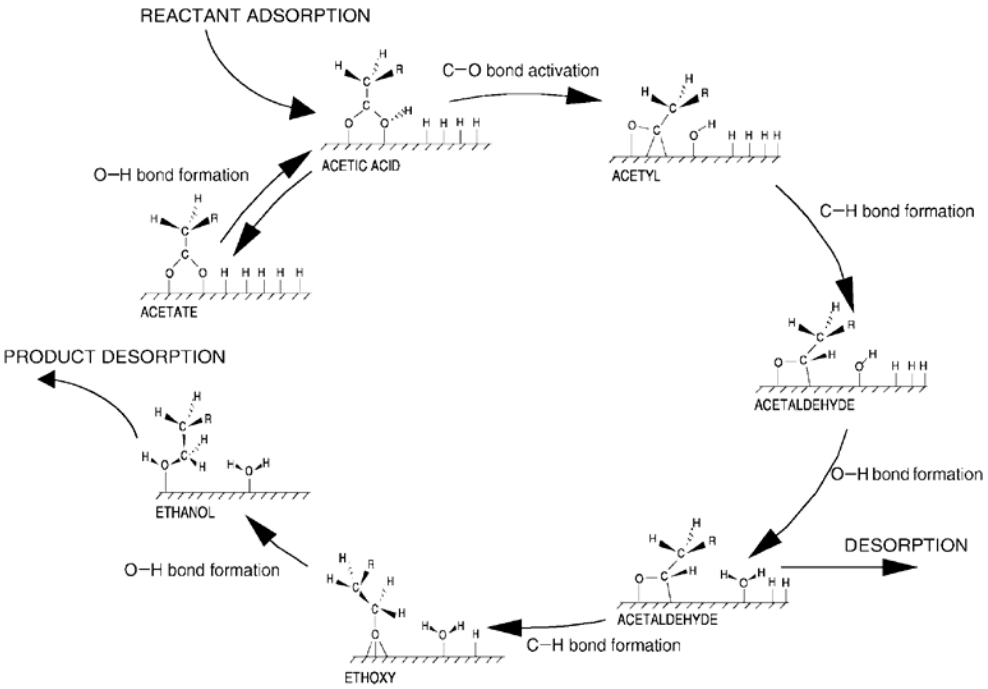

Figure A-1.8: Reaction network of acetic acid on Pd(111) surface. Cited from reference 49.

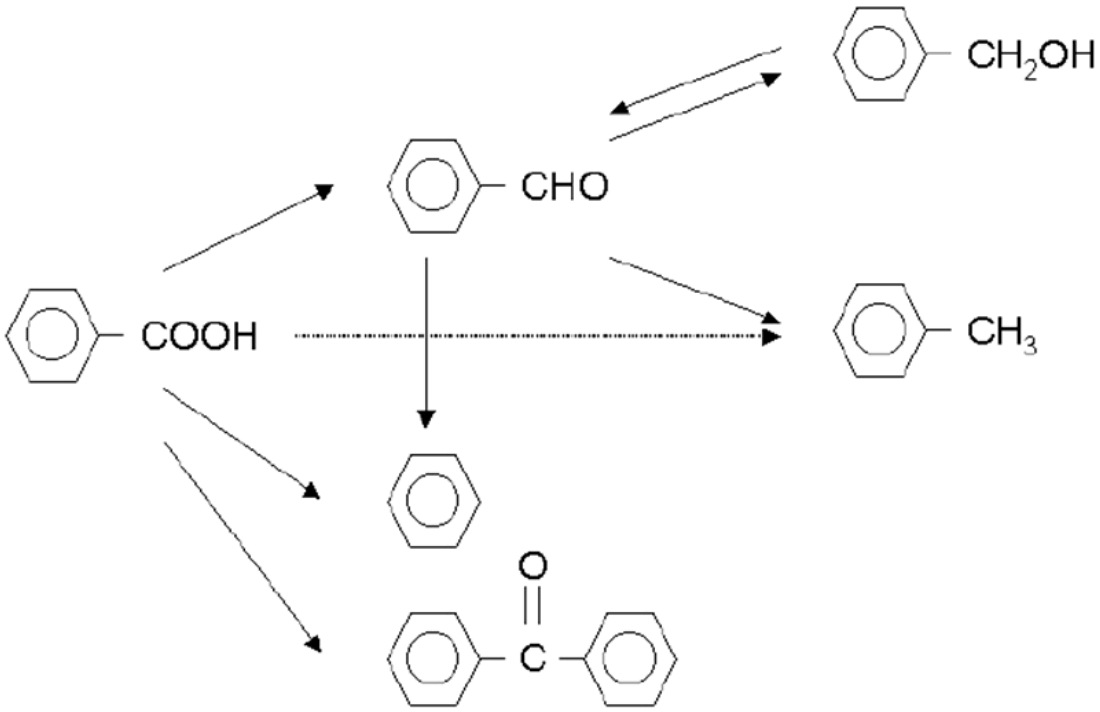

Figure A-1.9: Reaction network of benzoic acid on metal oxides. Cited from reference 27.

Not only metals are active for hydrogenation of carboxylic acids, a number of studies have reported the significant activity of metal oxides. According to Sakata et al., there are two separate mechanisms for hydrogenation of carboxylic acids (i.e. benzoic acid) over oxide catalysts: the selective Mars and Van Krevelen route to produce aldehyde and the non-selective radical-like decomposition of carboxylate species to form byproducts.[52] The Mars and Van Krevelen-type of mechanism involves the participation of lattice oxygen and oxygen vacancies in the reaction.[53] For example, on MgO and lanthanum oxides, the decomposition mechanism is operative. The transition metal oxides such as Fe, Co, and Mn are active for hydrogenation of carboxylic acids to aldehyde. However, they can contain too many oxygen vacancies, the complete hydro-deoxygenation can occur if the oxides are deeply reduced. Group IV oxides (Ti, Zr, and Hf) are the most selective catalysts. Particularly, Ponec et al. has shown that ZnO catalyst is effective in hydrogenating benzoic acid into benzaldehyde via oxygen vacancy mechanism.[27] The reaction network of benzoic acid on metal oxides is depicted in figure A-1.9. Figure A-1.10 shows the detailed product distribution of the reaction of benzoic acid on ZnO. There are three parallel reactions: deoxygenation to benzaldehyde, decarboxylation to benzene, and coupling to benzophenone. The deoxygenation reaction is favored with the presence of hydrogen, whereas the other two are prominent in the absence of hydrogen. Besides benzaldehyde, toluene is also the completely hydrogenated product from benzoic acid. Meanwhile, benzene and benzophenone come from the decomposition of carboxylate species, which are preferentially formed on the basic metal oxides (i.e. ZnO). However, the addition of small amount of Pt and Ru on ZnO catalyst does not improve the deoxygenation activity due to the maximum of oxygen vacancy on ZnO.

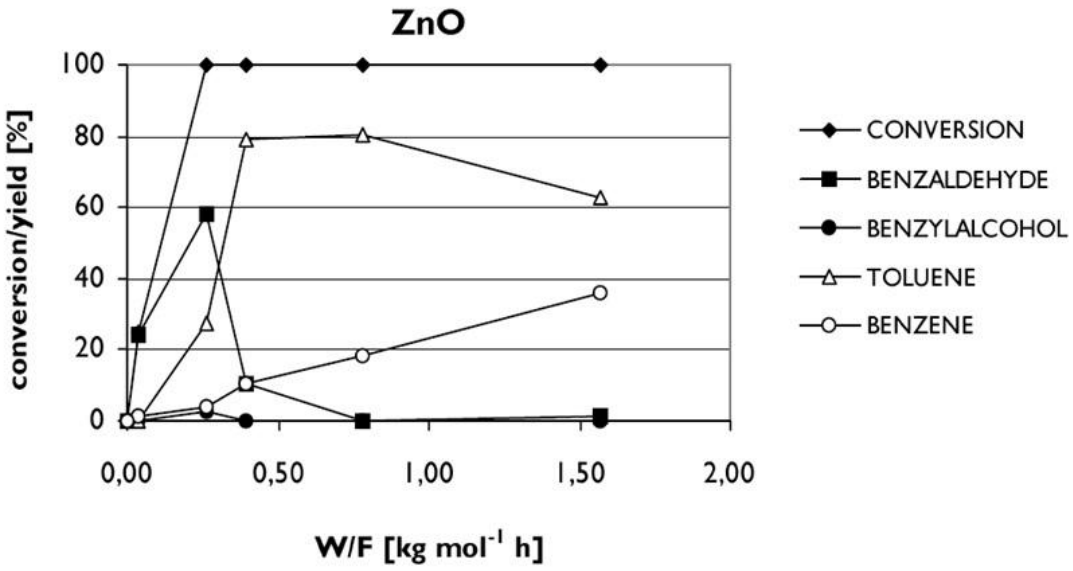

Figure A-1.10: Deoxygenation of benzoic acid at 673 K on ZnO catalyst as a function of contact time. Cited from reference 27.

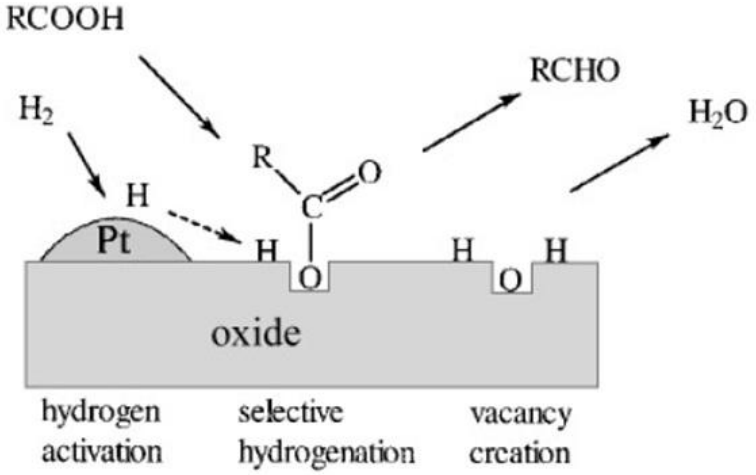

Figure A- 1.11: Schematic representation of the proposed reaction steps in the selective hydrogenation of acetic acid to acetaldehyde. Cited from reference 53.

In other cases, addition of hydrogen-dissociative metal (i.e. Pt) into oxides (i.e. TiO_2) has shown to increase the oxygen vacancy formation, consequently enhancing the hydrogenation activity on oxide catalyst. Hydrogen is dissociated readily on Pt and gets spilled over to the oxide surface (as seen in figure A-1.11). The increasing hydrogen availability on oxidic surface helps for the hydrogenation reaction to occur at lower temperatures and suppress the reactions that do not require hydrogen such as ketonization. In fact, Ponec et at. has reported that the addition of Pt into TiO_2 suppressed the formation of acetone when acetic acid is used as a feed.[54] He also concluded that oxides with intermediate metal-oxygen bond strength such as iron, tin or copper oxides are the best catalyst for selective deoxygenation of carboxylic acids and esters to aldehydes. Using the same model compound, acetic acid, through the kinetic study, Vannice et al. has claimed that the selectivity of reactions of acetic acid is controlled by the adsorption behavior of acetic acid on these oxide surfaces as well as the availability of activated hydrogen. [55] On Pt/oxide catalysts, the hydrogenation reaction may be favored over ketonization in the presence of activated hydrogen because the latter reaction has higher activation energy of 121-138 kJ/mol compared to values of 38-96 kJ/mol for the former. However, differently from dissociative adsorption of carboxylic acids and esters on copper metal, the adsorption of acetic acid on the oxides was proposed to be molecular.

2.3 Reactions of triglycerides and vegetable oils

Since alkyl esters can be directly derived from triglycerides of vegetable oils and they share the similar functional group (-COO-), it is worth reviewing the related reactions of these complex compounds. Before biodiesel or fatty acid methyl esters are used as potential diesel fuel components, many researchers have tried to convert the

original vegetable oils into hydrocarbon fuels. In the late 1980s, since direct use of vegetable oils is associated with viscosity and stability problems, Djega-Mariadassou and his group published several papers on production of diesel fuels by reacting vegetable oils over hydrotreating catalysts.[56] The reactions were carried in batch reactors. He found that sulfided Ni-Mo/γ-Al_2O_3 catalyst was active at elevated pressure (20 M Pa) and temperature (633 K). High selectivity of normal alkanes was obtained. When soybean oil was fed, products were formed by a 96% molar mixture of n-$C_{15}H_{32}$, n-$C_{16}H_{34}$, n-$C_{17}H_{36}$ and n-$C_{18}H_{38}$, which were obtained via decarboxylation/decarbonylation and hydro-deoxygenation of palmitic and stearic acid fragments in triglycerides. The hydrocarbons did not undergo any isomerization or hydrogenolysis activity, therefore; the carbon chains were close to that in acid molecules of the original triglycerides. When the hydrogen partial pressure was lower, some degree of isomerization, aromatization and cyclization reactions occurs. Figure A-1.12 depicts possible reactions happening during the hydrocracking reaction of vegetable oils. It is clearly seen that besides alkanes, cycloalkanes and alkylbenzenes were observed. In fact, the unsaturated fatty acid fragments can react via a decarboxylation and/or reduction to produce unsaturated hydrocarbons able to undergo cyclization into alkylcycloalkanes. At temperature of 633 K, a small fraction of alkylcycloalkanes can dehydrogenate and consequently aromatize to form aromatics. Other researchers also reported the presence of cycloalkanes as products in the pyrolysis of tropical vegetable oils at 573-773 K and atmospheric pressure.

More recently, a research group from Topsoe company has proposed new reaction pathways for hydrotreating of triglycerides and fatty acid methyl esters.[57]

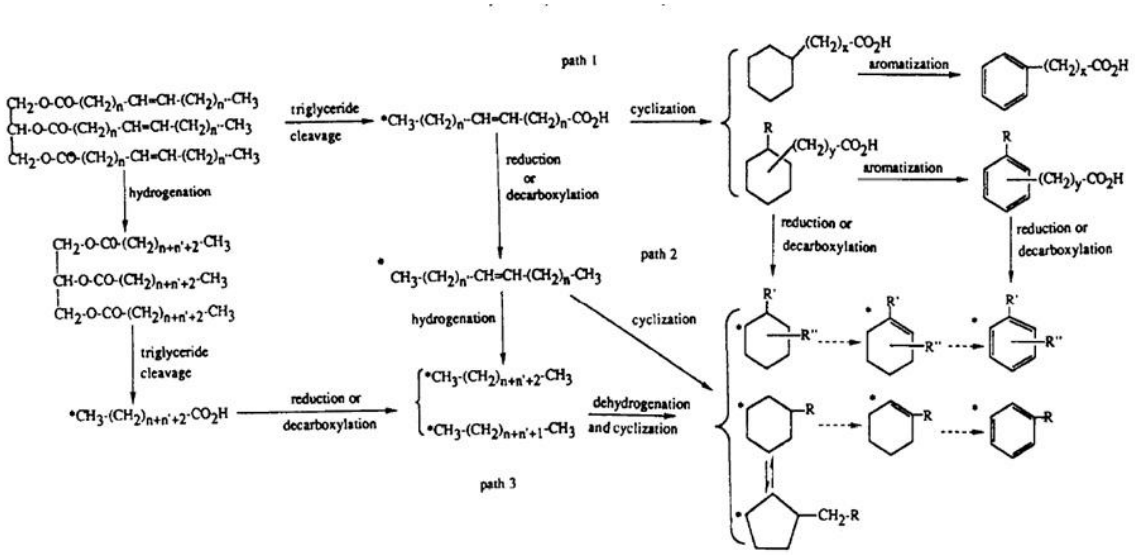

Figure A-1.12: Possible hydrocracking reaction mechanisms over $NiMo/Al_2O_3$ catalyst sulfided in situ (asterisks denote products observed). Cited from reference 56.

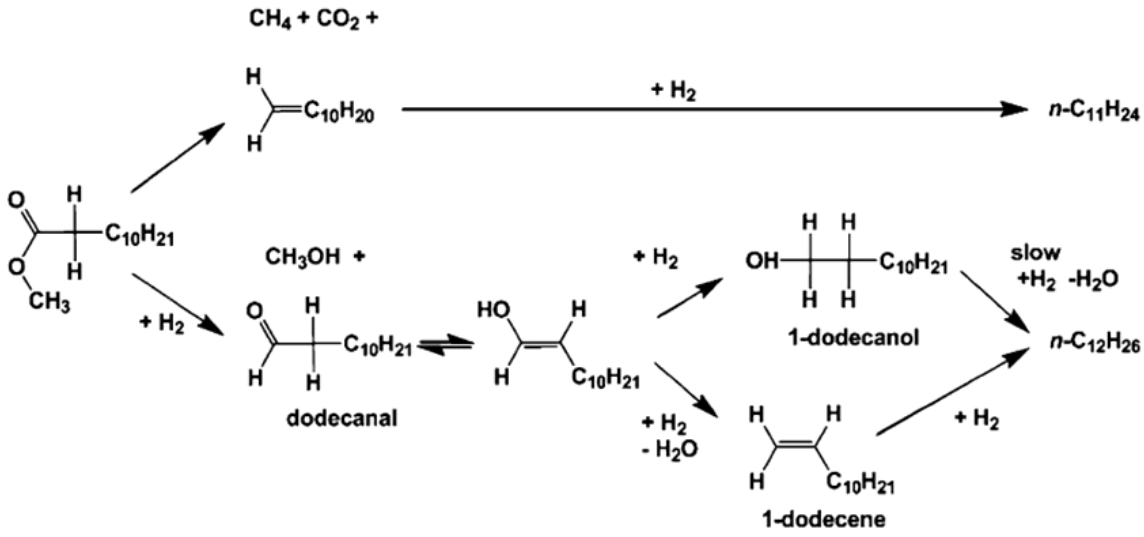

Figure A- 1.13: Overview of the proposed reaction routes when hydroprocessing methyl laurate. Cited from reference 57.

The hydrotreating of triglycerides and methyl laurate hydrotreating Ni-Mo catalysts involve both hydrogenation and decarboxylation/decarbonylation reactions. The major hydrogenation product is n-dodecane. As suggested by many other works, hydrogenation of methyl laurate is a step-wise reaction involving aldehyde as an intermediate. Here, the authors have claimed that since carbonylic compounds exist in equilibrium with the enol form, an obvious hypothesis would be that it is the (adsorbed) enol form of the dodecanoate or the dodecanal, which is the reactive intermediate. Figure A-1.13 describes the overall reaction scheme of hydrotreating reaction of methyl laurate. The decarboxylation/decarbonylation reactions yield CO_2 and CO as light gas products. When carbon dioxide and carbon monoxide are formed, there are two additional reactions which need to be taken into consideration. These are water gas shift and methanation. The water gas shift activity of the catalyst makes it difficult to establish whether the observed CO and CO_2 are produced by decarboxylation or by a similar decarbonylation route. Since the relative activities of the decarboxylation and hydro-deoxygenation reactions are of major importance for the hydrotreating process as these influences the hydrogen consumption, product yields, catalyst inhibition, treat gas composition and heat balance. The current tests showed that even though the decarboxylation route in itself constitutes a low-hydrogen consuming pathway to normal alkanes, the subsequent water-gas-shift and methanation reactions can increase the hydrogen consumption to a level, where the lower diesel yield in itself makes the HDO route more attractive.

2.4 Ketonization of carboxylic acids and alkyl esters

To increase the energy content of short biomass-derived molecules, the suggested pathways to fuel compounds involve the partial removal of oxygen, C-C bond formation

of functional molecules, and removal of the remaining oxygen.[58] The formation of C-C bonds between these oxygenated molecules can take place via aldol condensation, alkylation, or ketonization reactions. In the literature, it is reported that metal oxide catalysts are good options for catalyzing these reactions.[59]

The majority of the work relating to ketonization deals with oxide catalysts although some researchers have slightly talked about the presence of carboxylate species on metal surfaces. In this section, a brief review of how ketones are formed on oxides will be presented, together with some features that influence the ketone formation patterns. Between two reaction routes of carboxylic acids, ketonization is thermodynamically favored compared to dehydration. Therefore, ketonization reaction is well studied on polycrystalline oxide catalysts. Many oxides are found to be active in this reaction, including: γ -Al_2O_3, MgO, Fe_3O_4, Fe_2O_3, TiO_2, Cr_2O_3, ZrO_2, among others. Different mechanisms for the ketonization of carboxylic acids have been proposed and are under debate: [60]

- An acid anhydride species that release CO_2 to produce the ketone. This mechanism has been responsible for the production of cyclic ketones from dicarboxylic acids.
- A β-keto acid intermediate formed from two monodentate carboxylates via α-hydrogen abstraction. Carboxylic acids involved in this mechanism must have α-hydrogen atoms.
- A concerted mechanism involving two monodentate carboxylates. This mechanism is limited to form ketones from aromatic acids.
- An intermediate formed from two molecularly adsorbed carboxylic acids. However, the evidence shows that molecular acetic acid does not participate in ketonization reaction.
- A ketene-like intermediate that reacts with a carboxylate to produce the ketone.

- A bimolecular coupling of two carboxylates bound to the same cation.

Two proposed ketonization mechanisms relevant to this study are involving either ketene intermediate or bimolecular coupling of two carboxylates. Before discussing individual mechanisms, it is important to stress that many researchers have agreed on the capacity of oxides to dissociate carboxylic acids into surface carboxylates as an initial step. Dissociation of carboxylic acids on metal oxides appears to require only accessible cation-anion site pairs on the surface, with the conjugate base of the parent acid bound at a coordination vacancy of the metal cation. Ponec et al. has showed firm evidences on the participation of ketene-like species in formation of acetone from acetic acids.[53] The reaction intermediate is probably oriented parallel to the surface and interacts with the catalyst via both the carboxyl group and the α-carbon of the alkyl group. The latter interaction requires an α-hydrogen abstraction. The formed alkyldiene group can react with the adjacent carboxylate and a surface hydrogen atom to form ketone. The remaining carboxyl group would yield CO_2. The reaction intermediate might be in equilibrium with the ketene species. Meanwhile, using the same probe molecule, Barteau et al. has proposed the ketone formation via bimolecular mechanism.[60] From the studies using both TiO_2-functionalized silica monoliths and powder TiO_2, he concluded that ketonization requires the coordination of two acetates to a common titanium cation on a stoichiometric or fully oxide surface. The active sites are coordinatively unsaturated.

Although a variety of carboxylic acids such as straight-chain, branched, cyclic or even unsaturated, mono-carboxylic acids have been studied in ketonization reaction, the ketone yield is mostly influenced by the nature of the oxide catalysts.[61-62] Limited information is reported on ketonization of alkyl esters instead of carboxylic acids. The

work from Lomot et al. is one of the few studies on alkyl ester ketonization. [63] Lomot et al. has found that when studying ketonization of alkyl heptanoates over 20 wt.% MO_x/Al_2O_3 catalysts, where M = Mn, Ce or Zr, the yield of ketone depends strongly on the structure of alkyl group in the ester molecule. For heptanoates with primary alkyl groups the maximum yield of ketone increases with an elongation of alkyl group. Among isomeric butyl heptanoates an order of decreasing maximum yield of ketone is as follows: t-butyl > s-butyl > n-butyl > i-butyl. The highest reactivity was observed for t-butyl heptanoate. The reactivity of t-butyl ester exceeds that of heptanoic acid which has been measured before over the same catalyst.

Dumesic et al. has shown that supported rare-earth oxides (CeO_2/ZrO_2) can be used for C-C bond formation through ketonization reactions between carbohydrate-derived organic acids such as hexanoic acid.[64] The kinetic study has determined the value of the ketonization activation energy as 132 kJ/mol. Others have reported the value of 159 kJ/mol for different catalysts.[65] In regard to the ketonization activity of esters versus acids, Dumesic et al. has claimed that due to the stronger adsorption of acids on the catalyst surface, direct ketonization of esters will not take place as long as acids are present. Consequently, ketonization of acids takes place preferentially compared to ketonization of esters. While the reaction mechanism of ketonization of esters remain unknown,[66] it could be possible that the water formed by the ketonization of carboxylic acids causes the subsequent hydrolysis of esters to form carboxylic acids and alcohols, which is followed by the ketonization of these newly formed carboxylic acids. The ketonization reaction is between two carboxylic acid or ester molecules, whereas, the aldol condensation reaction involves two ketone or alcohol molecules react to form a

heavier branched ketone. Dumesic et al. has shown that a catalyst consisting of Pd-supported on $CeZrO_x$ is effective at 623 K for the condensation of ketones.[67] Since the support possesses high lattice oxygen mobility and the ability to interact strongly with supported metals, which leads to high resistance to the formation of carbonaceous species or deactivation.[68] Additionally, $CeZrO_x$ contains a combination of acidic and basic functionalities required for aldol condensation reactions.[69] The primary reaction products are C_{12} species, which will further undergo hydrogenolysis to C_9 species or sequential condensation to C_{18} species. The low Pd loading leads to enhanced selectivity to C_{12} products and suppressed de-oxygenation side reactions. Also, other oxygenated species such as alcohols and carboxylic acids, water and CO_2 were found to inhibit the self-coupling reaction of the tested ketone.

2.5 Isomerization reactions of long-chain alkanes

The deoxygenation reaction of triglycerides in vegetable oils and alkyl esters produces straight-chain hydrocarbons with 8 to 28 carbons. These compounds serve as great diesel fuel components and original feed stocks for chemicals production. However, these straight-chain hydrocarbons have high cloud points or waxing problems, which inhibits their uses in many applications. Therefore, converting these straight molecules into branched isomers becomes a desirable process.

The reactions of alkanes over solid acid catalysts involve a list of reactions such as cracking, alkylation, dehydrogenation, isomerization, and disproportionation. When bifunctional catalysts (i.e. Pt/zeolite) are used, the reactions proceed via carbenium ion, which is formed by protonation of olefin generated via dehydrogenation of alkane on the metal functionality. Consequently, the acid sites will catalyze the isomerization or β-

scission. The cracking/isomerization ratio can be used to interpret the information on pore size, temperature, diffusivity, location, density, number and strength of acid sites.[70] A number of works have reported the high isomerization selectivity of straight-chain alkanes over bifunctional Pt/solid acid catalysts. For example, catalysts, which are based on unidirectional 10-member ring zeolites (ZSM-22, ZSM-23, ZSM-35, ZSM-48) or silicoaluminophosphate molecular sieves (SAPO-11, SAPO-31, SAPO-41), loaded with a small amount of pure or bimetallic noble metal shows a high hydro-isomerization activity for long n-alkanes.[71-73] For tubular zeolites such as ZSM-22, the monobranching is preferred and often at terminal or close to terminal position.[74] In the meantime, on zeolites with wider pores, like HY, multi-branching and cracking are dominant. There are three main hypotheses explaining the high isomerization activity of tubular zeolites. First, the pore mouth chemistry plays an important role in the formation of terminal monobranching alkanes. The isomerization reaction, in fact, occurs at the acid site located at the entrance of the pore. The methyl substituent is formed at the part of the molecule residing at the pore mouth. The remaining carbon chain is positioned inside the pore. The second methyl substituent can be formed when the molecule penetrates into two more opening pore mouths. The thickness of the pore wall or the distance between two neighboring pore mouths will determine the position of the second methyl substituent. This mode is designated as key-lock mode. The second hypothesis is the transition state shape selectivity, in which the intermediate from linear to monobranched alkanes with terminal methyl group is as big as the zeolite channels. Thus, they can be formed. Their isomers with methyl group at different positions are bulkier and are favorably produced. The last hypothesis is the product shape selectivity, in which the isomers with a

distribution of methyl groups are formed inside the zeolites. However, alkanes with terminal methyl group are more mobile and diffuse out of the zeolite faster. Conversely, the alkanes with internal methyl reside inside the zeolite longer and are subject to cracking or further secondary reactions.

Besides zeolites, other solid acid catalysts such as WO_x-ZrO_2 are reported to be active in hydro-isomerization of long n-alkanes. [75] The study of isomerization of n-C_{16} over Pt/WO_x-ZrO_2 catalyst done by Martinez et al. has shown that the isomerization reaction can proceed via either classical bifunctional or non-classical bifunctional mechanisms. In the latter pathway, the original alkanes are activated during a redox step involving partially reduced W species.[76] The role of Pt here is to provide hydrogen to form Bronsted acid sites on partially reduced WO and assist the desorption of carbocation species. This catalyst requires lower reaction temperature to obtain the comparable level of isomerization than Pt/USY or Pt/amorphous silica-alumina catalysts do.

2.6 Trickle bed and monolith catalysts

Hydrocarbons produced from reactions of triglycerides and alkyl esters not only are used as fuel components but also are known as surfactant precursors. Among all of the hydrocarbon products, the terminal alkenes are the most preferred. Although the α-olefins are the primary hydrocarbon products from deoxygenation reactions, they quickly get isomerized to terminal olefins or hydrogenated to saturated alkanes. In order to maximize the yield and selectivity of α-olefins, the trickle-bed reactor and monolith catalysts are introduced. In fact, the vapor phase plug flow reactor and the supported mesoporous catalysts possess several issues leading to poor selectivity of α-olefins.

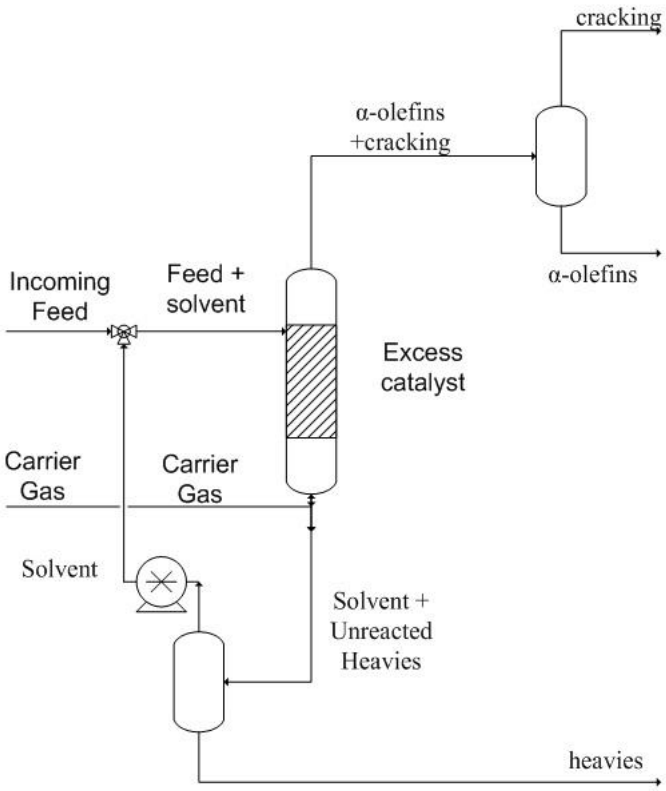

Figure A- 1.14: Counter-current reactor configuration to maximize α- alkenes production.

The secondary intra-particle re-adsorption easily occurs with the primary products, resulting in secondary reactions of the α-olefins. The isomerization activity either on catalyst surface or by re-adsorption before diffusing out of pore is commonly observed with mesoporous materials. The general solution for these problems is to minimize the retention of α-olefins inside the catalyst bed. This can be obtained by changing the feed rate and carrier gas rate. The trickle-bed reactor also offers some distinct features that could help to enhance the selectivity of α-olefins. Thin layer of liquid feed drips along the catalyst particles while the products formed desorb and diffuse through the liquid layer to the gas phase of carrier gas. The carrier gas and feed rates can be controlled so that the gas products, α-olefins in this reaction, are prevented from re-adsorbing on the catalyst surfaces. The use of monolith washcoat catalyst will add extra features to inhibit the re-adsorption of the primary products. The active catalyst component is coated on top of the washcoat attaching to the monolith support. The washcoat material is non porous, therefore; the diffusion of the primary products is not limited in any pore. This new support, in fact, contains uni-directional channels, where the gas or liquid only follow one direction. All of these features allow the formed products to desorb quickly and avoid re-adsorption. The counter-current reactor configuration is displayed in figure A-1.14. The α-alkenes will be carried out at the top of reactor in the gas phase and collected after the flash drum. The solvent or un-reacted material will be collected at the base of reactor and recycled. Several studies have proved the efficient use of coated MCM-41 catalyst on metallic and ceramic substrates for adsorption of volatile organic compounds and water vapors.[77] In some cases, the metallic substrates are favorable due to higher thermal conductivity. The substrates are etched to improve the contact with the catalyst support.

Thin layers of MCM-41 support are deposited on the substrates. The active components are then impregnated on the support.

3. References

[1] Kunkes, K. L., Simonetti, D. A., West, R. M., Serrano-Ruiz, J. C., Gärtner, C. A., and Dumesic, J. A. *Science* **322**, 417 (2008)

[2] Christensen, C.H., Rass-Hansen, J., Marsden, C.C., Taarning, E., and Egeblad, K. *Chem. Sus. Chem.* **1**, 283 (2008)

[3] Corma, A., Iborra, S., and Velty, A. *Chem. Rev.*, **107**, 2411 (2007)

[4] Chum, H. L., Overend, R. P., *Adv. Solar Energy* **15**, 83 (2003)

[5] DOE Report "Top Value Added Chemicals from Biomass Volume I—Results of Screening for Potential Candidates from Sugars and Synthesis Gas", August 2004

[6] Rennard, D.C., Dauenhauer, P.J., Tupy, S.A., Schmidt, L.D., *Energy Fuels* **22,** 1318 (2008)

[7] Lichtenthaler, F. W., *Acc. Chem. Res.* **35**, 728 (2002).

[8] NREL Report "Characterization of Biodiesel Oxidation and Oxidation Products", November 2005

[9] Demirbas, A., *Ener. Convers. Manage*. **44**, 2093 (2003)

[10] Da Rocha Filho, G. N, Brodzki, D., Djega-Mariadassou, G. *Fuel* **72,** 543 (1993)

[11] Corma A. ,Iborra, S., and Velty A., *Chem. Rev*. **107**, 2411 (2007)

[12] Renz, M., *Eur. J. Org. Chem*. 979 (2005)

[13] Gaertner, C.A., Serrano-Ruiz, J. C., Braden, D. J., and Dumesic J. A., *J. Catal.* **266** 71 (2009)

[14] Mavrikakis, M., and Barteau, M. A., *J. Mol. Catal. A: Chem.* **131,** 135 (1998)

[15] Houtman, C.J. and Barteau, M.A., *J. Catal.* **130**, 528 (1991)

[16] Gates, S.M., Russell Jr., J.N., and Yates Jr., J.T., *Surf. Sci.* **171,** 111 (1986)

[17] Avery, N.R., Weinberg, W.H., Anton, A.B., and Toby, B.H., *Phys. Rev. Lett.* **51,** 682 (1983)

[18] Henderson, M.A., Radloff, P.L., White, J. M., and Mims, C. A., *J., Phys. Chem.* **92** 4111 (1988)

[19] Vargas, A., Bürgi, T., and Baiker, A., *J. Catal.* **222**, 439 (2004)

[20] Ponec , V., *Appl. Catal. A: Gen.* **149,** 27 (1997)

[21] Sexton, B.A., Hughes, A.E., Avery, N.R., *Surf. Sci.* **155**, 366 (1985)

[22] Maier W.F., Bergmann, K., Bleicher, W., and Schleyer, P.V.R., *Tetrahedron Letters*, **22**, 4227 (1981)

[23] Durand, R., Geneste, P., Moreau, C., and Pirat, J. L. *J. Catal.* **90**, 147 (1984)

[24] Ferrari, M., Maggi, R., Delmon, B., and Grange, P. *J. Catal.* **198,** 47 (2001)

[25] Furimsky, E. *Appl. Catal. A: Gen.* **199**, 147 (2000)

[26] Bejblova, M., Zamostny, P., Cerveny, L., and Cejka, J. Collect. *Czech. Chem. Commun.* **68** (2003)

[27] De Lange, M. W., PhD Dissertation " Selective Deoxygenation of Carboxylic Acids", University of Twente, 2000

[28] Henrich, V.E. and Cox, P.A., " The Surface Science of Metal Oxides", Cambridge University Press, Cambridge, 1994

[29] Mahan, G. D. J. *Appl. Phys.* **54**, 3825 (1983)

[30] Wehner, P.S., Tustin, G.C., and Gustafson, B.L. *J. Catal.* **88,** 246 (1984)

[31] Hashimoto, K., Toukai, N., Hamada, R., and Imamaura, S., *Catal. Lett.*, **50**, 193 (1998)

[32] Davis, J. L., and Barteau, M. A., *Surf. Sci*. **256**, 50 (1991).

[33] King, S. T. and Strojny, E. J. *J. Catal.* **76**, 274 (1982)

[34] Turek, T. and Trimm, D. L., *Catal. Re. Sci. Eng.* **36**, 645 (1994)

[35] Davis, J. L., and Barteau, M. A., *J. Am. Chem. Soc.* **111**, 1782 (1989).

[36] Davis, J. L., and Barteau, M. A., *Surf. Sci.* **235**, 235 (1990).

[37] Shekhar, R., Barteau, M. A., Plank, R. V., and Vohs, J. M., *J. Phys. Chem. B* **101**, 7939 (1997)

[38] Maier, W. F., Roth, W., Thies, I., and Rague Schleyer P. v., *Chem. Ber.* **115**, 808 (1982)

[39] Snare, M., Kubickova, I., Maki-Arvela, P., Eranen, K., Murzin, D.Y., *Chem. Ind.* **115,** 415 (2005)

[40] Snare, M., Kubickova, I., Maeki-Arvela, P., Eraenen, K., Murzin, D.Y., *Ind. Eng. Chem. Res*. **45**, 5708 (2006)

[41] Adjaye, J. D., and Bakhshi, N. N. *Biomass and Bioenergy* **8**, 131 (1995)

[42] Agarwal, A. K., Cant, N. W., Wainwright, M. S., and Trimm, D. L., *J. Mol. Catal.* **43**, 79 (1987)

[43] Brands, D. S., Poels, E. K., and Bliek, A., *Appl. Catal. A: Gen.* **184**, 279 (1999)

[44] Aring, H., Burch, K.., Franke, P., Honetzke, G., Tietz, W., Weidemann, R. DD Patent 213430, 1984.

[45] Bradley, M. W., Harris, N., Turner, K. US Patent 258733, 1981

[46] Kohler, M. A., Cant, N. W., Wainwright, M. S., and Trimm, D. L., *in* "Proceedings of the 9th International Congress on Catalysis, Calgary,1988" (M. J. Phillips and M. Ternan, Eds.), p. 1043. Chem. Institute of Canada, Ottawa, 1988.

[47] Natal Santiago, M. A., S´anchez-Castillo, M. A., Cortright, R. D., and Dumesic, J. A. *J. Catal.* **193,** 16 (2000)

[48] Pallassana, V. and Neurock, M. *J. Catal.* **209**, 289 (2002)

[49] Neurock, M., *Appl. Catal. A: Gen.* **160**, 169 (1997).

[50] Snappe, R., and Bourneville, J. P., DE Patent 3217429, 1982.

[51] Cressely, J., Farkhani, D., Deluzarche, A., and Kiennemann, A., *Mater.Chem. Phys.* **11**, 413 (1984).

[52] Sakata, Y., van Tol-Koutstaal, C.A., and Ponec, V., *J of Catal* **169**, 13 (1997)

[53] Pestman, R., Koster, R. M., Van Duijne, A., Pieterse, J.A.Z., and Ponec , V., *J. Catal.* **168**, 265 (1997)

[54] R. Pestman, R. M. Koster, J. A. Z. Pieterse, and V. Ponec, *J. Catal.* **168**, 255 (1997)

[55] Rachmady, W., and Vannice, M. A., *J. Catal.* **192**, 322 (2000)

[56] Da Rocha Filho, G. N., Brodzki, D., and Djega-Mariadassou, G., *Fuel* **72** 543 (1993)

[57] Donnis, B., Gottschalck R. E., Blom, P., Knudsen, K. G. *Top Catal* **52**, 229 (2009)

[58] Simonetti, D. A. and Dumesic, J. A. *ChemSusChem* **1**, 725 (2008)

[59] Dooley, K.M., Bhat, A.K., Plaisance, C.P., and Roy, A.D. *Appl. Catal. A* **320**, 122 (2007)

[60] Martinez, R., Huff, M.C., and Barteau, M.A., *J. Catal.* **222,** 404 (2004)

[61] Glinski, M., and Kijenski, J., *Appl. Catal. A: Gen.* **190**, 87 (2000)

[62] Nagashima, O., Sato, S., Takahashi, R., and Sodesawa, T. *J. Mol. Catal. A* **227**, 231 (2005)

[63] Glinski, M. , Szymanski, W., and Lomot, D., *Appl. Catal. A: Gen.* **281,** 107 (2005)

[64] Gaertner, C.A., Serrano-Ruiz, J. C., Braden, D. J., and Dumesic J. A., *J. Catal.* **266** 71 (2009)

[65] Rajadurai, S. *Catal. Rev.-Sci. Eng.* **36**, 385 (1994)

[66] Klimkiewicz, R., Grabowska, H., and Syper, L. *Kinet. Catal.* **44**, 283 (2003)

[67] Kunkesa, E. L., Gürbüza, E. I, and Dumesic, J. A. *J. Catal.* **266**, 236 (2009)

[68] S.M. de Lima, I.O. da Cruz, G. Jacobs, B.H. Davis, L.V. Mattos and F.B. Noronha, *J. Catal.* **257** (2008), p. 356

[69] V. Solinos, E. Rombi, I. Ferino, M.G. Cutrufello, G. Colon and J.A. Navio, *J. Mol. Catal. A Chem.* **204-205** (2003), p. 629.

[70] Sastre, G., Chica, A., and Corma, A. *J. Catal.* **195**, 227 (2000)

[71] Meriaudeau, P., Tuan, V.A., Nghiem, V.T., Lai, S.Y., Hung, L.N., and Naccache, C. *J. Catal.* **169**, 5 (1997)

[72] Sinha, A.K., Sivasanker, S., and Ratnasamy, P. *Ind. Eng. Chem. Res.* **37**, 2208 (1998)

[73] Liu, Y., Liu, C., Tian, Z., and Lin, L. *Energy Fuels* **18**, 1266 (2004)

[74] Martens, J. A.; Jacobs, P. A. *Angew. Chem. Int. Ed. Engl.* **1995**, *34, No. 22*, 2528

[75] Martínez, A., Prieto, G., Arribas, M.A., and Concepción, P. *Appl. Catal. A: Gen.* **309,** 224 (2006)

[76] Kuba, S., Lukinskas, P., Grasselli, R.K., Gates, B.C., and Knozinger, H. *J. Catal.* **216**, 353 (2003)

[77] Shima, W.G., Moona, H., and Lee, J. W. *Micro. Meso. Mat.* 94, 15 (2006)

CHAPTER II: EXPERIMENTAL SETUP

1. Catalyst Preparation

Platinum was incorporated by incipient wetness impregnation using aqueous solutions of chloroplatinic acid hexahydrate (Aldrich) to obtain a 1 wt % Pt loading. The copper catalyst was prepared using copper (II) nitrate (Alfar-Aesar) as a precursor. Silica gel (from Sigma-Aldrich, surface area = 500 m^2/g), γ-alumina, and titania were used as the catalyst supports. All catalysts were prepared via incipient wetness impregnation method. The bimetallic Pt-Sn was prepared by using "chloride complex" method. Both chloroplatinic acid hexahydrate and tin (II) chloride (from Alfar-Aesar) were dissolved in 0.1M solution of hydrochloric acid. After stabilizing for two hours, the dark red solution is then doped into silica. It is our intention to keep the same molar ratio of Pt:Sn as the ratio in $[PtCl_2(SnCl_3)_2]^{-2}$ complex,[1] therefore; the loading of Sn was calculated to be 1.3 wt%. In the making of Pt-Sn-K catalysts, platinum and tin were introduced similarly as above. The liquid to support ratio is 0.8 mL/1 gram. The sample was then dried overnight at 383 K before potassium hydroxide (from Alfar-Aesar) was doped. The Pt supported on acidic supports were prepared by using HY zeolite (Si/Al= 15 from International Zeolyst) and W-Zr mixed oxide prepared by co-impregnation. After impregnation all the samples were kept at ambient temperature for 4 hours, then dried at 383 K overnight, and finally calcined in flowing air ($100cm^3$/min) at 673 K for 2 hours.

The metal-foam-supported Pt-Sn-K catalysts were prepared in two consecutive steps. First, the carbon fibers were grown on the metal foam substrate. The fresh foams was either treated or not treated with concentrated HCl solution. This treatment was thought to create more surface roughness to increase the active sites for carbon fiber

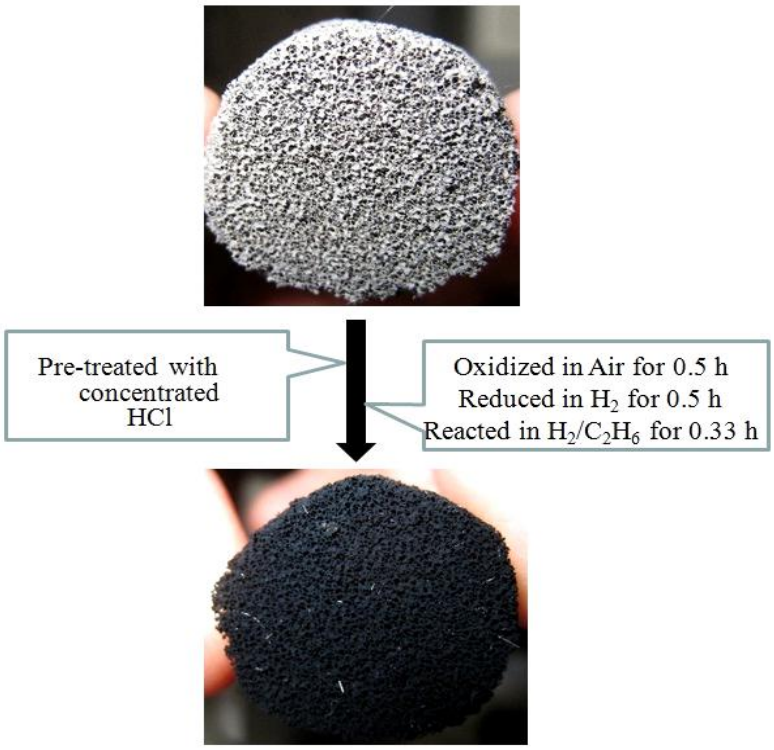

Figure A-2.1: Step-wise deposition of carbon fiber on Inconel metal foam

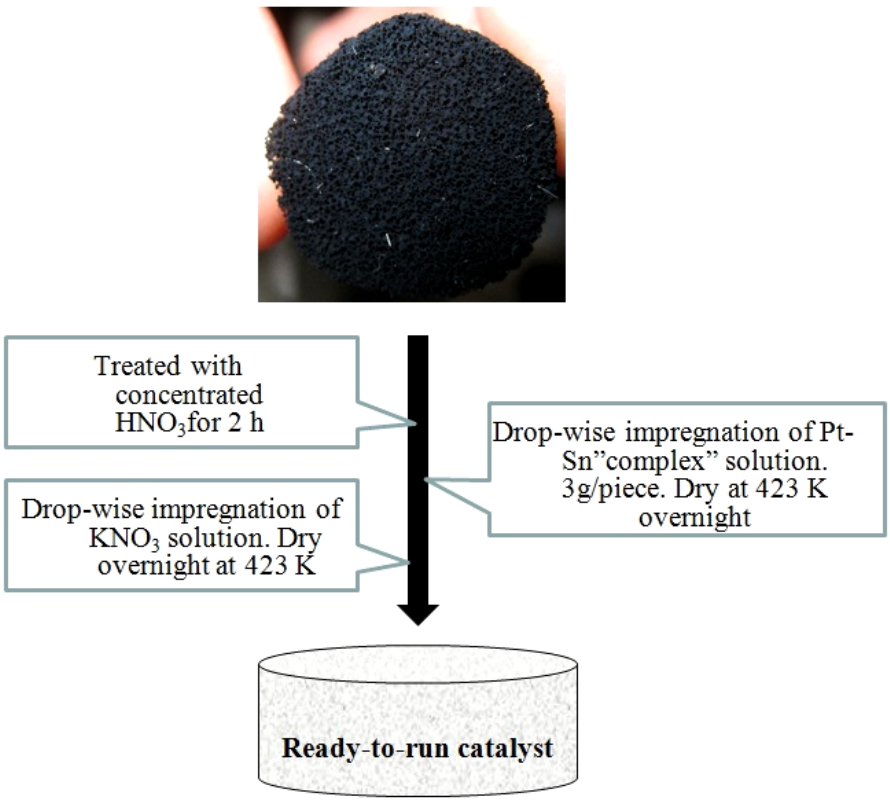

Figure A-2.2: Step-wise deposition of Pt-Sn-K on metal foam substrate

growth. After that the foam was oxidized in air for 0.5 hour and reduced in hydrogen for 0.5 hour. The reduced sample was then reacted with mixture of ethane in hydrogen for 0.33 hour. The process of carbon fiber growth is depicted in figure A-2.1, in which the color of the fresh foam changed from grey to black due to the coating of carbon fiber. Figure A-2.2 shows the step-wise deposition of Pt-Sn-K on the substrate. The coated foam was treated with concentrated HNO_3 solution for 2 hours to functionalize the carbon fiber, which could lead to higher dispersion of Pt-Sn-K active element. The drop-wise impregnation of Pt-Sn "complex" species was carried after the functionalization step. The sample was then dried in stagnant air at 423 K for 12 hours before being impregnated with KNO_3 solution (0.2 mL). The final catalyst was again dried in stagnant air at 423 K for 12 hours.

2. Catalyst Characterization

2.1 Carbon monoxide chemisorption

Carbon monoxide chemisorption data was obtained with 75 mg of the catalyst sample, which was then reduced in H_2 flow (100 cm^3/min) at 603 K for Pt/Al_2O_3 and Pt/TiO_2 and 653 K for Pt-Sn-K/SiO_2 series for 1.5 hour before switching to He (100 cm^3/min) at the same respective temperatures for 0.5 hour to remove surface-adsorbed hydrogen. The samples were then cooled to the room temperature, when 100μL pulses of CO were introduced. An online SRI 310C TCD was used to monitor the evolution of CO signal. Pulses of calibrating CO was sent for quantification after the surface became saturated with adsorbed CO. The ratio of CO to metal (CO/Pt) was calculated by moles of adsorbed CO per moles of Pt impregnated into catalyst supports.

2.2 Temperature-programmed reduction (TPR)

TPR experiments were carried out by feeding gas mixture of 5% H_2 in Argon (20 cm^3/min) to 130 mg of catalyst samples. The temperature program was set up to 1073 K at ramp of 10 K/min. The effluent gases were analyzed using online SRI 110 thermo conductivity detector (TCD).

2.3 Temperature-programmed oxidation (TPO)

Prior to the temperature-programmed oxidation step, 100 mg of each spent catalyst sample was heated from room temperature up to 773 K in He (80 cm^3/min) flow (ramp rate at 10 K/min and holding at 773 K for 40 min) to remove all of volatile materials on the actual carbon deposit. During the TPO experiments, the sample was oxidized in flow of 5%O_2 in He (80 cm^3/min) while heating up to 1073 K (ramp at rate 10 K/min) to assure the complete burning of deposited coke. The main oxidation product, CO_2, was passed through 1% Ni/Al_2O_3 bed to convert into CH_4, which was then detected by an SRI 110 equipped with a FID detector. The amount of deposited coke was quantified by using a standard 100μL CO_2 sample loop.

2.4 X-ray photoelectric spectroscopy (XPS)

XPS information was recorded on a Physical Electronics PHI 5800 ESCA system equipped with an Al*Kα* X-ray anode operated at 350 W and 15 kV. The base pressure of the UHV XPS chamber was ~1.0×10^{-8} Torr. A 400 μm spot size and 187.85 eV pass energy were implemented during the data acquisition. For XPS analysis of the reduced samples, the catalysts were pre-reduced in flow of H_2 (100 cm^3/min) at 603 K or 653 K for 2.5 hours, and then transferred into ex-situ cell in He atmosphere to avoid exposing

with oxidizing medium. Sputtering depth profiles of reduced supported Pt catalysts was been done by using argon ion beam bombardment.

2.5 Transmission electron microscopy (TEM)

2.5.1 Transmission electron microscopy of powder catalyst

A small amount (5mg) of catalyst powder was dispersed in 15 mL of iso-propanol solution before being sonicated for 10 minutes. Three drops of the dispersed solution were deposited on the copper grids, which were then left to dry at 333 K overnight.

2.5.2 Same-spot transmission electron microscopy

The same-spot TEM experiments were carried on the SPI silicon nitride membrane window grids. First, thin layers of silica were formed after three drops of tetraethyl orthosilicate (Aldrich) were introduced into the grids, which were let to dry and hydrolyze to form SiO_2 at 333K for three continuous days. Second, three drops of aqueous solution of chloroplatinic acid hexahydrate and mixed aqueous solution of chloroplatinic acid hexahydrate and tin chloride ($SnCl_2$) in HCl were deposited on Pt grid and Pt-Sn grid, respectively. The molar ratio of Pt:Sn in the mixed solution was fixed at 1:2. The samples were then heated at 373 K overnight in the open atmosphere before being calcined in the flowing air (100 cm^3/min) at 573 K for 2 hours. The first TEM were taken with the calcined grids. Since the grids contain a matrix of tiny windows, the windows, in which metal particles were detected, were numbered to reassure that the same spots will be spotted after each treatment. The second TEM experiments were done after the calcined grids were reduced in hydrogen (100 cm^3/min) at 653 K for 2.5 hours. During TEM, the grids were in contact with air, therefore; they were slightly treated with

hydrogen before being exposed to the feeding of methyl hexanoate at 653K in helium (100cm/min). After four hours of reaction, these grids were analyzed by TEM.

2.6 Iodine number measurements

The Iodine number is defined as the number of grams of iodine adsorbed by 100 g of liquid. The added iodine reacts with the molecule containing double bond, therefore; the iodine number can be used to interpret unsaturation degree of the liquid sample. One flask containing 100 g of liquid in chloroform and one flask containing only chloroform were prepared. Fixed amounts of Wijs solution (0.2M of ICl) were added into each flask, which was then left under the dark for the reaction of double bond with ICl. Next, certain quantities of KI solutions were added to react with the unreacted ICl. The last step is to titrate the formed I_2 using measured amounts of $Na_2S_2O_3$ solution mixed with starch solution. The iodine number is calculated based on the difference in amount of $Na_2S_2O_3$ solution added to two flasks.

3. Catalytic Activity Measurements

3.1 Vapor phase plug flow reactor

The reactions of both methyl octanoate ($CH_3(CH_2)_6COOCH_3$ from Aldrich) and methyl hexanoate ($CH_3(CH_2)_4COOCH_3$ from Aldrich) were carried out in a fixed-bed tubular reactor (1/2" OD stainless steel tube), equipped with a thermo well in the center of the catalyst bed. To minimize the heat accumulated, the catalyst was diluted with an inert material (α-alumina from Aldrich). Reactions were conducted in the gas phase at at 603 K for methyl octanoate and 653 K for methyl hexanoate, at atmospheric pressure and using gas/liquid feed molar ratio of 30. The catalyst was first reduced for 2.5 hours under flowing H_2 at same reaction temperatures. In the helium reactions, the catalyst was then

treated with helium for 0.5 hour to remove surface-adsorbed hydrogen. After that the liquid reactant was fed using an Isco LC-500 high-pressure syringe pump. The line after the reactor was heated up to 543 K to maintain products and reactant in the gas phase. Reactor effluent was analyzed online using a Hewlett Packard 6890 GC. Product identifications were using a Shimadzu GC-MS-QP5000. Chemical standards were also used to confirm product identification.

3.2 Trickle-bed reactor

The coated metal foam catalyst was placed in the center of a fixed-bed tubular reactor (1" OD stainless steel tube). To create evenly distributed liquid flow, liquid feed was introduced through a constricted tube from the top of the reactor. Both hydrogen and nitrogen were fed co-current with the liquid. The metal foam catalyst was reduced under 200 mL/min of hydrogen at 653 K for 2.5 hours before the reaction under nitrogen. The reactions were carried at 653K and 2.72 MPa or 1.36 MPa. The liquid products were collected after the reactor and analyzed manually by Hewlett Packard 6890 GC. Products were identified using Shimadzu GC-MS-QP5000.

4. References

[1]De Miguel, S.R. , Baronetti, G.T., Castro. A.A., and Scelzaa, O.A., *Appl. Catal.* **45** 61 (1988)

CHAPTER III: REACTION OF METHYL OCTANOTE

Since alkyl esters, particularly methyl esters, are renewable and abundant, it is efficient to convert them into valuable chemicals and fuel products, which are currently originated from petroleum sources. The decarboxylation of carboxylic acids to the corresponding hydrocarbons in the gas phase over heterogeneous metal catalysts has been known for many years. [1] Liquid-phase deoxygenation of vegetable oils over supported metals, acidic, and basic catalysts has been reported by several groups.[2-6] Other studies have focused on elucidating the mechanism of deoxygenation of small carboxylic acids.[7]

In this work, although methyl octanoate is not quite in the range of natural fatty acid methyl esters, it was first chosen as a model molecule to study reactions of methyl esters. The reactions were carried out in vapor phase and the products were analyzed by an online GC. In details, the targeted chemicals and fuel products are alpha olefins and fungible fuel compounds from methyl octanoate. In order to achieve these products, important operating parameters such as catalysts, temperature, pressure, and hydrogen partial pressures need to be well controlled. The manipulations of these parameters will focus on (1) maximize the deoxygenation of esters into hydrocarbons, (2) design the stable catalysts for the reactions without hydrogen and selective catalyst sfor alpha olefin production and (3) tailor the catalysts that can simultaneously deoxygenate the original ester and isomerize its products. First, the deoxygenation of methyl octanoate will be carried out over two supported Pt and Cu catalysts. Two supports used for Pt catalysts are non-reducible alumina and reducible titania. The product distribution is also affected as one varies the support. Decarbonylation/decarboxylation reactions are found to mostly occur on 1%Pt/Al_2O_3. Meanwhile, on 1%Pt/TiO_2, hydrogenation/hydrogenolysis pathway

competes with decarbonylation/decarboxylation. However, different behavior is observed with Cu catalyst. Hydrogenation reactions become dominant on 10%Cu/SiO_2. Second, since bimetallic Pt-Sn catalysts show high coke tolerance activity, they will be used to optimize the selectivity of α-alkenes in the reaction without hydrogen. Inert support, silica, was chosen to maximize the interactions between Pt and Sn. Changing Pt:Sn atomic ratio also affects these interaction, which has direct impacts on selectivity of α-alkenes. Last, different reactor configurations will be proposed in making the fungible fuel components. That includes deoxygenating the ester into straight-chain hydrocarbons, isomerizing these products into branched hydrocarbons, and dehydrogenating saturated alkanes into alkenes. The supported Pt-Sn catalysts were used in both deoxygenation and dehydrogenation reactions. In the mean time, bifunctional catalysts of Pt on acidic support will catalyze the isomerization reactions of hydrocarbons.

1. Reaction of Methyl Octanoate on Supported Pt and Cu Catalysts

1.1. Catalyst characterization analysis

Figure A-3.1 shows the temperature-programmed reduction of 1%Pt/Al_2O_3 and 1%Pt/TiO_2 catalysts. For the alumina-supported catalyst, two reduction peaks are evidently in good agreement with other TPR reported in the literature.[8] The hydrogen consumption peak at low temperature is due to reduction of Pt oxide particles that do not interact strongly with the alumina, while the high-temperature peak is associated those strongly interacting with it. [9]Decomposition of the Pt precursor that remains after the calcination step may also shift the reduction temperature. The reduction temperature chosen for the reaction (603 K) is a compromise between maximum reduction and minimum particle growth by high-temperature sintering. It must be taken into

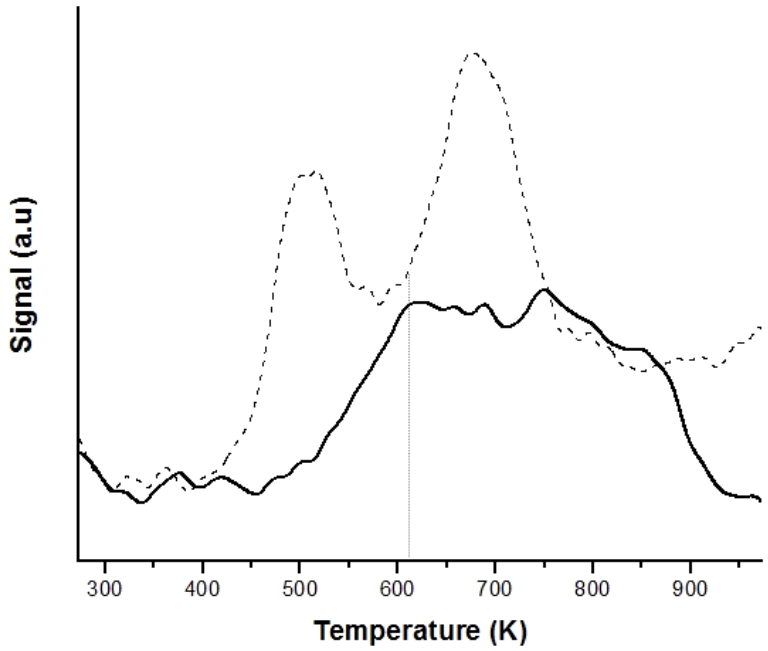

Figure A-3.1: Temperature-programmed reduction (TPR) of 1%Pt/Al_2O_3 (dash line) and 1% Pt/TiO_2 catalysts (solid line)

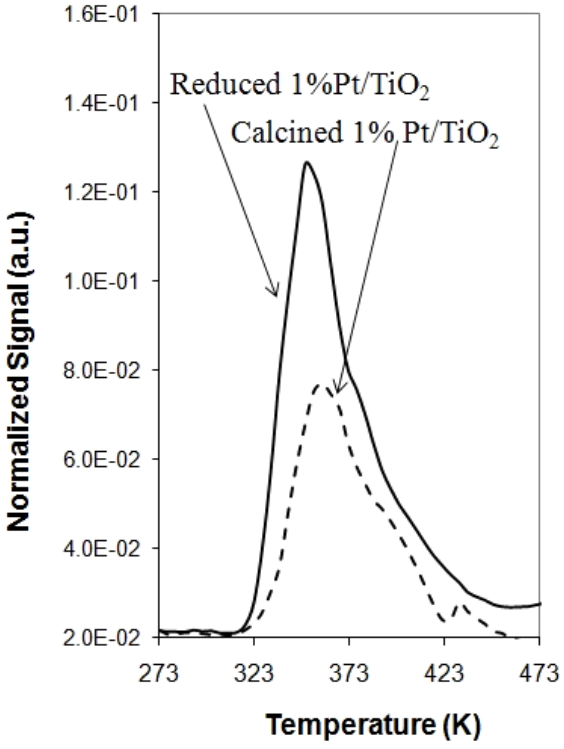

Figure A-3.2: Temperature-programmed desorption profiles of CO_2 over calcined and reduced 1%Pt/TiO_2 catalysts

consideration that during the pre-reduction step, a much higher hydrogen pressure than in the TPR experiments is employed, which will enhance the reduction of Pt oxides. Therefore, while a small fraction of PtO_x species stabilized by alumina support might not be reduced, a high CO/M ratio of Pt/Al_2O_3 catalyst (shown in Table A-3.1) was still obtained. On the titania-supported catalyst, reduction of PtO_x stabilized by TiO_2 plus partial reduction of some TiO_2 support species lead the board peak in TPR profile of Pt/TiO_2 catalyst.[9] Since reduction of Pt/TiO_2 performed at high temperature might result in strong metal-support interaction, which leads to loss of Pt active sites,[10] this catalyst has also been chosen to reduce at 603 K.

The XPS results for the oxidized and reduced catalysts are shown in Table A-3.2. The pre-reduced sample of Pt/Al_2O_3 shows a high fraction of metallic Pt after 603 K reduction, which together with the TPR and CO-chemisorption data described above indicate that 603 K is a suitable reduction temperature. For the titania-supported catalyst, Pt appears only partially reduced after 603K reduction. It must be taken into account that the residual Cl from Pt precursor (chloroplatinic acid hexahydrate) in both reduced samples probably generates some residual acidity, which is likely to participate in side reactions such as isomerization, cracking and transesterification during methyl octanoate reactions.

The temperature-programmed desorption of CO_2 was carried to quantify the amount of basic sites $1\%Pt/TiO_2$ catalysts. In fact, similarly to Hasegawa et al. observed, [11]figure A-3.2 shows higher quantity of basic sites (or corresponding amount of desorbed CO_2 in the temperature-programmed desorption experiments) on reduced $1\%Pt/TiO_2$ compared to calcined catalyst

Catalysts	Support surface area (m^2/g)	CO / Pt
1% Pt/Al_2O_3	220	0.9
1% Pt/TiO_2	50	-

Table A-3.1: CO-chemisorption and BET data of 1% Pt/Al_2O_3 and 1% Pt/TiO_2 catalysts

	Atomic Surface Concentration (%)					Atomic Ratios		
Sample	O (1s)	Al (2p)	Ti (3d)	Cl (2p)	Pt (4d)	Pt/Al	Pt/Ti	Cl/Pt
1%Pt/Al_2O_3 (oxidized)	66.6	31.6	0	1	0.9	0.03		1.1
1%Pt/Al_2O_3 (reduced)	68.2	30.5	0	0.8	0.6	0.02		1.3
1%Pt/TiO_2 (oxidized)	65.7	0	30.7	2	1.7		0.05	1.2
1%Pt/TiO_2 (reduced)	68.4	0	30.8	0.2	0.6		0.02	0.3

Table A-3.2: X-ray photoelectron spectra (XPS) data of 1% Pt/Al_2O_3 and 1% Pt/TiO_2 catalysts. The pre-reduced samples are reduced ex-situ in hydrogen at 603 K for 2 hours and then transferred into XPS equipment by ex-situ cell.

1.2. Catalytic activity of methyl octanoate on Pt/Al_2O_3 catalyst

1.2.1 Formation of C_7 and C_8 hydrocarbons

The conversion of methyl octanoate over 1%Pt/γ-Al_2O_3 catalyst in the vapor phase yields various products including hydrocarbons (C_7 and C_8 alkane and alkenes), other oxygenates (octanal, 1-octanol, octanoic acid), condensation products (diheptyl ketone, n-pentadecane and octyloctanoate), and light compounds (CO, CO_2, CH_4, CH_3OH, and H_2CO). If one would use these reactions as probe conversions of biodiesel into normal diesel, desirable products would be then the straight chain hydrocarbons. In the studies reported here, at a high H_2/HC ratio, saturated C_7 and C_8 hydrocarbons are the dominant hydrocarbon products. Only a small fraction of unsaturated hydrocarbons and trace amounts of aromatics were obtained.

Figure A-3.3 shows the distribution of products from conversion of methyl octanoate at a time-on stream of 1.0 h, excluding light gases, over a 1% Pt/Al_2O_3 catalyst under flow of hydrogen at various W/F. Almost no cracking products is observed for conversions up to 60%. At higher conversions, small fractions of light hydrocarbons are detected. C_7 hydrocarbons are the major product, while C_8 hydrocarbons and other oxygenates account for less than 10% of the products. From figure A-3.3, at low conversion (below 5%), the calculated selectivity to the C_8 hydrocarbon is negligible, while the combined octanal – octanol selectivity is around 10% and that to octanoic acid is close to 40%. At higher conversions, selectivity of octanal and 1-octanol drops with increasing selectivity of C_8 hydrocarbons.

Both C_7 and C_8 hydrocarbons are the dominant products of methyl octanoate conversion, so it is valuable to understand the reaction pathways that result in the

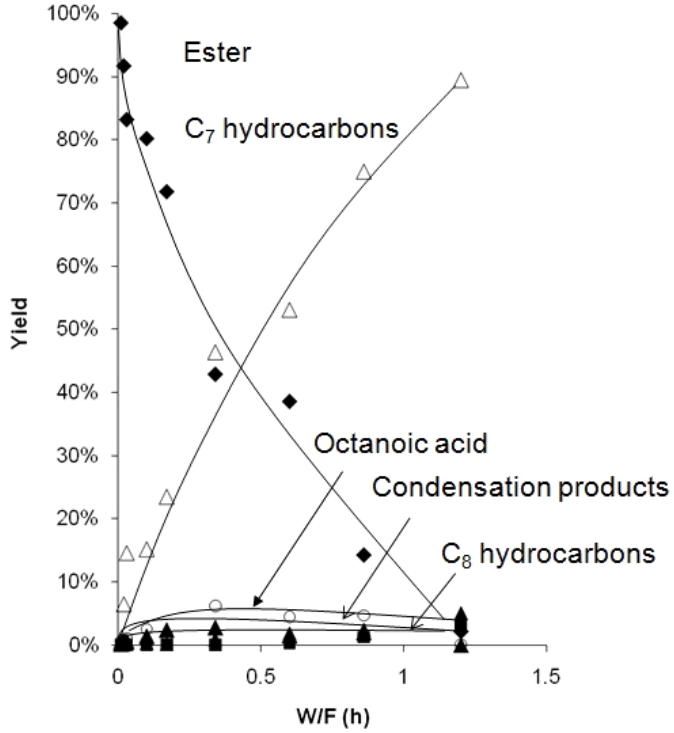

Figure A-3.3 : Product distributions of reaction of methyl octanoate on 1%Pt/Al_2O_3 at 603 K in hydrogen

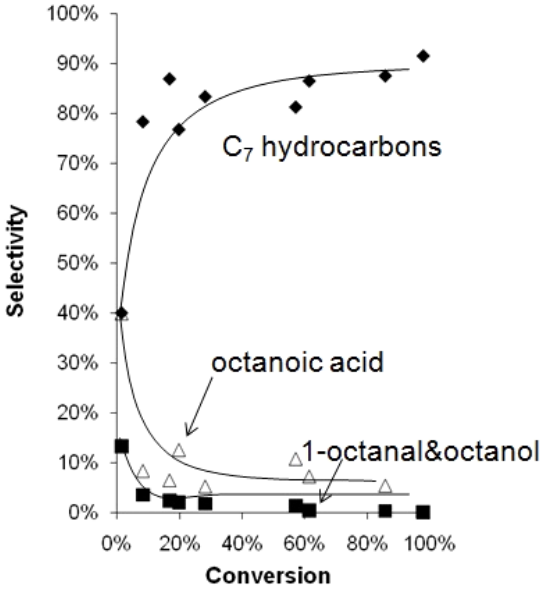

Figure A-3.4 : Selectivity of C_7 hydrocarbons, octanoic acid, and 1-octanal/octanol in the conversion of methyl octanoate over 1% Pt/Al_2O_3.

formation of these two hydrocarbon products, as well as the pathways leading to condensation (heavy) products which can deactivate the catalyst. The appearance of mostly C_7 hydrocarbons octanoic acid at low conversions (seen in figure A-3.4) suggests that C_7s can be produced by two parallel paths via decarboxylation and decarbonylation. That is, indirectly via octanoic acid and other oxygenates or directly from methyl octanoate. Both CO_2 (from decarboxylation) and CO (from decarbonylation) are also detected by online mass spectroscopy. The metal-catalyzed decarbonylation of one-oxygen-containing compounds such as aldehydes, alcohols and ketones to the corresponding hydrocarbons with one C less than the parent oxygenated feed is a well-known reaction.[12-13] Similar results were found by Murzin in the conversion of ethyl stearate (C_{18}) over Pd/C catalysts in presence of H_2, yielding mostly n-heptadecane.[2] As illustrated in the reaction scheme shown in figure A-3.5, 1-octanol and octanal are formed via hydrogenation/hydrogenolysis, while heavier oxygenates can be obtained by condensation reactions such as ketonization and transesterification of the ester molecules. These oxygenates can also contribute to the production of C_7 hydrocarbons via decarboxylation/decarbonylation. In contrast, C_8 hydrocarbons are not primary products, i.e., they are formed via a 2-step reaction. As depicted in figure A-3.5, C_8 hydrocarbons, which are the hydrogenated products in this case, are directly derived from C_8 aldehyde/alcohol, which originally are generated from either the methyl ester or the acid.

In a separate experiment, when we fed 1-octanal over 1% Pt/γ-Al_2O_3, we observed C_7 hydrocarbons as the main product, with much less C_8 hydrocarbons and 1-octanol. This result supports the concept that in the methyl octanoate conversion, primary products are octanoic acid and C_8 aldehyde/alcohol, which subsequently mainly convert

Figure A-3.5 : Proposed reaction pathways for conversion of methyl octanoate on supported Pt catalysts

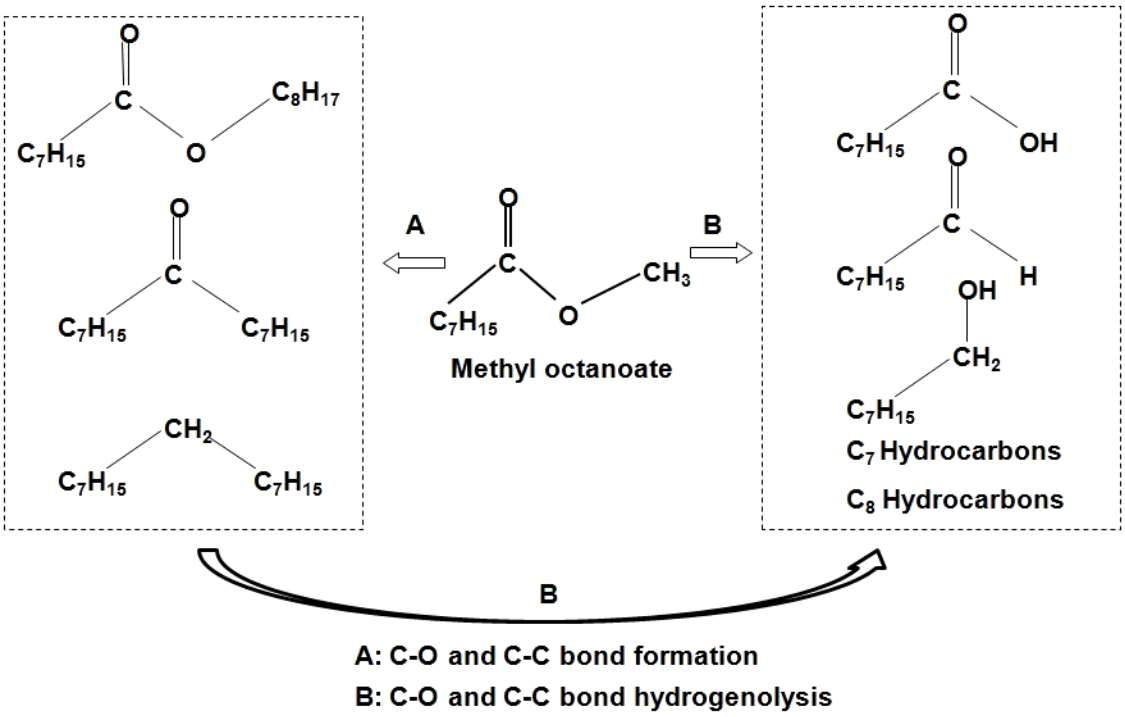

to C_7 hydrocarbons via decarbonylation and to a lesser extent to C_8 hydrocarbons via C-O hydrogenolysis. No C_6 or lower hydrocarbons (from demethylation of C_7) have been observed, which suggests that the alumina-supported Pt catalyst has negligible cracking activity.

In summary, these studies suggest that in the presence of hydrogen conversion of methyl octanoate to octanoic acid is dominant. Formation of C_7 hydrocarbons can stem from direct decarboxylation/decarbonylation of the ester, acid, aldehyde, and alcohol. At the same time, C_8 hydrocarbons come from direct C-O hydrogenolysis of the alcohol/aldehyde following hydrogenation of the ester and acid.

1.2.2 Formation of heavy products

Although decarboxylation and decarbonylation routes are dominant in the conversion of methyl octanoate in hydrogen, condensation of the ester molecules to heavy products such as diheptyl ketone, n-pentadecane, and octyloctanoate is also an important side reaction. According to Ponec et al.,[14] the symmetrical ketone is formed via the interaction of one carboxylate and one ketene carboxylate species on the oxide surface. A second observed heavy product in our experiments was octyloctanoate, which results from either esterification of octanoic acid with 1-octanol or transesterification of methyloctanoate with the alcohol. These two reactions can be catalyzed by Brönsted acid sites. [15]A third heavy product, n-pentadecane, is probably formed via C-O hydrogenolysis of the diheptyl ketone.

The ketonization reaction is only favored under a hydrogen-deficient environment. Therefore, when the oxides were reduced by the presence of spilled-over hydrogen from Pt (on Pt/TiO_2 catalyst), the ketone formation on TiO_2 was greatly suppressed by the

availability of hydrogen on reduced TiO_2 surface. Since none of the hydrogenated product of the ketone, a secondary alcohol, was detected, the heavy hydrocarbon is probably produced via C-O hydrogenolysis. Barteau et al. [16]also observed propane, the product from acetone, over Pd/CeO_2 and Co/CeO_2 catalysts. Although the presence of surface Cl, which may generate acid sites, is still detected on the reduced Pt/Al_2O_3 (as shown by XPS in Table A-3.2) the production of octyloctanoate remains low throughout the course of the reaction. The yields of undesirable heavy ketone and hydrocarbon are also suppressed by the presence of hydrogen.

1.3. Deactivation study

Figure A-3.6 displays the conversion of methyl octanoate over the Pt/Al_2O_3 catalyst as a function of time on stream, at a W/F of 0.6 h. It is seen that, in H_2 flow, the conversion drops from 61% to 42 % over 5-h on stream. The observed deactivation is due to site blocking by oligomerization of unsaturated hydrocarbons and heavy compounds (i.e. symmetrical ketone) that lead to coke. This deactivation is accelerated when no H_2 is used. The first conversion point under He gas is 40% compared to 61% for hydrogen. Moreover, at a TOS of 2 h, the conversion further drops to 15%. This dramatic drop in catalyst activity parallels the increase in unsaturated hydrocarbons and heavy substances observed in the product distribution. Instead of the C_7 and C_8 alkanes that dominate in the presence of excess H_2, alkenes become dominant in He. Interestingly, a large activity recovery is observed when the carrier gas is switched from He to H_2. At the same time, saturated hydrocarbons are again the dominant products and formation of heavy products is much inhibited.

1.4. Decarboxylation/decarbonylation versus hydrogenation reactions

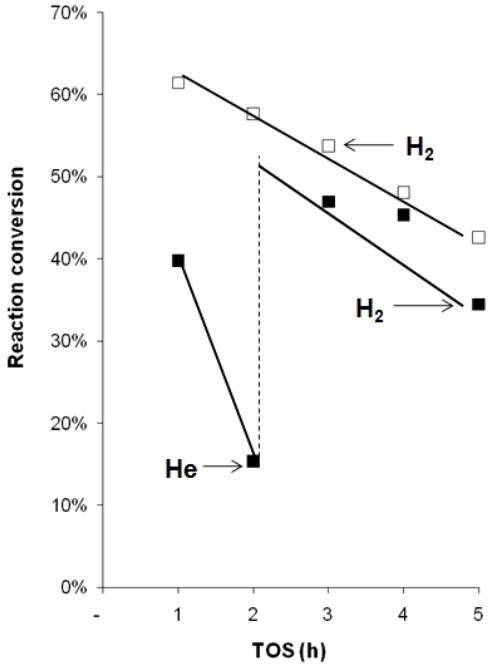

Figure A-3.6 : Conversions of methyl octanoate over 1% Pt/Al_2O_3 catalyst with and without hydrogen

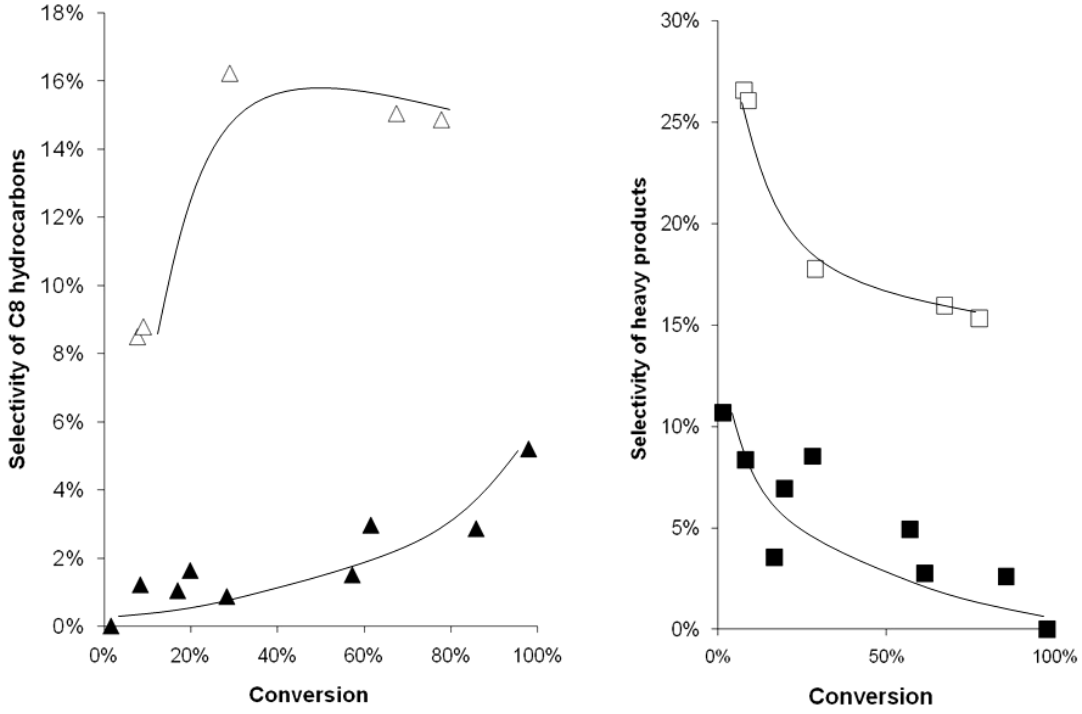

Figure A-3.7: Selectivity of C_8 hydrocarbons as varying methyl octanoate conversion for 1% Pt/Al_2O_3 (filled) and 1% Pt/TiO_2 (unfilled).

One of the characteristics of decarboxylation and decarbonylation is the loss of carbon via release of CO_2 and CO, respectively, which results in product with one C less than the feed. By contrast, catalysts that are active for C-O hydrogenolysis may reduce the carbon loss. In this case, we compare the conversion of methyl octanoate to C_8 hydrocarbons as opposed to C_7 hydrocarbons. In this sense, Pt supported on reducible oxide catalysts such as TiO_2 and $CeO\text{-}ZrO_2$ seems to be better candidates. Selectivity to C_8 hydrocarbons is significantly higher for Pt/TiO_2 than for Pt/Al_2O_3 as illustrated in figure A-3.7. This difference is due to a higher C-O cleavage activity, perhaps related to the higher reducibility of the titania support compared to alumina. It is well known that spilled-over hydrogen from Pt to titania helps reducing TiO_2 into TiO_x ($x<2$) at 603 K.[17] The large availability of Ti cations can enhance the adsorption of methyl octanoate via bond of an ester oxygen and a Ti cation. The activation of the C-O bond can occur through the so-called oxygen-vacancy mechanism.[18] Titania may appear attractive for enhancing the C-O cleavage reaction. In addition, both Pt/TiO_2 and $Pt/CeO\text{-}ZrO_2$ all have higher activity compared to that of Pt/Al_2O_3. With the same amount of catalyst, the yield toward C_7 hydrocarbons is higher on the former than on the latter. This is probably due to the participation of Ti and Ce/Zr cations in decarboxylation/decarbonylation reactions as similarly observed elsewhere.[14]

However, a drawback of titania-supported Pt catalyst is its high selectivity towards production of heavy products (i.e. symmetrical ketone and octyloctanoate) as shown in figure A-3.7. The formation of heavy ketone from carboxylic acids is reported to occur on basic sites.[19] Given the chlorine content of pre-reduced TiO_2 and Al_2O_3 from the XPS data in Table A-3.2, one could predict that the density of acid sites for

transesterification reaction of methyl octanoate would be higher on Al_2O_3 than on TiO_2. Higher acidity would lead to higher production of octyloctanoate from alumina catalyst. However, the contribution of the formation of symmetrical ketone on TiO_2 dominates, as seen in the heavy product distribution. Although the spilled-over hydrogen from Pt helps limiting ketone formation, methyl octanoate molecules adsorb preferably on reduced TiO_2 surface than on the more refractory Al_2O_3 surface.

As observed before, Pt on alumina is active for decarboxylation/decarbonylation of methyl octanoate since Pt is an effective metal that catalyzes C-C bond cleavage. On 1%Pt/TiO_2, this reaction pathway is still dominant; however; the hydrogenation pathway is greatly enhanced by the hydrogenation activity of reduced TiO_2 support. This hydrogenation activity is resulted from high affinity to break C-O bond via oxygen vacancies on reduced TiO_2. Besides reducible oxides, there are also other metals that are selectively active for hydrogenation reaction. One of them is copper. Copper chromite and supported copper catalysts are widely used to produce alcohols from fatty acids and fatty acid alkyl esters.[20 -21]It has been observed that 10%Cu/SiO_2 is an effective catalyst for conversion of methyl octanoate in hydrogen. Table A-3.3 shows the effect of hydrogen partial pressure on the catalyst activity and product distribution. It is clearly seen that the catalyst is much more active at high hydrogen partial pressure. The reaction temperature required to achieve similar conversion (around 50%) is much lower at 3.4 MPa than that at 0.1 MPa. Additionally, the amount of catalyst at the former pressure is much less. It is of interest to analyze the changes in decarboxylation/decarbonylation products (C_7s), hydrogenation products (C_8s), and condensation compounds as one varies the operating pressure. At atmospheric pressure, C_8 oxygenates (octanal and octanol) and

10% Cu/SiO_2 at W/F =0.45 h		
Compounds	**P = 101 kPa and T = 673 K**	**P = 3.4 M Pa and T = 588 K**
C_7 hydrocarbons	2.4%	14.7%
C_8 hydrocarbons	3.2%	7.9%
C_8 oxygenates	17.7%	32.8%
Methyl octanoate	56.4%	42.8%
Octanoic acid	4.4%	1.8%
Heavy product + Ketones	15.9%	0.0%
Conversion	**43.6%**	**57.2%**

Table A-3.3: Product distribution of 10% Cu/SiO_2 catalysts at different operating conditions in the reactions of methyl octanoate

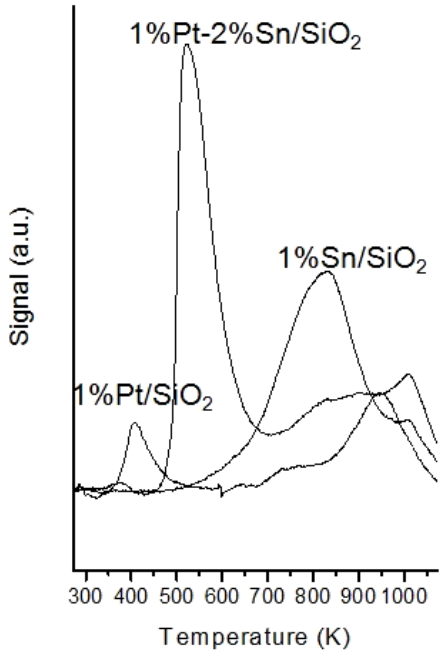

Figure A-3.8 : Temperature-programmed reduction profiles of supported Pt-Sn catalysts

condensation products are dominant. Meanwhile, C_8 oxygenates and hydrocarbons are populated at 3.4 MPa. Copper catalyst is active for C-O bond rupture; therefore; methyl octanoate reacts with hydrogen to form one-oxygen-containing oxygenates after one C-O bond cleavage and C_8 hydrocarbons after the second C-O bond rupture. Although one-oxygen-containing compounds are dominant products in both cases, the secondary conversion of these oxygenates into C_8 hydrocarbons is observed greater at elevated pressure. This is due to the higher hydrogen availability on the surface for the secondary hydrogenation reaction. In contrast, less hydrogen available at atmospheric pressure leading to higher coverage of ester on the surface or higher selectivity of condensation products, which derive from coupling of two esters molecules. Since copper selectively breaks C-O bonds; therefore; the decarboxylation/decarbonylation activity, which results from C-C bond cleavage or the selectivity of C_7 hydrocarbons is less dominant compared to hydrogenation to C_8 hydrocarbons. However, at the elevated pressure, the decarboxylation/decarbonylation activity is also enhanced. It could be possible that the condensation reactions are suppressed at higher hydrogen partial pressures, leading to higher selectivities toward both hydrogenation and decarboxylation/decarbonylation.

2. Reactions of Methyl Octanoate on Supported Pt-Sn Catalysts: Maximizing α-Alkene Selectivity

2.1 Catalyst characterization

Figure A-3.8 shows the temperature-programmed reduction of silica-supported Pt-Sn catalyst series. 1% Pt/SiO_2 is reduced at relatively low temperature ranging from 373 K to 473 K. The high-temperature peak in Pt/SiO_2 profile might be contributed to the

decomposition of remaining precursors left after the calcination step. On the other hand, 1%Sn/SiO_2 requires higher reduction temperature from 573 K to 1073 K. TPR profile of the bimetallic 1%Pt-2%Sn/SiO_2 contains a sharp peak at 473 K to 673 K. This peak, which corresponds to the reduction temperature of the Pt-Sn alloy phase, is positioned in between Pt and Sn reduction peaks. This catalyst has none or very little free Pt phase since there is no visible reduction peak around 373 K to 473 K. However, a portion of free Sn is observed through a board peak at high reduction temperature. For this catalyst, most of the Pt participates in the Pt-Sn alloy; however; the alloy only composes of a fraction of Sn.

2.2 Reaction of methyl octanoate on Pt-Sn catalysts

2.2.1 Reaction on alumina-supported Pt catalyst

1%Pt/Al_2O_3 is proven to be effective in reaction of methyl octanoate in both hydrogen and helium. The major products in both cases are decarboxylated/decarbonylated products: C_7 hydrocarbons. Under the inert gas flow, the catalyst deactivates faster and the hydrocarbon products are mostly alkenes instead of alkanes as in the case of hydrogen flow. Therefore, in order to maximize the selectivity of α-alkene products, inert gas is preferred over hydrogen. When inert gas is used as a carrier gas, α-heptene is formed prior to heptane and other heptene isomers since the ester functional group is located at α-position of the C_7 carbon chain. Once α-heptene is produced, it is quickly either hydrogenated to form n-heptane or undergone through double-bond isomerization reaction to internal heptenes. The secondary reaction of α-heptene is limited at elevated temperatures since hydrogenation and α-to-internal double-bond isomerization reactions are thermodynamically less favored. In order to evaluate

performance of each catalyst toward maximizing α-alkene selectivity, the percentage of α-heptene to sum of n-heptane and internal heptenes is a useful tool. Figure A-3.9 shows the above percentage as a function of time on stream or conversion for one particular 1%Pt/Al_2O_3 reaction at 623 K. As the catalyst deactivates or coke was piling up on the catalyst surface, the ratio increases from 11 % to 70%. It is the coverage of coke on active Pt sites that boosts up the selectivity of α-heptene. In another word, when Pt particles get smaller either by coking or catalyst modification, the selectivity toward the desired product is enhanced. This result prompts next step in catalyst design: modifying Pt with added Sn. In fact, Dumesic et. al. and other researchers have reported the significant stability and selectivity improvement in isobutane dehydrogenation reactions by adding Sn into Pt catalysts.[22-23]

2.2.2 Reaction on silica-supported Pt-Sn catalysts

Table A-3.4 exhibits the selectivity of 1-heptene for different Pt catalysts. Together with the activity, figure A-3.10 visualizes three different gas chromatograms of C_7 products for three tested catalysts. The relative intensity of α-heptene peak increases as the catalyst is changed from 1%Pt/Al_2O_3 to 1%Pt-1%Sn/SiO_2 and finally to 1%Pt-2%Sn/SiO_2. The conversion level for three tested catalysts is low since at higher conversion or longer catalyst bed, more active sites are available for secondary reactions. At relatively similar conversions, the selectivity of 1-heptene is enhanced by adding 1% Sn and further with 2% Sn into Pt. This improvement might be originated from two contributing effects: geometric and electronic. Addition of Sn into Pt helps to dilute Pt ensembles so that less isomerization reactions take place. The more Sn is added, the smaller Pt ensembles are. Electronically, modification of Sn onto Pt will lead to lower the

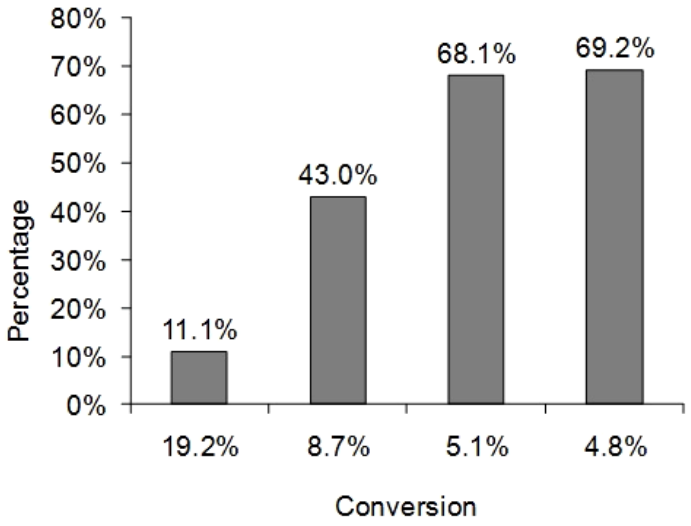

Figure A-3.9: Selectivity of 1-heptene over all C_7 hydrocarbons in reactions of methyl octanoate over 1% Pt/Al_2O_3 catalyst at 623K, 3.4 M Pa, and W/F = 0.03h

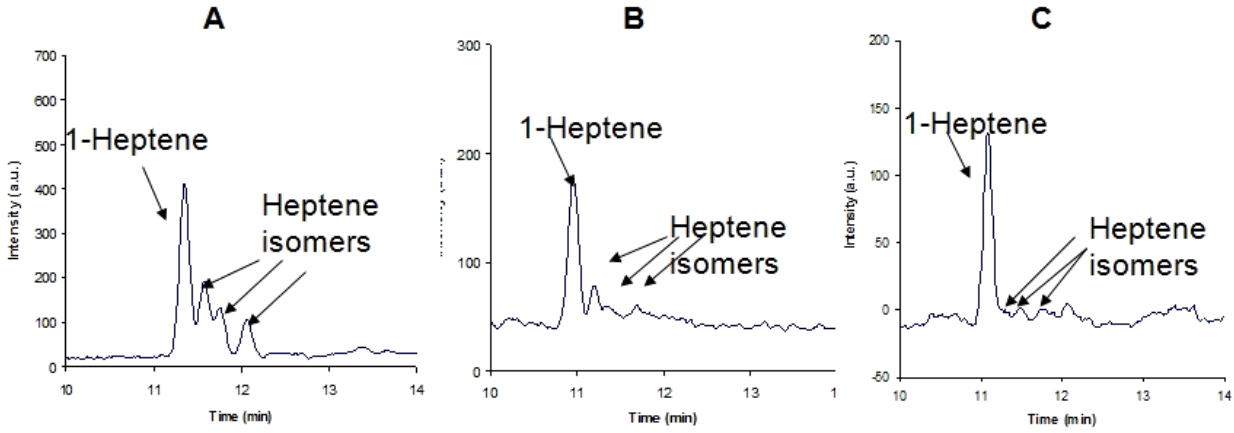

Figure A-3.10: Chromatogram of C_7 hydrocarbons in the reaction of methyl octanoate over different catalysts: 1%Pt/Al_2O_3 (A), 1%Pt-1%Sn/SiO_2 (B), and 1%Pt-2%Sn/SiO_2 (C)

T = 623 K, P = 3.4 M Pa, He/O_x = 40			
Catalysts	Conversion	Overall selectivity of 1-heptene	Selectivity of 1-heptene over all C_7
1%Pt/Al_2O_3	7.8 %	31.5 %	55.6 %
1%Pt-1% Sn/SiO_2	3.6 %	26.2 %	74.4 %
1%Pt-2% Sn/SiO_2	6.9 %	23.1 %	87.6 %

Table A-3.4: Selectivity of 1-heptene over supported Pt and Pt-Sn catalysts in the reaction of methyl octanoate

Catalysts	**Pt/SAPO-34**	**Pt/Amorphous Silica-alumia**	**Pt/SAPO-11**	**Pt/Al_2O_3>>Pt/SAPO-11 (two beds)**
Gas	10% H_2 in Argon	10% H_2 in Argon	10% H_2 in Argon	10% H_2 in Argon
W/F (h)	0.17	0.17	0.13	0.57>>0.34
T of reduction/reaction (K)	588	588	588	588>> 571
Pressure (M Pa)	3.4	3.4	3.4	3.4
		YIELD (%)		
Cracking	4.2%	0.0%	0.0%	0.0%
Methyl hexanes/hexenes	2.0%	0.4%	0.8%	0.0%
Heptanes/Heptenes	78.0%	70.4%	81.2%	82.0%
Methyl heptanes/heptenes	1.0%	0.0%	0.6%	0.0%
Octanes/octenes	5.2%	5.7%	3.2%	2.2%
Unknown(aromatics + light esters)	0.8%	0.0%	0.0%	0.0%
Octanal+Octanol	0.2%	1.0%	0.8%	0.7%
Methyl octanoate	7.8%	21.9%	12.0%	14.2%
Octanoic acid	0.3%	0.0%	0.0%	0.4%
Heavy products	0.5%	0.5%	1.2%	0.5%
Conversion	**92.2%**	**78.1%**	**88.0%**	**85.8%**
Isomerization yield	**3.0%**	**0.4%**	**1.4%**	**0.0%**

Table A-3.5: Product distribution of reactions of methyl octanoate over different zeolite-supported Pt catalysts (loading of Pt is 1%)

adsorption strength of the dehydrogenated compounds, resulting in quicker desorption of the produced α-heptene or less isomerization. In the next chapter, a detailed analysis of effects of adding Sn and K on the stability and selectivity will be presented.

3. Reaction of Methyl Octanoate on Bifunctional Pt/Zeolite Catalysts: Optimizing the Production of Branched Alkenes

Previously, all supported Pt catalysts (i.e. Pt/Al_2O_3, Pt/TiO_2 and $Pt\text{-}Sn/SiO_2$) are shown to be effective in deoxygenating methyl octanoate into C_7 and C_8 hydrocarbons. In fact, almost all of the deoxygenated hydrocarbons are linear since the isomerization activity on Pt here is highly limited. Although Pt is known for its ability to isomerizes hydrocarbons, the oxygenate species are populated on Pt surfaces, leading to strictly limited active sites for isomerization of hydrocarbon products. In order to make hydrocarbons, which are fungible and can serve as fuel compounds, some level of branching is required. This prompts for the use of bifunctional Pt/zeolite catalysts, in which Pt will deoxygenate the methyl ester and zeolites will isomerizes the linear hydrocarbons. This concept is illustrated in the proposed reaction scheme in figure A-3.11. As mention in the preceding section, Pt supported on SAPO-34 and SAPO-11 shows high activity and selectivity for the isomerization of linear saturated alkanes (i.e. C_{12}).[24-26] The role of Pt here is to dehydrogenate the saturated alkanes, which will then be protonated and isomerized by zeolite acid sites. Due to the specific structure of these two zeolites, the isomerization reactions of these long alkanes occur at the pore mouths. Other researchers also reported the high activity of Pt supported on amorphous silica-alumina and $W\text{-}ZrO_2$ in dodecane isomerization reactions.[27] For these reactions, the activity of

these catalysts in the reaction of methyl octanoate will be analyzed in this work. The results will be compared with that of 1%Pt/HY zeolite.

Tables A-3.5 and A-3.6 display the overall activity and isomerization activity of the above catalysts. The isomerization activity is the sum of yields of branched C_7 and C_8 hydrocarbons. Compared at the same W/F, 1%Pt/SAPO-34 is the most active catalyst. Although high deoxygenation activity (selectivity >80%) is observed with all Pt/zeolite catalysts, the isomerization selectivity remains quite low. This selectivity also increases with the ester conversion. It could be explained that the coverage of unreacted ester and other oxygenate species, in fact, impairs the isomerization activity of these catalysts. The oxygenate species might adsorb stronger on the surface compared to the hydrocarbon products. This prompts the idea of two-bed configurations, in which the complete deoxygenation of ester takes place over 1%Pt/Al_2O_3 catalyst and isomerization occurs on 1%Pt/SAPO-11 catalyst. However, there is still remaining unreacted ester from the first bed and the temperature in the second bed (around 571K) is a bit low, leading to negligible isomerization activity.

Among all tested catalysts, 1%Pt/21%W-ZrO_2 catalyst is the most selective toward isomerization. At the conversion of 78%, the isomerization yield is computed as 10%. On this catalyst, the hydrogenolysis activity of ester dominates the decarboxylation/decarbonylation activity, which is reflected by 60% selectivity of C_8 hydrocarbons. However, the former is reduced significantly with lower hydrogen partial pressure. Similarly to what is observed on 1%Pt/TiO_2 catalyst, under hydrogen flow, the partially reduced support W-ZrO_2 might participate in the hydrogenolysis/hydrogenation reactions to produce C_8 compounds since the level of reduction is strongly depends on the

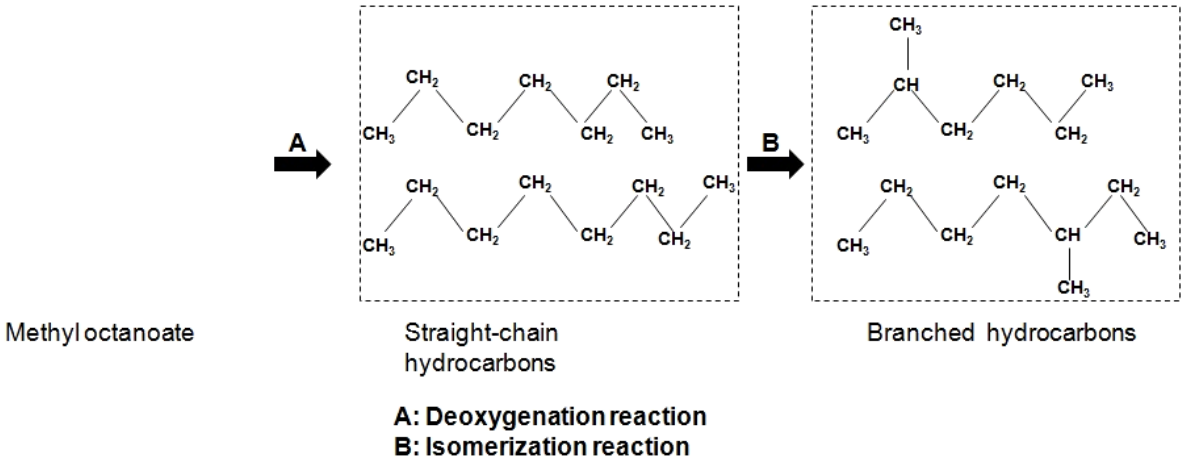

Figure A-3.11: Reaction scheme of methyl octanote to form branched hydrocarbons

1%Pt / 21% W on ZrO_2 catalyst $T_{reduction} = T_{reaction}$ = 623 K, W/F = 0.15 h, P = 3.4 MPa, Reaction in H_2		
Compounds	**H_2**	**5%H_2 in He**
Cracking	6.1%	0.4%
Methyl hexanes	1.7%	0.2%
Heptane	15.4%	38.1%
Methyl heptanes	8.4%	0.2%
Octanes	39.0%	14.7%
Aromatics	3.3%	0.7%
C_8 oxygenates	0.4%	0.5%
Methyloctanoate	21.8%	44.7%
Octanoic acid	3.6%	0.3%
Heavy product + Ketone	0.2%	0.2%
Conversion	**78.2%**	**55.3%**

Table A-3.6: Product distribution of reactions of methyl octanoate over 1%Pt on 21%W/ZrO_2 catalyst

Catalysts	**1% Pt/HY (Si/Al =15)**	**1% Pt/HY (Si/Al =15)**
Gas	10% H_2 in Argon	H_2
W/F (h)	0.34	0.34
T of reduction/reaction (K)	588	588
Pressure (M Pa)	3.4	3.4
YIELD (%)		
Cracking (hydrocarbons)	3.1%	17.9%
Methyl hexanes/hexenes	1.9%	4.5%
Heptanes/Heptenes	51.9%	33.3%
Methyl heptanes/heptenes	2.1%	8.1%
Octanes/octenes	8.9%	32.4%
Unknown(aromatics + light esters)	1.8%	3.1%
Octanal+Octanol	0.7%	0.6%
Methyl octanoate	28.6%	0.0%
Octanoic acid	0.5%	0.0%
Heavy products	0.5%	0.0%
Conversion	**71.4%**	**100.0%**
Isomerization yield	**4.0%**	**12.6%**

Table A-3.7: Product distribution of reactions of methyl octanoate over 1%Pt on HY

concentration of fed hydrogen. In addition, the high isomerization selectivity of W-ZrO_2 catalyst comes from the strong acid sites on the support, which is able to catalyze isomerization reaction of C_8 hydrocarbons.

The last tested catalyst is 1%Pt/HY (Si/Al =15) catalyst. At conversion of 70%, this catalyst shows less than 10% isomerization selectivity. However, at 100%, the isomerization activity is tripled. It could be possible that when the surface is free of unreacted ester and other oxygenates (100% conversion), the coverage of hydrocarbons is enhanced, corresponding to higher isomerization activity. The drawback of this catalyst is excessive cracking due to greater amount of acid density.

From these results, two possible reactor configurations were proposed to maximize the productions of branched alkenes from methyl octanoate feed. Both options include two reactors in series. The first option involves deoxygenation plus isomerization in the first reactor and dehydrogenation in the second reactor. Platinum supported on zeolite or acidic supports could be used as the catalyst for dual task in the first reactor. Bimetallic Pt-Sn on silica is the dehydrogenation catalyst. In order to dehydrogenate the alkanes, the second temperature needs to be high and in turn less hydrogen is required. The second set-up includes deoxygenation plus dehydrogenation in the first reactor. Isomerization activity will be accomplished in the next one. Here either bimetallic Pt-Sn on silica or Cu-based catalysts could be used in the first reactor. Isomerization reactors will occur on bi-functional Pt on zeolite catalysts. Both reactors requires high operating temperatures, however, the first one needs less hydrogen than the second one.

4. Conclusion

The reaction of methyl octanoate serves as a model reaction to produce valuable chemicals and fuel components from renewable methyl esters. The specifically targeted chemicals are alpha alkenes and fuel compounds are branched alkenes. In this section, catalyst and operating condition selections will be chosen to maximize the productions of these above components. It is shown that 1%Pt/Al_2O_3 catalyst is an active and selective catalyst for conversion of methyl octanoate in flow of hydrogen. The dominant products, C_7 hydrocarbons, result from decarboxylation and decarbonylation of various oxygenates including the original ester, the produced carboxylic acid, 1-oxygen containing compounds (1-octanol/octanal), and condensation products. However, one major drawback of this catalyst is quick deactivation in helium atmosphere. When titanium replaces alumina, hydrogenation activity of methyl octanoate, together with C_8 product formations, is enhanced although decarboxylation/decarbonylation reaction is still dominant. Further enhancement in hydrogenation activity is observed when copper is used instead of platinum. 10% Cu/SiO_2 is less active than Pt catalyst in the reaction of methyl octanoate; therefore; the former requires higher reaction temperature and total pressure.

To improve the coke tolerance of Pt catalyst, Sn is added. The bimetallic Pt-Sn not only shows slower catalyst deactivation but also exhibits higher selectivity toward alpha alkenes. In details, an inert atmosphere is preferred over hydrogen in maximizing the selectivity of α-alkene products since the hydrogenation reaction of alkenes occurs fast with hydrogen. On 1%Pt/Al_2O_3 catalyst, high selectivity of 1-heptene is achieved with low methyl octanoate conversion and with deactivated catalyst since secondary

hydrogenation and double-bond isomerization reactions are restricted. Sn-added Pt catalyst and deactivated Pt/Al_2O_3 catalyst share the common effect. That is the rupture of Pt ensembles leading to less isomerization. Therefore, the more Sn is doped, the higher fraction of 1-heptene in entire C_7 hydrocarbons is accomplished.

In fact, adding Sn into pure Pt catalyst not only does not impair the high deoxygenation activity of the Pt catalyst but also makes this catalyst more tolerant to coking. The same fashion is observed with doping Pt on acidic supports. The bi-functional Pt/zeolite catalysts still show high deoxygenation activity of methyl octanoate. Besides, isomerization reactions, an important side reaction to produce fungible fuel compounds, occur on acid function of the supports. Among all the tested bi-functional catalysts, 1%Pt/ 21%W-ZrO_2 catalyst shows highest isomerization selectivity under hydrogen flow. This catalyst is also selective for hydrogenolysis of methyl octanoate to form C_8 hydrocarbons. Significant isomerization activity is observed on 1%Pt/HY, however, this catalyst is prone to cracking due to its high acid density.

5. References

[1] Maier, W.F., Roth, W., Thies, I., and Schleyer, P.v.R. , *Chem. Ber.* **115**, 808 (1982)

[2] Kubickova, I., Snare, M., Eranen, K., Maki-Arvela, P., and Murzin, D.Y.., *Catal. Today* **106**, 197 (2005)

[3] Snare, M., Kubickova, I., Maeki-Arvela, P., Eraenen, K., and Murzin, D.Y., *Ind. Eng. Chem. Res.* **45**, 5708 (2006)

[4] Maeki-Arvela, P., Kubickova, I., Snre, M., Eraenen, K., and Murzin, D.Y.., *Energy & Fuels* **21**, 30 (2007)

[5] Snare, M., Kubickova, I., Maki-Arvela, P., Eranen, K., and Murzin, D.Y., *Chem. Ind.* **115**, 415 (2005)

[6] Snare, M., Kubickova, I.,Maeki-Arvela, P., Eraenen, K., Waerna, J., and Murzin, D. Yu., *Chem.Eng. J.* **134**, 29 (2007)

[7] Houtman, C., and Barteau, A., *Surf. Sci.* **248**, 57 (1991)

[8] De Miguel, S. R., Román-Martınez, M. C., Cazorla-Amorós, D., Jablonski, E. L., and Scelza, O. A., *Catal. Today* **66,** 289 (2001)

[9] Huizinga, T., Van Grondelle, J., and Prins, R., *Appl. Catal.* **10**, 199 (1984)

[10] Haller, G. L., and Resasco D. E., *Advances in Catalysis* **36**, 173 (1989)

[11] Hasegawa, *J. Catal.* 127, 221 (1991)

[12] McCabe, R. W., DiMaggio, C. L., and Madix, R.J. *J. Phys. Chem.* **89**, 854 (1985)

[13] Davis, J. L., and Barteau, M. A. *J. Am. Chem. Soc*. **111**, 1782 (1989)

[14] Pestman, R., Koster, R. M., Duijne, A. V., Pieterse, J. A. Z. , and Ponec, V. *J. Catal.* **168**, 265 (1997)

[15] López, D. E., Suwannakarn, K., Bruce, D.A., and Goodwin Jr, J. G. *J. Catal.* **247**, 43 (2007)

[16] Idriss, H., Diagne, C., Hindermann, J. P., Kiennemann, A. , and Barteau, M. A. *J. Catal.* **155** (1995)

[17] Huizinga, T., and Prins, R., *J. Phys. Chem*. **85**, 2156 (1981)

[18] Barteau, M. A., *J. Vac. Sci. Technol. A* **11**, 2162 (1993)

[19] Gaertner, C.A., Serrano-Ruiz, J. C., Braden, D. J., and Dumesic J. A., *J. Catal.* **266** 71 (2009)

[20] Aring, H., Burch, K.., Franke, P., Honetzke, G., Tietz, W., Weidemann, R. DD Patent 213430, 1984

[21] Bradley, M. W., Harris, N., Turner, K. US Patent 258733, 1981

[22] Cortright, R. D., and Dumesic, J. A., *Appl. Catal. A* **129**, 101 (1995)

[23] Cortright, R.D., and Dumesic, J. A., *J. Catal.* **148**, 771 (1994)

[24] Meriaudeau, P., Tuan, V.A., Nghiem, V.T., Lai, S.Y., Hung, L.N., and Naccache, C. *J. Catal.* **169**, 5 (1997)

[25] Sinha, A.K., Sivasanker, S., and Ratnasamy, P. *Ind. Eng. Chem. Res*. **37**, 2208 (1998)

[26] Liu, Y., Liu, C., Tian, Z., and Lin, L. *Energy Fuels* **18**, 1266 (2004)

[27] Martínez, A., Prieto, G., Arribas, M.A., and Concepción, P. *Appl. Catal. A: Gen.* **309,** 224 (2006)

CHAPTER IV: REACTIONS OF METHYL HEXANOATE

1. Introduction

As fossil fuels are becoming less abundant, and the need for green house gas neutral fuels has been accepted, tremendous attention has turned into maximizing the use of renewable energy resources such as biomass, vegetable oils, animal fat, and algae. Although those sustainable materials compose of variety of structural building blocks at different compositions, alkyl esters, along with others such as furans, phenols, aldehydes/alcohols, carboxylic acids, appear as commonly derived components from those blocks.[1] Although the reactions of alkyl esters draw considerable research attention today, for many years in the past, researchers have excessively examined the reaction chemistry of other oxygen-containing functional groups such as carboxylic acid, ketones, aldehyde and alcohol.[2-18] For instance, the reactions of carboxylic acids on single crystals and supported catalysts have been well-characterized. The typical reactions for carboxylic acids involve hydrogenation/hydrogenolysis, decarboxylation/decarbonylation, and ketonization. The studies have shown that noble metals (i.e. Pd), [7] transitional metals (i.e. Cu),[9] and reducible oxides (i.e. TiO_2)[10] are all active for hydrogenating the acids to corresponding alcohols/aldehydes. Both noble metals and transition metals are able to catalyze decaboxylation/decarbonylation of carboxylic acids; however, the former is more active.[17] While two above reactions only require the presence of one acid molecule, ketonization reaction necessitates the participation of two acid molecules.[14-16] The formation of a longer ketone has been observed over a variety of metal oxides: both reducible (i.e. TiO_2, SnO_2) and non-reducible (i.e.K_2O, MgO).

Together with the increasing demand of sustainable energy resources nowadays, alkyl esters, as derived products from renewable vegetable oils, are becoming subjects to exclusive studies. Since alkyl esters still maintain similar functional group (-COO-), they also undergo three typical reaction pathways as carboxylic acids do. [19-24] Although all used catalysts target the same –COO- group, it is clearly seen that the product distributions vary with different catalyst functions. In the previous section, it has been shown that supported Pt catalysts are active for the reactions of methyl octanoate and methyl stearate under hydrogen-rich condition. [25] Also, changes in supports strongly affect the catalyst activities, reaction pathways, and consequently the product distributions. 1%Pt/TiO_2 catalyst is more active than 1%Pt/Al_2O_3 since the titanium oxide, which is partially reduced under reaction conditions, is capable of hydrodeoxygenating the esters via oxygen-vacancy mechanism. However, 1%Pt/Al_2O_3 catalyst is more selective toward decarboxylation/decarbonylation reactions than 1%Pt/TiO_2 catalyst. Another important finding was observed with the changes in hydrogen concentration. When inert carrier gas replaced hydrogen, the activity and selectivity of two catalysts were immediately impaired. This is probably due to the formation of condensates or cokes, which are suppressed under the reactions with hydrogen. These species inhibit the activity of Pt catalysts.

In the effort of seeking for the catalysts that are more resistant to coking, bimetallic Pt-Sn catalysts turn out as promising candidates. Silica supported Pt-Sn catalyst is a well-studied catalyst for dehydrogenation of short alkanes.[26-29] In fact, tin interacts with Pt to form Pt-Sn alloy particles.[30-31] Dumesic et al. has found that this formation inhibits the formation of highly dehydrogenated species, or coke precursors,

during isobutene dehydrogenation reactions.[26] The addition of a third metal, potassium, into Pt-Sn is primarily to neutralize the acid sites of alumina support and inhibit the hydrocarbon cracking on the support.[32] Dumesic showed that addition of potassium helps to improve the selectivity of Pt-Sn/SiO_2 catalyst as well.[27] There are two interesting things about these combination Pt-Sn-K catalysts. They not only show high resistance to coking but also possess two functions that are active for converting the methyl esters: metal function (i.e. Pt, Pt-Sn), and oxide function (i.e. SnO_x, K_2O). Therefore, in this work, a range of silica-supported Pt-Sn-K catalysts have been tested in the reaction of a model methyl ester compound, methyl hexanoate, under hydrogen-deficient conditions. It was found that the additions of Sn and K have several strong impacts on the catalyst performances. One hand, stability of the pure Pt catalyst without hydrogen is significantly improved. On the other hand, Sn and K-related species are proven to facilitate the conversion of methyl hexanoate. Various characterization techniques have shown that interactions among three metals are key elements to the better performances of Pt-Sn-K catalysts. In fact, Sn was believed to interact with both Pt and K. In agreement with other studies, it is the formation of Pt-Sn alloys that leads to the increasing coke tolerance of the pure Pt catalyst. Beside the activities of pure Pt and Pt-Sn alloys in decarboxylation/decarbonylation reactions of the ester, Sn-associated K species were found to convert the original feed into intermediate products, which are eventually transformed into final hydrocarbon products by either pure Pt or Pt-Sn alloys.

2. **Catalyst Characterization Analysis**

2.1 Carbon monoxide chemisorptions and BET surface areas

Table A-4.1 shows the calculated ratio of adsorbed CO/Pt for series of Pt-Sn-K catalysts. It is clearly seen that Pt/SiO_2, with 30% dispersion, has the most available Pt sites for carbon monoxide to adsorb. Additions of Sn and K all reduce the CO/Pt ratio and catalyst BET surface areas. The above trend of CO/metal is also in the same line with reduced carbon monoxide coverage reported by Dumesic et al. when adding Sn and K into Pt/SiO_2 and Pt/KL catalysts.[27,33] The dispersion drops might be originated from the coverage of Sn and K over Pt surfaces and the formation of Pt-Sn alloys. Since the Pt-Sn alloy does not adsorb carbon monoxide, which has been clearly pointed out in the previous paper by Resasco et al., CO only adsorbs on monometallic Pt sites.[34] Verbeek and Sachlter have shown that the extents of adsorption for carbon monoxide decrease on Pt-Sn alloy particles with increasing tin content.[35] Besides the Pt present in the alloys, some other part of Pt surfaces are covered by both Sn and K, therefore; the Pt active sites available for CO adsorption are reduced, leading to lower CO/Pt ratio. This is consistent with the decreases in BET surface areas. The additions of Sn and K not only cover support surfaces but also block some pores of silica, causing a huge surface area drop in the case of 1%Pt-1.3%Sn-1.5%K/SiO_2 catalyst.

2.2 Temperature-programmed reduction (TPR)

TPR profiles of different silica-supported catalysts are displayed in figure A-4.1. The fact that PtO_x is reduced in a broad range of temperature (from 373 K to 523 K) indicates a wide distribution of Pt particle sizes. The various particle sizes might come from the weak interaction of Pt with inert silica gel support. Two very small peaks at higher temperatures might be due to the decomposition of precursor residual left on the

Catalysts	CO/Pt	BET surface area (m^2/g)
SiO_2	N/A	500
1%Pt/SiO_2	0.30	450
1%Pt-1.3%Sn/SiO_2	< 0.05	440
1%Pt-0.5%K/SiO_2	0.10	440
1.3%Sn-0.5%K/SiO_2	< 0.05	430
1%Pt-1.3%Sn-0.5%K/SiO_2	< 0.05	450
1%Pt-1.3%Sn-1.5%K/SiO_2	< 0.05	300

Table A-4.1: Carbon mono-oxide chemisorption data and BET surface areas of different silica-supported Pt-Sn-K catalysts. Pt loadings are 1 wt% for all catalysts.

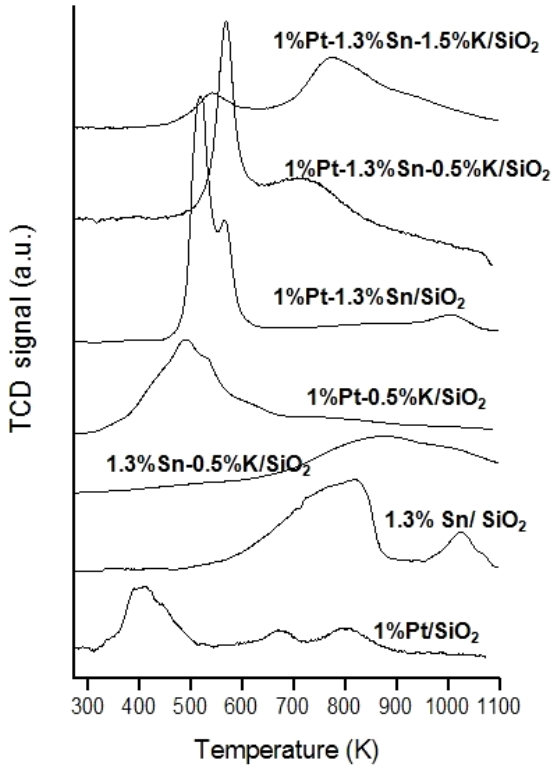

Figure A-4.1: Temperature-programmed reduction profiles of different silica-supported Pt-Sn-K catalysts

sample after calcination step. In the mean time, Sn oxide on silica gets reduced at relatively high temperature ranging from 673 K to 873 K. Although potassium oxidation stage does not change at all during the reduction period, the addition of K onto both Pt and Sn has broadened the reduction peaks in profiles of 1%Pt-0.5%K/SiO_2 and 1.3%Sn-0.5%K/SiO_2 catalysts, respectively. This might indicate the interactions between Sn and Pt species with oxygen atom from K oxide, which could consequently require higher temperatures to reduce both Sn and Pt.

When Pt and Sn are co-impregnated with molar ratio of 1:2, different peaks appear. Similarly to what has been reported in the literature, these peaks correspond to different alloy compositions of Pt-Sn.[36] Since the bimetallic Pt-Sn phases containing both Pt and Sn, the reduction temperatures of those phases are in between these of monometallic Pt and Sn. Phase separation is observed when potassium is added as a third component incorporated into Pt-Sn catalysts. While no free-Pt peaks appear, some of Sn gets segregated out of the alloy to form a separate Sn-oxide peak. This might indicate a closer interaction between K and Sn. When only 0.5 % K is present, a sharp reduction peak around 573 K and relative intensity between the alloy and Sn oxide peaks indicate that most of the Sn might be still present in the Pt-Sn alloys. However, the composition of Pt-Sn alloys might slightly alter, therefore; this alloy peak has been shifted to higher reduction temperature compared to the peaks of 1%Pt-1.3%Sn/SiO_2 catalyst. The segregation is more pronounced with increasing loading of potassium. With 1%Pt-1.3%Sn-1.5%K/SiO_2 catalyst, the relative intensity between the Pt-Sn bimetallic peak and Sn-oxides peak has suggested us that almost of the Sn is present in the separate oxide phase, leaving only small portion in the Pt-Sn alloy. Additionally, the decrease in overall

intensity of 1%Pt-1.3%Sn-1.5%K/SiO_2 profile might be explained by the coverage of excessive K as shown in the BET surface area. In short, the addition of K has tremendous effects on the interaction between Pt and Sn. That is: K interacts closely with Sn, leading to the segregation of Sn out of the Pt-Sn alloy as Sn-oxide species, and consequently changing the composition of Pt-Sn alloys.

2.3 Temperature-programmed oxidation (TPO)

Figure A-4.2 exhibits the TPO plots of together with quantification of carbon deposits on various spent catalysts. Since silica support is not totally inert in the methyl hexanoate reaction, the deposited species remain on the spent catalyst after the reaction. These species are oxidized during TPO step over a range of temperatures (from 550 K to 900 K), leading to low-intensity-multiple-peak profile. Differently from silica sample, 1%Pt/SiO_2 and 1%Pt-1.3%Sn/SiO_2 profiles both have only one sharp peak at higher temperature around 823 K and 873 K, respectively. The oxidation peaks for Pt and Pt-Sn all fall in the same region as the oxidation temperature of the refractory coke formed during the reaction of 1-pentene over 1%Pt/SiO_2 catalyst. This might indicate the similar nature of deposited species on three catalysts. The difference between pure Pt and Pt-Sn profiles is that the slightly lower oxidation temperature is required for the former catalyst. However, a slight reduction in carbon amount is observed with the alloy catalyst. In fact, 1%Pt-1.3%Sn/SiO_2 catalyst produces the least amount of carbon deposit among all tested samples. Although the presence of Sn in the alloy has inhibited the formation of coke precursor species, Pt-Sn alloy is not able to catalyze coke oxidation reaction as effectively as pure Pt.

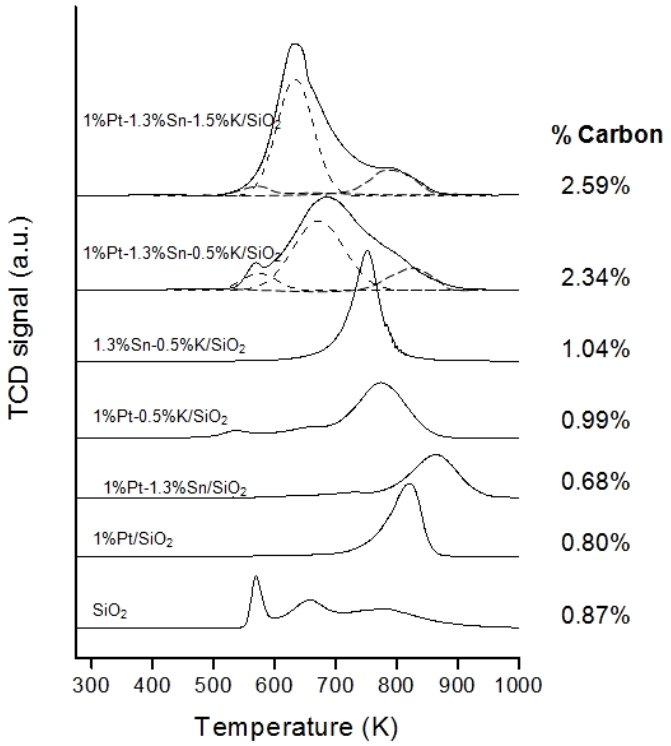

Figure A-4.2: Temperature-programmed oxidation profiles of different spent silica-supported Pt-Sn-K catalysts together with weight percent of carbon on 100 mg of spent samples ($T_{reaction}$ = 653 K, P= 101 kPa, W/F= 2.8 h). All of the spent samples were collected at 4 hour TOS.

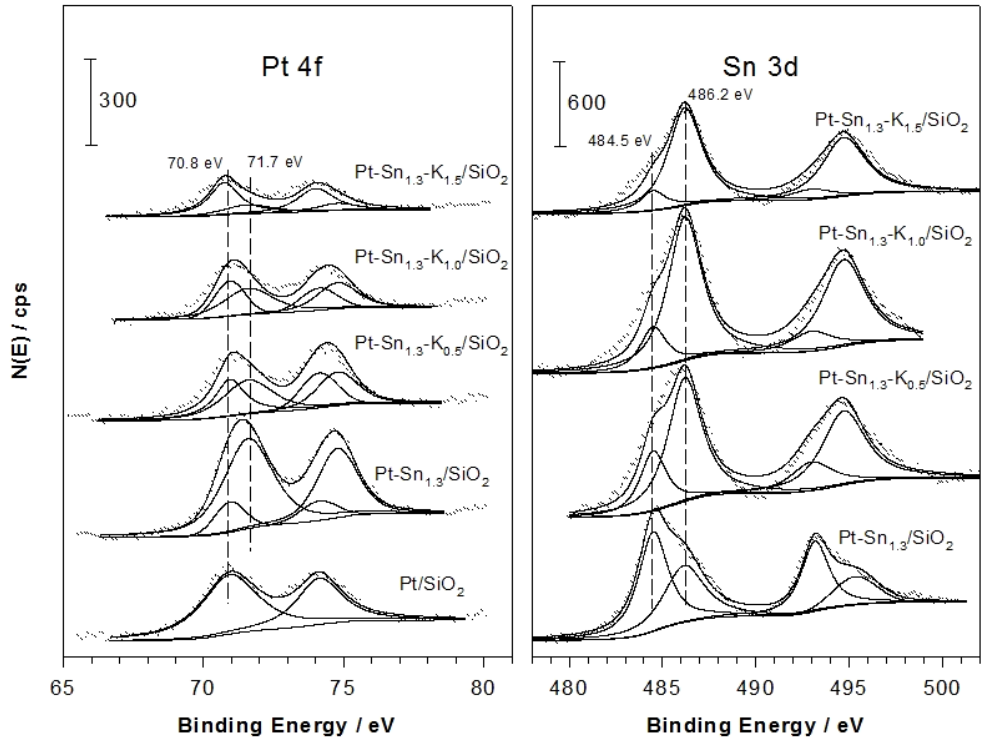

Figure A-4.3: X-Ray Photon Spectroscopy profiles of Pt 4f and Sn 3d for different silica-supported Pt-Sn-K catalysts .

In contrast to the addition of Sn, the additions of K into pure Pt and pure Sn lead to lower oxidation peaks, but greater amount of carbon deposits. This suggests that tin and potassium might contribute to different activities during the methyl hexanoate reactions. When three metals are added together in 1%Pt-1.3%Sn-0.5%K/SiO_2 and 1%Pt-1.3%Sn-1.5%K/SiO_2 catalysts, the oxidation profiles are broadened over a range of temperature from 550 K to 850 K. Although the oxidation takes place over the same temperature range for these two catalysts and silica support, the shape of oxidation peaks differ. Despite of the fact that those peaks are broader, they look more like the ones obtained with 1%Pt/SiO_2 and 1.3%Sn-0.5%K/SiO_2 catalysts. This could means that deposited species from both support and metal catalysts contributes to coke existing on the surfaces of two combination catalysts. Increasing potassium loading from 0.5 % to 1.5% not only results in lower oxidation peaks, but also leads to elevated amount of coke. Highest amount of coke is recorded with 1%Pt-1.3%Sn-1.5%K/SiO_2 catalyst

2.4 X-ray photonelectric spectroscopy (XPS)

The XPS results for all reduced silica-supported Pt catalysts are displayed in Figure A-4.3. It is interesting to note that apparent binding energy shifts were observed with the addition of both Sn and K into pure Pt. Initially, binding energies of Pt 4f peak for 1%Pt/SiO_2 is at 70.8 eV and 74.0 eV, which is assigned for metallic Pt component.[37-38] When only potassium is added into Pt/SiO_2, the positions of this peak are not changed. However, the first shift (around 0.5eV) toward higher binding energy is seen with bimetallic 1%Pt-1.3%Sn/SiO_2 catalyst. In fact, other researchers have reported the shift to lower binding energy with Pt-Sn catalysts with respect to pure Pt catalyst. [38] They explain the change in term of electron transfer from tin to Pt in the alloy. The higher binding

energy peak here might be due to the closer contact of metallic Pt with Sn oxide species. In fact, Sn 3d peak are made of two fragments attributing to metallic Sn^0 and oxide Sn (Sn^{+2} and Sn^{+4}). However, the higher binding energy of Pt 4f gradually shifts back to the lower position with increasing potassium loadings. In the mean time, Figure A-4.4 shows that the relative percent of oxide Sn over metallic Sn goes up with more potassium. One hand, this might indicate the Pt-Sn alloys are affected with the introduction of K. On the other hand, a portion of tin now is in closer contact with oxide potassium. These results are in a good agreement with segregated Sn peak and suppressed Pt-Sn alloy peaks observed with TPR as potassium is introduced into 1%Pt-1.3%Sn/SiO_2 catalyst. Dumesic et al. also reported that the K-Sn interaction is more dominant than that of K-Pt. [27] Similar to what has been reported in the literature, potassium is expected to be present as a hydroxide.[39] Since tin is thought to have a stronger affinity for oxygen than does Pt,[40] tin might have a stronger affinity for the oxygen atom of KOH than Pt. For a better visualization of the surface compositions, argon sputtering experiments were carried out with reduced 1%Pt-1.3%Sn-1.5%K/SiO_2 catalyst. Figure A-4.5 plots the atomic ratio of Pt/Si, Sn/Si, and K/Si as a function of sputtering time. At zero sputtering time, ratio of Pt/Si is lower than both Sn/Si and K/Si. As one penetrates deeper into the catalyst surface, the concentrations of Sn and K decrease together with increase in Pt concentration. This could lead to the conclusion that Pt is partially buried under layers of Sn and K, where they both closely interacts with each other.

2.5 Same-spot transmission electron spectroscopy (TEM)

In the dehydrogenation reactions of short alkanes, the catalyst deactivation is much more rapid on pure Pt catalysts than on bimetallic Pt-Sn catalysts. [26]In our previous

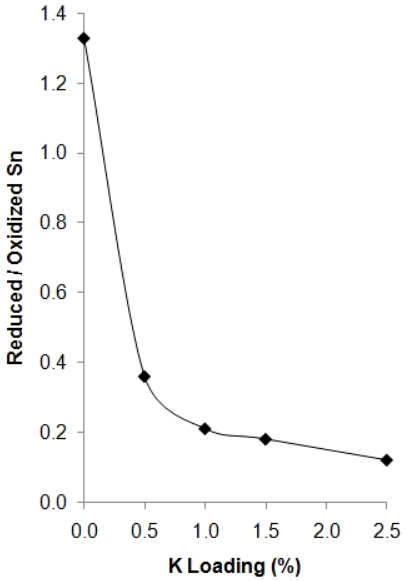

Figure A-4.4: Ratio of reduced Sn/oxidized Sn signal obtained from XPS Sn profiles

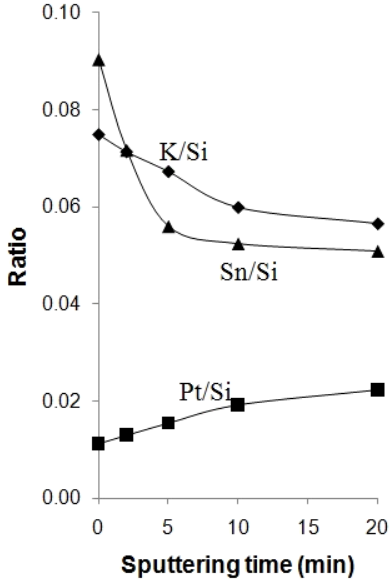

Figure A-4.5: Ratio of Pt/Si, Sn/Si and K/Si at different sputtering time for 1%Pt-1.3%Sn-1.5%K/SiO_2 reduced catalyst

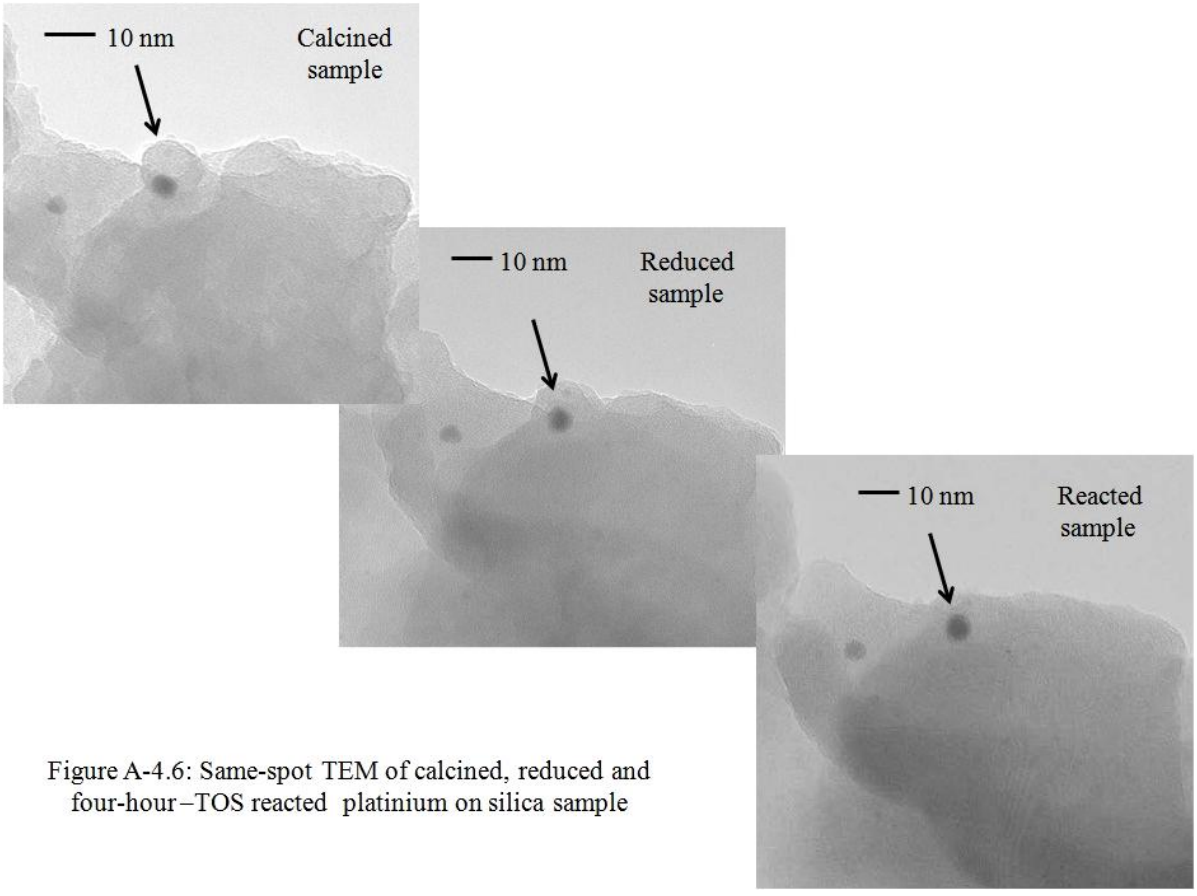

Figure A-4.6: Same-spot TEM of calcined, reduced and four-hour−TOS reacted platinium on silica sample

publication, we also reported that reactions of methyl esters under hydrogen-deficient conditions over supported-Pt catalysts are subject to severe deactivation, which can be caused by several factors such as coking or particle growth. Therefore, same-spot TEM experiments of Pt and Pt-Sn samples were done in order to monitor changes in metal particle sizes during the reactions. Figures A-4.6 and A-4.7 show the TEM images of calcined, reduced, and 4-hour-TOS reacted Pt and Pt-Sn (molar ratio 1:2) on silica. The average particle size is 2 to 8 nm. Over the course of reactions, it is obviously seen that the metal particles do not sinter significantly. Therefore, one might conclude that coking is the major cause for catalyst deactivation in methyl hexanoate reactions.

3. Catalytic Activity of Methyl Hexanoate

3.1 Activity of a series of Pt-Sn-K catalysts

Since deactivation was previously the major issue in the reaction of methyl octanote over 1%Pt/Al_2O_3, [25] in this work, we have worked on selection of several new catalysts that will be potentially more resistant to deactivation than this pure Pt catalyst. The combinational Pt-Sn-K/SiO_2 catalysts appear as good options for several reasons. First, the bimetallic Pt-Sn component is proved to be coke-tolerant in many other studies. Second, the oxide functions (i.e. SiO_2, SnO_2, K_2O) might exhibit some activity in the reaction of methyl esters similar to that of carboxylic acids. Figure A-4.8 compares the performances of silica support, 1%Pt/SiO_2, and the most effective catalyst 1%Pt-1.3%Sn-0.5%K/SiO_2 over reaction time. Silica shows low level of activity and slowly deactivates. Initially, 1%Pt/SiO_2 catalyst is highly active. However, this catalyst quickly deactivates to the same level of activity as silica after 1 hour time-on-stream (TOS). 1%Pt-1.3%Sn-0.5%K/SiO_2 catalyst also shows high initial conversion. In contrast to pure Pt catalyst,

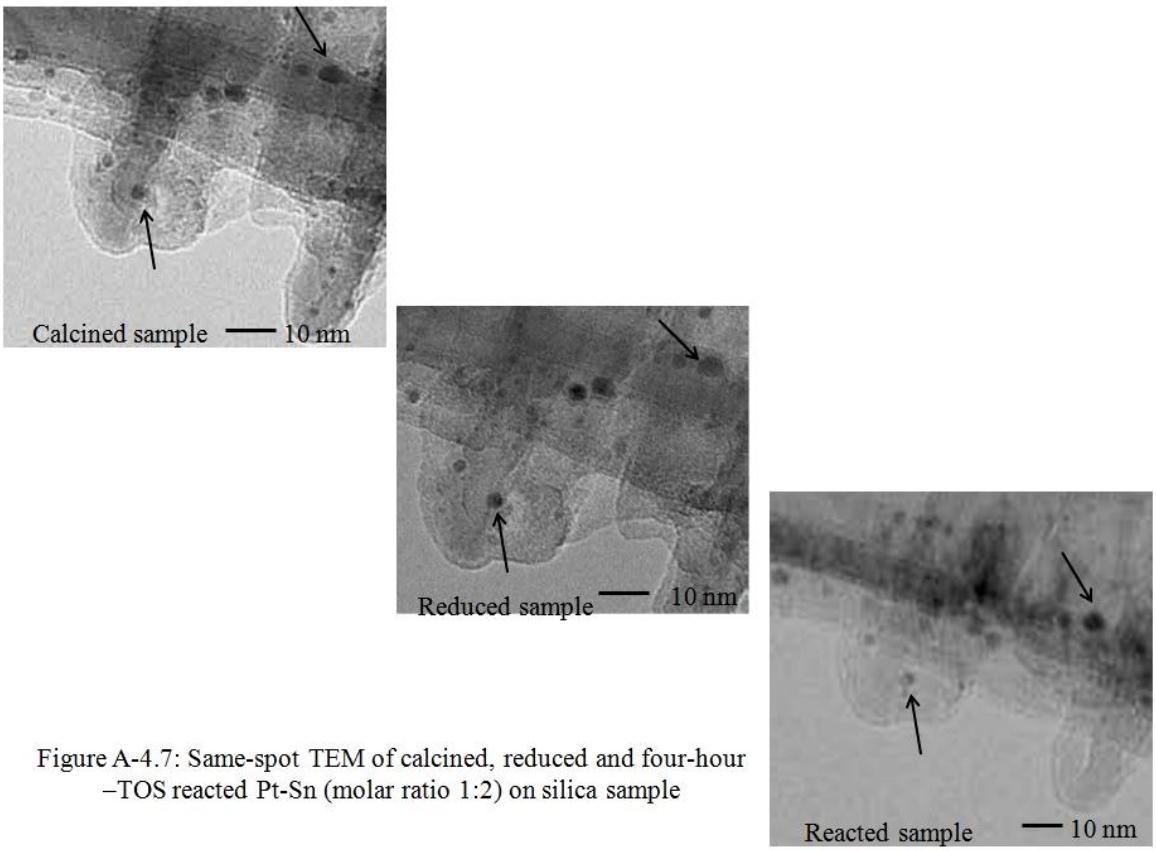

Figure A-4.7: Same-spot TEM of calcined, reduced and four-hour –TOS reacted Pt-Sn (molar ratio 1:2) on silica sample

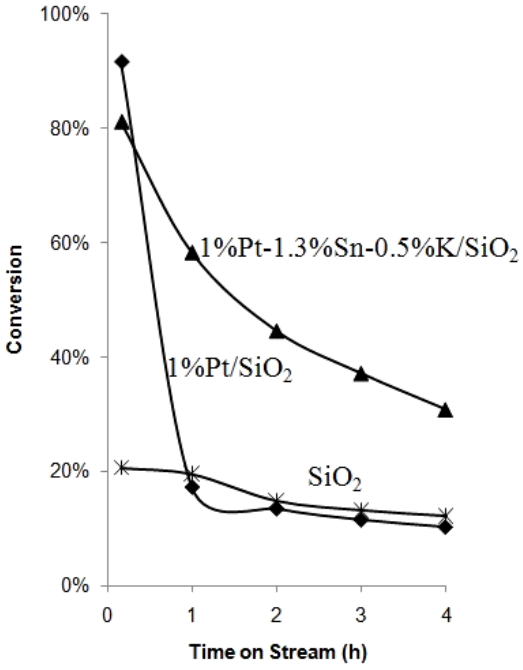

Figure A-4.8: Conversion of methyl hexanoate at various times on stream over silica, 1%Pt/SiO_2, and 1%Pt-1.3%Sn-0.5%K/SiO_2 catalysts ($T_{reaction}$ = 653 K, P= 101 kPa, W/F= 2.8 h). Feeding liquid via small-diameter feeding tube

this combinational catalyst still maintains considerable level of conversion over the course of 4-hour reaction.

To understand the performance of each catalyst, it is worth identifying different reaction pathways and associated products. Figure A-4.9 depicts four possible ways to produce final products, which are C_5 and C_6 hydrocarbons. The reactions also release some light compounds such as H_2, CO_2, CH_4, CO, methanol, and formaldehyde. Different intermediates separate these pathways. C_5 and C_6 hydrocarbons are produced directly and indirectly from the original ester in route (c) and routes (a), (b), (d), respectively. Besides, route (d) is the only pathway that involves two feed molecules. Those ester molecules condense to form condensation products (i.e. 6-undecanone). The evolutions of the major products along the catalyst bed in the reaction of methyl hexanoate over 1%Pt-1.3%Sn-0.5%K/SiO_2 catalyst in Figure A-4.10a will serve as a better visualization of the proposed reaction pathways. Although there is a direct conversion of methyl hexanoate to C_5 and C_6 hydrocarbons, it is clearly seen that methyl hexanoate are transformed via hexanol/hexanal, hexanoic acid and condensation products intermediates. These trends are in good conjunction with the results previously reported from our group with CsNaX catalyst.[41] Among those intermediates, condensation products are dominant intermediates, and consequently contribute heavily in methyl hexanoate conversion. In the effort of gaining more insights on this conversion pathway, it comes to our intention to design reaction conditions that maximize the formation of these coupling products. By changing the size of the feeding device, we are able to maximize the yield of condensation products. Figure A-4.10b shows evolutions of four major products obtained with new feeding conditions, in which contributions from the acid and alcohol/aldehyde are negligible

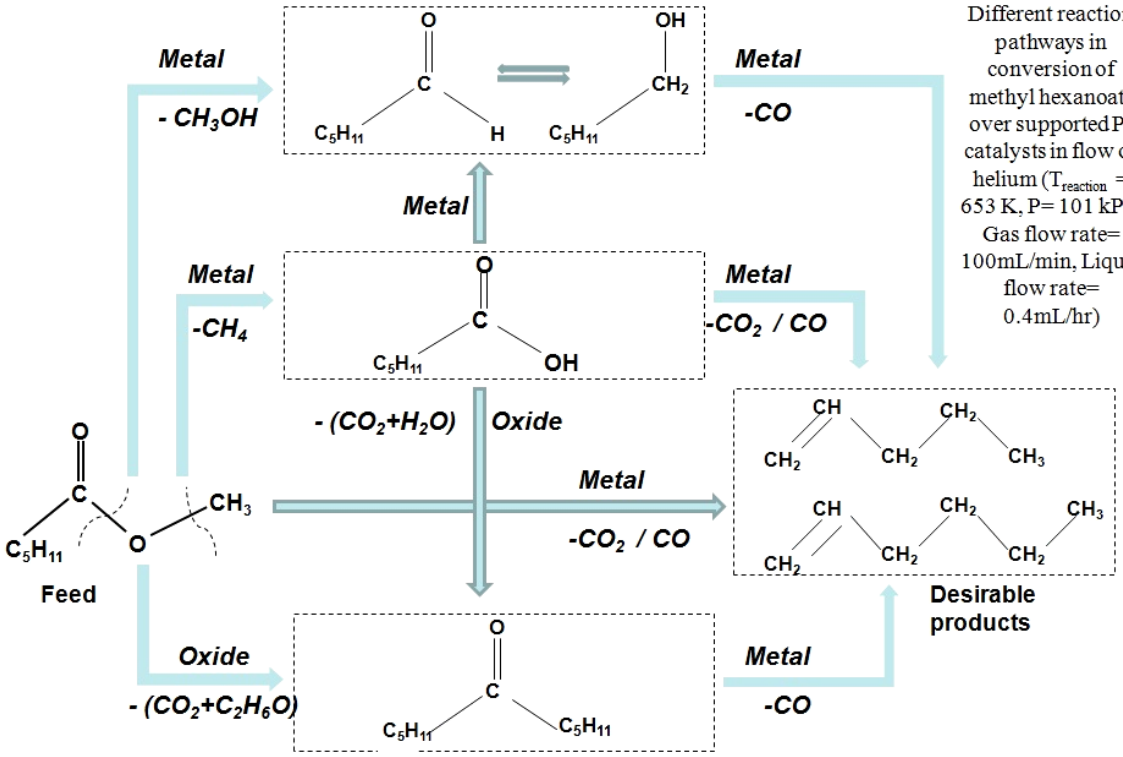

Figure A-4.9: Different reaction pathways in conversion of methyl hexanoate over supported Pt catalysts in flow of helium ($T_{reaction}$ = 653 K, P= 101 kPa, Gas flow rate= 100mL/min, Liquid flow rate= 0.4mL/hr)

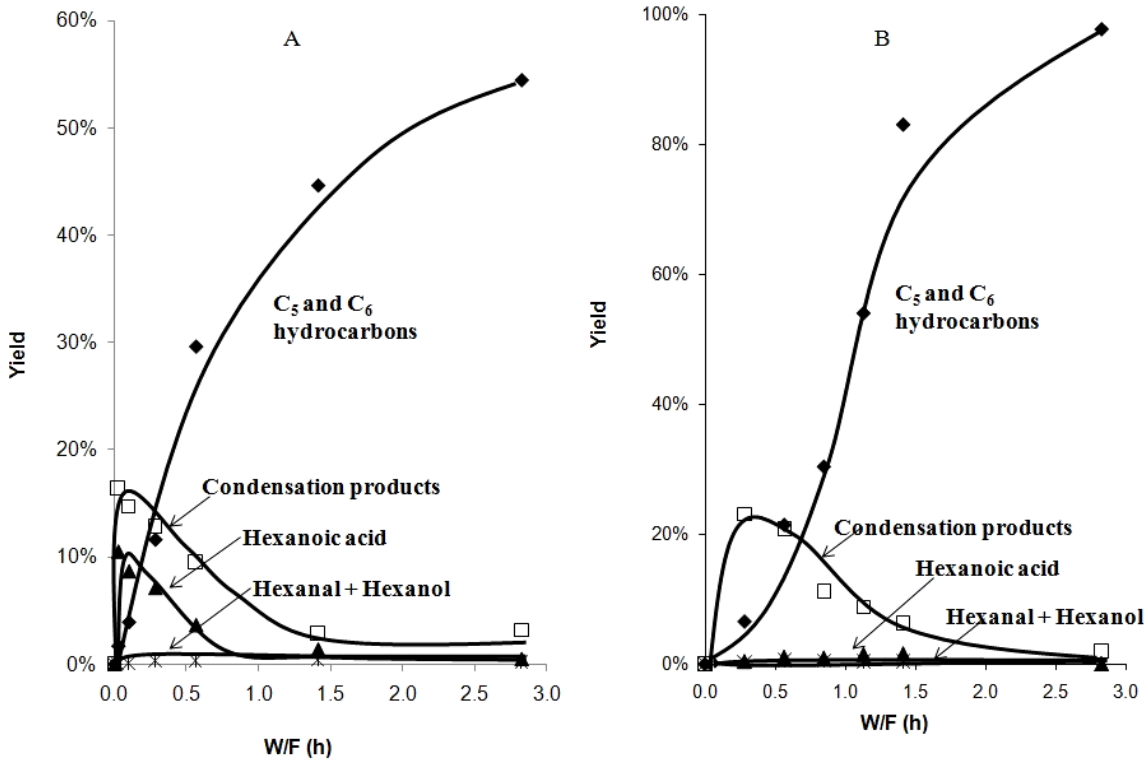

Figure A-4.10: Yields of major products from methyl hexanoate reactions over 1%Pt-1.3%Sn-0.5%K/SiO_2 catalyst at various W/F ($T_{reaction}$ = 653 K, P= 101 kPa, TOS = 1h). Graph A: Small-diameter feeding tube. Graph B: Large-diameter feeding tube.

while the condensation products become the main reaction intermediates. Consequently, indirect production of C_5 and C_6 hydrocarbons via condensation intermediates also becomes dominant, causing the suppression of direct ester-to-hydrocarbon transformation, which is reflected by lower rate of hydrocarbon formation at zero W/F.

As mentioned previously, condensation reactions can be catalyzed by some oxides (i.e. SnO_2, K_2O). In the mean time, transformation of those condensation products into C_5 and C_6 hydrocarbons involves C-C cleavages, therefore; active noble metal catalysts (i.e. Pt, Pt-Sn) are required. Since the overall reaction of methyl hexanoate is sequential, in the following section, we will show how to incorporate both oxide and metal functions to tailor the most effective catalyst. The abilities to form intermediates and to convert intermediates into final products strongly affect the catalyst stability and subsequently are keys for catalyst design. Thus, for each tested catalyst, the overall conversion, formation of condensation compounds, and production of C_5 and C_6 hydrocarbons will be reported. Figure A-4.11 shows the conversion of methyl hexanoate over silica support and different supported Pt catalysts at the same W/F over the course of 4-hour reactions. It should be noted here that the behaviors of silica, 1%Pt/SiO_2 and 1%Pt-1.3%Sn-0.5%K/SiO_2 catalysts are similar to what is reported in Figure A-4.8. Even though the conversions of 1% Pt/SiO_2 remains as low as 20% after one-hour TOS, as previously mentioned, one might assume that initially this catalyst is highly active. Besides, the activity of 1%Pt/SiO_2 is slightly higher than that of silica after one-hour TOS. The stability of pure Pt catalyst is improved by addition of either Sn or K. In fact, 1%Pt-1.3%Sn/SiO_2 catalyst is slightly more stable than 1%Pt-0.5%K/SiO_2 catalyst. Without any Pt, the conversion of 1.3%Sn-0.5%K/SiO_2 catalyst levels at around 38% over four

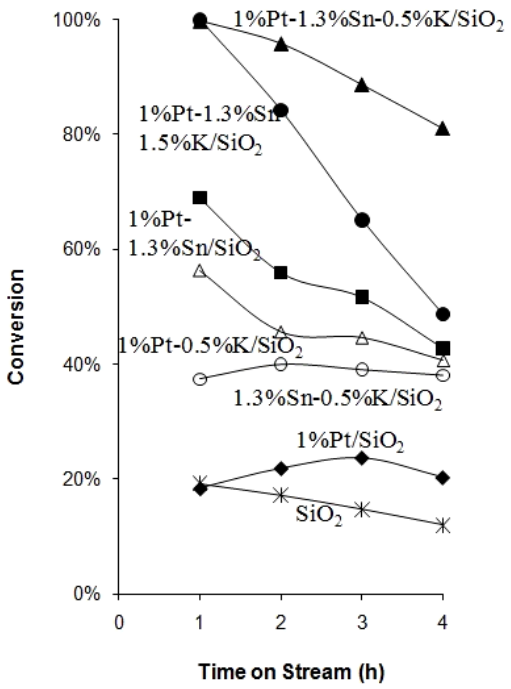

Figure A-4.11: Conversion of methyl hexanoate at various times on stream over all tested catalysts ($T_{reaction}$ = 653 K, P= 101 kPa, W/F= 2.8 h). Feeding liquid via large-diameter feeding tube

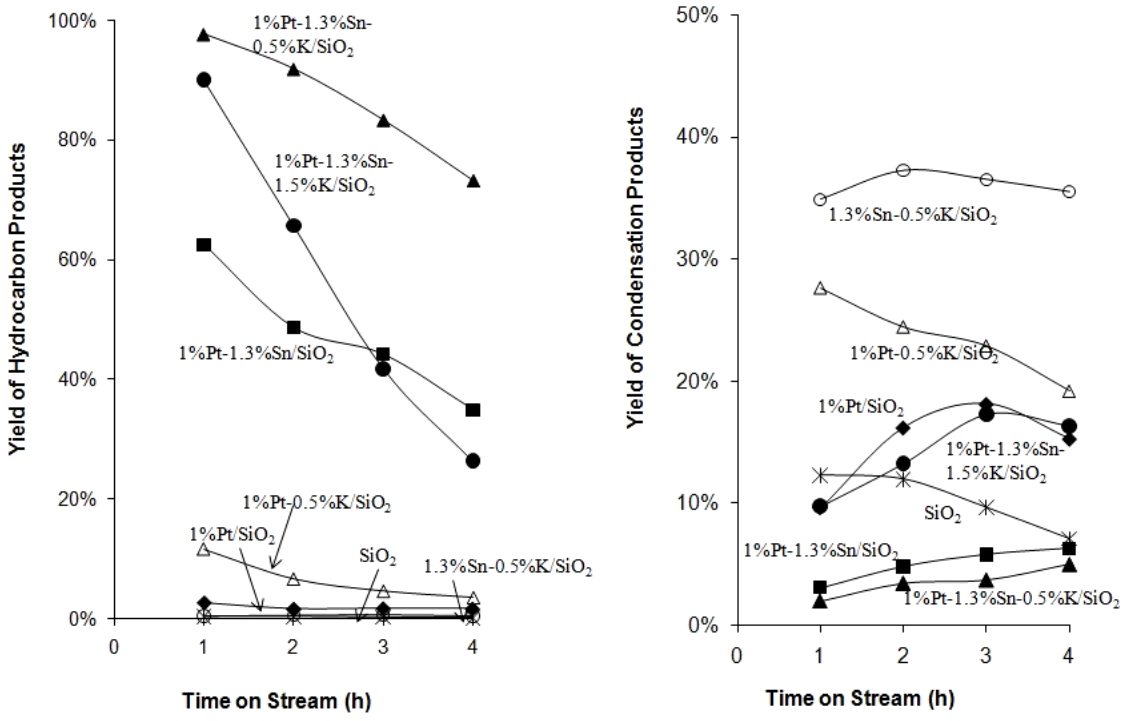

Figure A-4.12: Yields of C_5 and C_6 hydrocarbons at various TOS all tested catalysts($T_{reaction}$ = 653 K, P= 101 kPa, W/F= 2.8h). Feeding liquid via large-diameter feeding tube

hours of reaction. The marked improvement is seen with the introduction of potassium into 1%Pt-1.3%Sn/SiO_2 catalyst. As one varies the loading of potassium, the optimal performance is achieved with 0.5 wt % K. When comparing between 1%Pt-1.3%Sn-0.5%K/SiO_2 and 1%Pt-1.3%Sn-1.5%K/SiO_2 catalysts, the conversion drops might indicate that the latter possesses higher initial activity the former. However, the latter deactivates more quickly as the reaction proceeds.

As stated before, the formation of coupling compounds and the conversion of those compounds into final products have great influences on catalyst performances. Thus, it is informative to examine the yields of condensation products and C_5 and C_6 hydrocarbons at different TOS for all tested catalysts (figures A-4.12a and A-4.12b). On the both silica, 1.3%Sn-0.5%K/SiO_2, and 1%Pt/SiO_2 catalysts, most of the activities after one-hour of reaction go to formation of coupling compounds. In fact, condensation activity for silica continuously decreases. When Sn and K are added into silica, the condensation yield of Sn-K catalyst is much higher than that of the original support (35% versus 10%). Thus, there are Sn and K species that are responsible for this high coupling activity. Conversely to silica support, the condensation production on pure Pt catalyst continuously increases and goes through a maximum at three-hour TOS. The production of C_5 and C_6 hydrocarbons on these three catalysts are minimal after TOS of 1 hour. The addition of K into pure Pt catalyst slightly facilitates the production of C_5 and C_6 hydrocarbons. However, the condensation products are still the dominant products on the 1%Pt-0.5%K/SiO_2 catalyst. The further improvements in formation of hydrocarbons were observed with addition of Sn and later K into pure Pt catalyst. On 1%Pt-1.3%Sn/SiO_2 catalyst, the amount of produced coupling products appears to be much less than that of

the pure Pt, but the yield of hydrocarbons is much higher on the bimetallic catalyst. The fact that higher yield of hydrocarbons, together with the limited yield of coupling products, on Pt-Sn catalyst indicates that the bimetallic is more stable or more coke-tolerant than the monometallic Pt. In other words, 1%Pt-1.3%Sn/SiO_2 catalyst shows a higher ability in maintaining the conversion of heavy compound into hydrocarbons over the course of reaction. By comparing the relative yields of these two products, one can easily see that 1%Pt-1.3%Sn-0.5%K/SiO_2 catalyst is even more effective than the bimetallic Pt-Sn catalyst. When varying the concentration potassium, the performances of 0.5%K and 1.5%K catalysts differ. In fact, excessive potassium (1.5% loading) results in rapid drop in hydrocarbon yields and quick accumulation of condensates as the reaction proceeds.

Since the formation reactions of heavy compounds, the decomposition reactions of those compounds to hydrocarbons, and other side reactions release some light gases, it is possible that more insights can be gained by interpreting these light gas outputs. While the former reactions produce CO_2, carbon mono oxide is observed as one of the by-products in the latter reaction. In details, the decomposition reaction of one of the condensation products, 6-undecanone, yields CO. Carbon mono oxide and hydrogen can also come from water-gas-shift (WGS) reactions and decomposition reactions of other side products such as methanol/formaldehyde and dimethyl ether, similarly to other researchers observed. It is worth pointing out that the production of CO only occurs on metal function of the catalyst. Thus, it could be possible that the catalyst that produces higher amount of CO under the same condition is the more stable and effective catalyst in deoxygenation reaction. In fact, other researchers also observed similar reactions during

the conversion of vegetable oils over hydrotreating catalysts.[42] Another source of hydrogen is from coking reaction. These gas production reactions occur simultaneously with other main reactions, thus; the gas productions reflect the catalyst activity with time on stream.

Figures A-4.13 exhibits the gas distributions all tested catalysts. The concentrations of produced H_2, CO, CO_2, and CH_4 decrease as the catalyst deactivates. Seven tested catalysts produce CO_2. Hydrogen was seen with five catalysts, except silica gel and Sn-K/SiO_2. These observations are in good agreement with the results reported in figures A-4.12. The condensation reactions (i.e. ketonization) occur on silica support and supported- metal catalysts, therefore; it is expected to see CO_2 at all time. Silica with its low condensation activity only produces small amount of CO_2. Sn-K catalyst exhibits a higher condensation activity than the support alone, therefore; higher quantity of CO_2 was detected on this catalyst. In fact, the carbon dioxide productions go hand in hand with potassium loadings. The K-doped catalyst produces more CO_2 than the one without any potassium. The highest CO_2 concentration was observed with the catalyst containing 1.5% K. Almost no hydrogen was seen on silica and Sn-K samples. In fact, the considerable amounts of hydrogen produced were only observed with the Pt-containing catalysts, on which Pt metal is active in catalyzing WGS, decomposition, and dehydrogenation reactions to form carbon species. However, the deactivated pure Pt and Pt-K catalysts only produce small or negligible amount of hydrogen via those above reactions. Consequently, the remaining activity is condensation, which releases CO_2, on these two catalysts. Besides, H_2 and CO_2, considerable amount CO start appearing on Pt-Sn and two Pt-Sn-K catalysts. The production of CO is closely related to the reactions

that are catalyzed by metal function of the catalyst such as deoxygenation, light oxygenate decomposition, and water gas shift reactions. Therefore, CO is only observed on the catalysts containing Pt-Sn bimetallic or the stable catalyst over the reaction period. Figure A-4.14a shows the proportional relationship between CO evolution and deoxygenated products, C_5 and C_6 hydrocarbons as one varies both W/F and time on stream. Since, CO is one of the products from decomposition reaction of light oxygenates (i.e. methanol, formaldehyde, and dimethyl ether) the amount of remaining light oxygenates per reacted ester coincides with the CO evolution as shown in figure A-4.14b. C_xH_yO is converted to more CO and other products as the catalyst bed expands. Similarly when the catalyst deactivates, together with decreasing CO production, the conversion of light oxygenates is suppressed as well. The fact that CO was present in the largest quantity on 1%Pt-1.3%Sn-0.5%K/SiO_2 catalyst refers to the highest activity of this catalyst among Pt-Sn and two Pt-Sn-K catalysts. Lastly, only on this catalyst, CH_4 was present in small amount.

In short, the results of the overall activities and gas distributions on all tested catalysts enable us to draw several conclusions. That is: pure Pt on silica is very active for the methyl hexanoate reaction in the absence of hydrogen. However, this catalyst deactivates quickly. Addition of K into Pt does not significantly improve its stability because the condensation intermediates formed on K species cannot be converted on deactivated Pt sites. Substantial enhancement is only observed with addition of both Sn and K into Pt. Here, the heavies, which are formed on Sn and K species, are effectively transformed into final hydrocarbon products. Additionally, the Pt-Sn alloys exhibit higher

Catalyst	H_2	CO_2	CH_4	CO
SiO_2		√		
1%Pt/SiO_2	√	√		
1%Pt-1.3%Sn-0.5%K/SiO_2	√	√	√	√
1.3%Sn-0.5%K/SiO_2		√		
1%Pt-0.5%K/SiO_2	√	√		
1%Pt-1.3%Sn/SiO_2	√	√		√
1%Pt-1.3%Sn-1.5%K/SiO_2	√	√		√

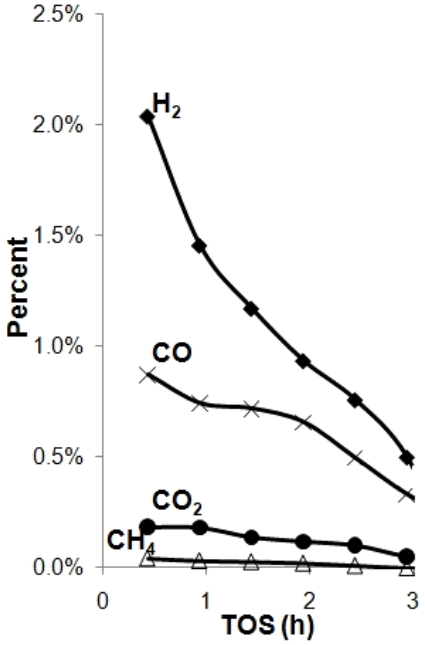

Figure A-4.13: (A) Different light gas product (H_2, CO_2, CH_4, and CO) in methyl hexanoate conversions over different tested catalysts; (B)Typical light gas concentration

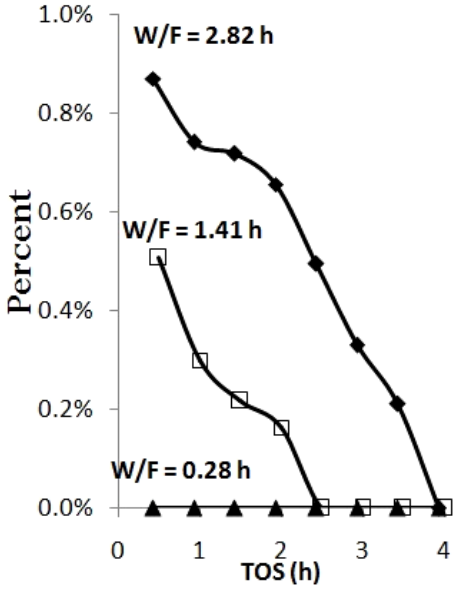

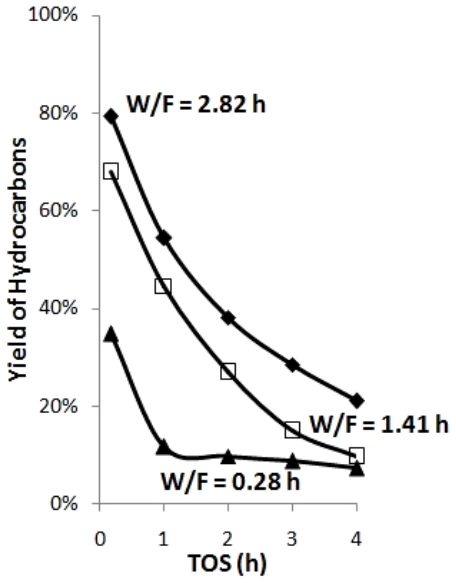

Figure A-4.14a: Evolution of carbon monoxide in the reaction of methyl hexanoate on 1%Pt-1.3%Sn-0.5%K/SiO_2 catalysts and deoxygenated hydrocarbon products at various W/F and time on stream

coke tolerant than pure Pt, leading to improvement in catalyst stability. 1%Pt-1.3%Sn-0.5%K/SiO_2 was found to be the optimal catalyst configuration.

3.2 C_5 hydrocarbon distribution

Reaction of methyl hexanaote over supported Pt catalysts yield a distribution of C_5 and C_6 hydrocarbons. As reported in our previous paper, without hydrogen, the hydrogenation activity of methyl ester strongly impaired compared to decarboxylation/decarbonylation activity.[43] Consequently, under the studied conditions, C_5 compounds are more dominant than C_6 compounds. In the previous sections, it is known that altering catalyst composition strongly affects the total yields of condensation and hydrocarbon products. C_5 hydrocarbons were believed to come from decarbonylation/decarboxylation reaction of methyl hexanoate and mostly decomposition reactions of coupling compounds. In the following section, we will show that the changes in composition create significantly impacts on C_5 distribution, which consists of mostly pentane and isomers of pentene, and negligible amounts of di-en C_5s. Among all C_5 pentene isomers, one would expect to have 1-pentene or alpha pentene as the first C_5 hydrocarbon product due to the position of the original ester functional group. However, a distribution of C_5 alkenes was usually observed since the double-bond isomerization reaction between alpha pentene and internal pentenes, 2-pentene and 3-pentene, can occur on platinum catalysts. C_5 alkane can be also produced from hydrogenation of C_5 alkenes on platinum with hydrogen released from the methyl hexanoate reactions. The hydrogenation/dehydrogenation reaction is generally accepted as reactions which run with small ensembles of contiguous metal surface atoms, or even with single-atom. [44-45]

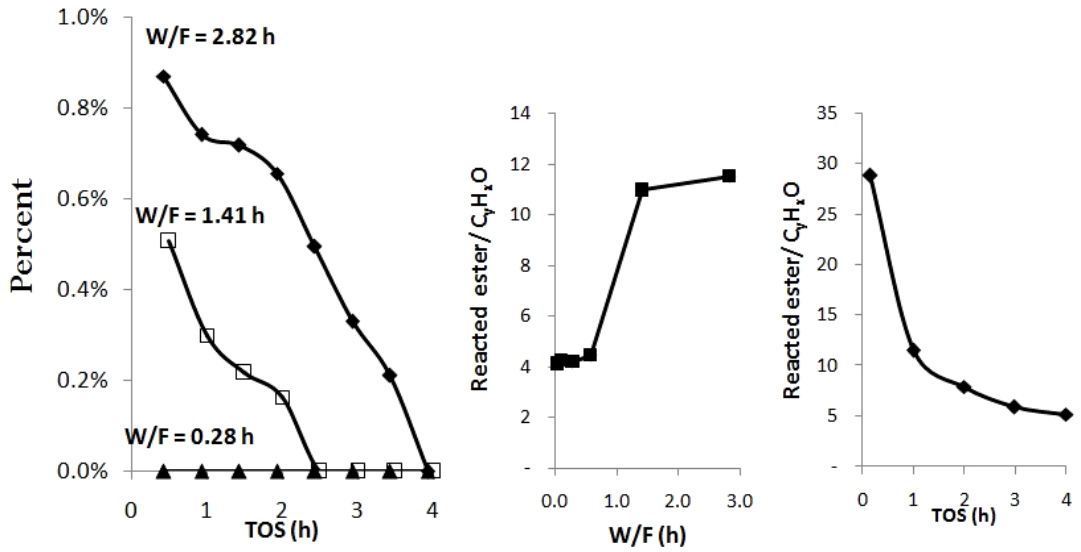

Figure A-4.14b: Evolution of carbon monoxide in the reaction of methyl hexanoate on 1%Pt-1.3%Sn-0.5%K/SiO_2 catalysts and the conversion of light oxygenates at various W/F and time on stream

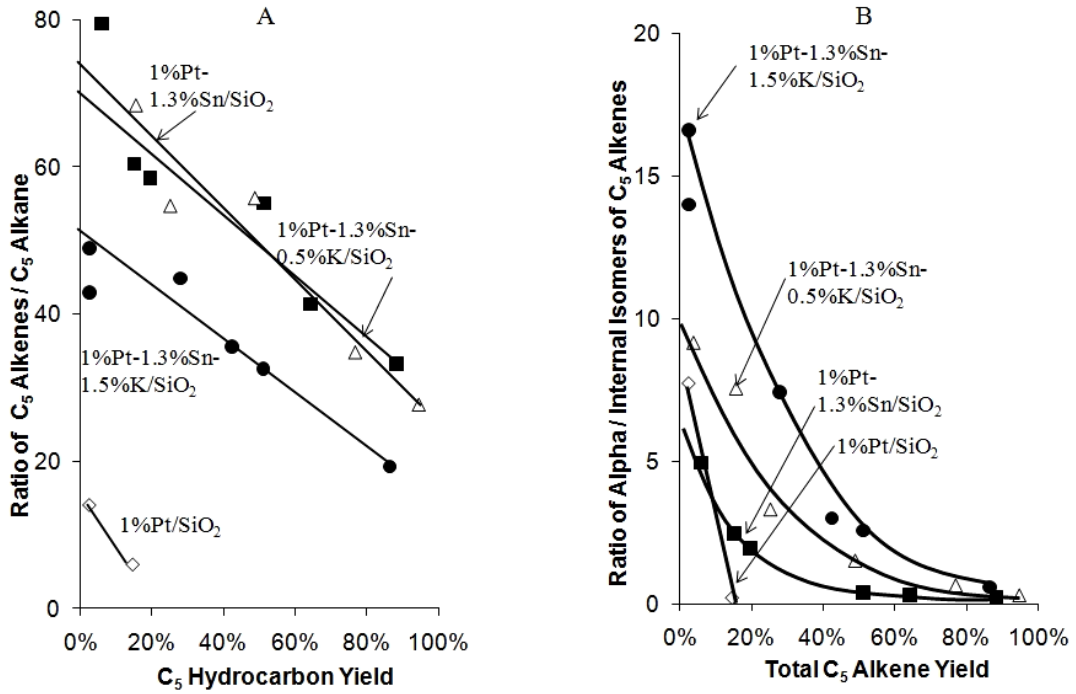

Figure A-4.15: Ratios of C_5 alkenes / C_5 alkane (graph A) and alpha/internal C_5 alkenes (graph B) as a function of total C_5 hydrocarbon yield for Pt-Sn-K/SiO_2 catalysts ($T_{reaction}$ = 653 K, P= 101 kPa, TOS=1h)

Additionally, strong adsorption of highly dehydrogenated or alkene-derived intermediates can quickly deactivate the catalysts. [26]Therefore, the ratio of alkane C_5/alkene C_5 and alpha/internal C_5 alkenes would give some insights to the hydrogen availability on catalyst surface, the size of active ensembles, and the coking tendency of the studied catalysts.

Since the additions of Sn and K have tremendous impacts on the overall performances of pure Pt catalyst, it is very likely that these introductions will influence the selectivities of C_5 alkane and alkenes. Figure A-4.15a depicts the ratio of C_5 alkenes/alkane as varying total C_5 hydrocarbon yields or overall conversions. For all catalysts, the ratio decreases with increasing C_5 yields. As conversion proceeds, pentenes get hydrogenated into pentane, which makes the ratio decrease. At the same total C_5 yield, this ratio follows the order: 1%Pt/SiO_2 < 1%Pt-1.3%Sn-1.5%K/SiO_2 < 1%Pt-1.3%Sn/SiO_2 ≈ 1%Pt-1.3%Sn-0.5%K/SiO_2. It should be noted that all the data points are taken at 1 hour TOS, where catalyst deactivations have happened to some extent. Consequently, the data point at zero C_5 yield (or zero conversion) does not tell us about the intrinsic differences among the deactivation-free catalysts, but rather about the extent of hydrogenation reaction of C_5 alkenes on slightly deactivated catalysts. As mentioned above, 1%Pt/SiO_2 deactivates very fast during the first hour of the reaction. The hydrogen released in the coking reactions is in turn used to hydrogenate the alkenes to alkane. It is the decrease in alkene concentrations due to their great consumptions in the coke formation reactions that leads to low ratio of alkenes/alkane on pure Pt catalyst. Conversely, these ratios are markedly higher on three other catalysts that exhibit significantly lower level of deactivations. Among those three catalysts, more alkenes

were converted into alkane on 1%Pt-1.3%Sn-1.5%K/SiO_2 catalyst, which can be caused by the greater availability of hydrogen produced on this catalyst as depicted in figure A-4.13a.

Not only the ratio of C_5 alkene/alkane varies with catalysts and conversion, the ratio of alpha/internal C_5 alkenes deviates as shown in figure A-4.15b. Alpha pentene is initially formed, however; more active sites available for alpha-to-internal-alkene isomerization activity as the catalyst bed size increases, leading to the decreasing ratio for all four catalysts. The isomerization reactions are structure sensitive, [45-46] therefore; the ratio drop rapidly on pure Pt. As the size of catalyst bed manifests, more clusters of Pt sites become available for isomerization. Nevertheless, this trend is not observed with other three catalysts since Pt ensembles were possibly affected with introductions of Sn and K. In fact, the changes in alpha/internal C_5 alkenes for three Pt-Sn-K catalysts go hand in hand with potassium loadings and the condensation concentrations on the catalyst surfaces. As shown in XPS results, Pt surfaces are covered with potassium, leading to reducing metal sites (i.e. Pt, Pt-Sn) available for isomerization or reducing alpha/internal ratio with increasing potassium loadings. In details, increase in potassium loadings (0.5% to 1.5%) leads to more populated condensation product concentrations, as seen in figure A-4.12, and consequently inhibits the double-bond isomerization of C_5 alkenes. Thus, higher alpha/internal ratio is found on the 1.5% K catalyst. The influence of potassium loadings on alpha/internal C_5 alkene ratio is further supported by the deviations of selectivities of C_5 hydrocarbons and coupling products during the course of reaction on figure A-4.16. 1%Pt-1.3%Sn-0.5%K/SiO_2 catalyst was chosen as a typical sample. As the catalyst deactivates, C_5 hydrocarbons are produced in less quantity and coupling products

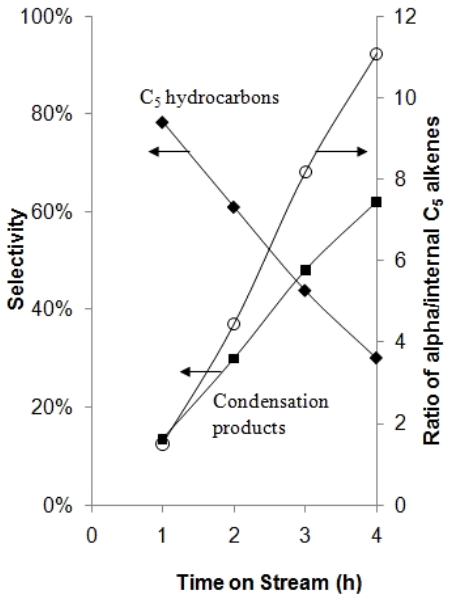

Figure A-4.16: Reaction of methyl hexanoate on 1%Pt-1.3%Sn-0.5%K/SiO_2 catalyst for 4 hours. Left Y-axis: selectivities of condensation products and C_5 hydrocarbons. Right Y-axis: Alpha/internal C_5 alkene isomer ratio ($T_{reaction}$ = 653 K, P= 101 kPa, W/F= 1.1h)

are accumulated. The increasing coverage of these heavy compounds on the catalyst surface makes the double-bond isomerization more difficult. In another word, the more catalyst deactivates, the more alpha alkenes are preserved.

4. General Discussion

Pt is one of the noble metals that are active and selective for deoxygenation of methyl esters under mild operating conditions.[21] In the previous publication, we have shown that 1% Pt/Al_2O_3 is active for conversion of not only small methyl esters (i.e. methyl octanoate) but also fatty acid methyl esters (i.e. methyl stearate) in hydrogen.[25] The presence of hydrogen not only facilitates the overall conversion of the ester but also suppresses the formation of coupling products (i.e. symmetrical ketone). [11] Although this catalyst is very active in reactions with hydrogen, it deactivates rapidly under helium medium, leading to a higher yield of condensation products. These markedly different

activities prompt us to tailor for catalysts that are more coke-resistant and still active for conversion of methyl esters. Both metal and oxide functions should be incorporated in the optimal catalysts since the metals are able to catalyze decarboxylation/decarbonylation reactions and oxides add additional activities. In this study, the combinational Pt-Sn-K/SiO_2 catalysts were chosen because they are known for their high coke tolerance in dehydrogenation reactions of short alkanes and exhibit above essential functions: metal (i.e. Pt, Pt-Sn) and oxide (i.e. SnO_2, K_2O).

Before analyzing the impacts of new catalyst on the reaction, an important piece of information needs to be addressed in the first place. That is, the conversion of a model ester feed, methyl hexanoate, occurs via different reaction pathways as depicted in figure A-4.9. Since the route via condensation intermediates play an important role in the transformation of the ester into final hydrocarbon products and the catalyst stability, the performances of all tested catalysts will be analyzed under the maximizing conditions of this pathway. Here, it is seen that the coupling products are formed as first products from the reaction of methyl hexanoate. As the conversion proceeds, those compounds are transformed into C_5 and C_6 hydrocarbons via decomposition reactions.

As shown in figures A-4.11 and A-4.12, the silica support, similar to other reported oxides, [16] is able to catalyze the coupling reaction of methyl hexanoate at low extent, particularly ketonization reaction. The reaction yields two main products: 6-undecanone and hexanoic acid. At lower conversion of silica, the acid becomes the dominant product. It could be possible that carboxylate species resulting from dissociation of ester are responsible for formation of hexanoic acid and the heavy ketone. In fact, carboxylate species are commonly observed when having carboxylic acids

adsorbed on oxide surfaces.[47] One hand, those species then react with atomic surface hydrogen produced from methyl group decomposition, which has been well-documented in the literature[15], to form hexanoic acid. On the other hand, they can form the symmetrical ketone via either bimolecular mechanism suggested by Barteau et al. [15] or ketene-like intermediate proposed by Ponec et al. [16] It is reported in the literature that at 653 K some portion of bridged hydroxyl groups could undergo dehydroxylation resulting in coordinatively unsaturated sites on silica.[48] These types of sites could be active for adsorption of carboxylates as proposed by Barteau et al. The carboxylate species can also oligomerize or condense to form the type of residual observed in oxidation profile of spent silica. The fact that no hydrogen is detected on deactivated silica in figure A-4.13 further confirms the coking via condensation reactions instead of dehydrogenation reactions

Compared to silica support, 1%Pt/SiO_2 catalyst exhibits a slightly enhanced selectivity for final hydrocarbons despite of being quickly deactivated. In fact, both direct decarboxylation/decarbonylation of ester and indirect deoxygenation of condensation intermediates into hydrocarbons require ensembles of active sites and is structure-sensitive. [49 - 50] At the beginning of the ester reaction, C_5 and C_6 hydrocarbons are produced favorably on platinum surface due to the availability of large and clean active ensembles. Since pure Pt is highly prone to coking, the overall activity quickly drops as seen in figure A-4.11. In fact, the high-temperature peak in TPO profile of spent 1%Pt/SiO_2 catalyst has suggested that the carbon residuals are refractory and mostly located on Pt surfaces, where formation of C_5 and C_6 hydrocarbons occurs. The produced alkenes might quickly turn to highly dehydrogenated species or cokes on platinum.

Literature suggested that an ensemble of surface Pt atoms, which are available on pure Pt catalyst, might be required for decomposition reactions leading to coke formation.[51] However, the deactivated Pt/SiO_2 is still able to maintain some coupling activity, even higher than on deactivated silica. It is possible that the coke on platinum can still catalyze dehydrogenation reaction of oxygenates in a similar fashion as the activity of coke in oxydehydrogenation of ethylbenzene. [52 - 53] These two cokes might resemble similar structures with the aromatic structure and contain oxygen atom in the form of quinone/hydroquinone- or aroxyl/phenol-type complexes. [52] It is very likely that the hydrogen evolved from both dehydrogenation reactions forming coke and reactions catalyzed by coke can be spilled-over and help to maintain silica surface active for the condensation reactions. The hydrogen cleaning effect does not happen with silica itself; therefore, the condensation activity is lower for spent silica compared to spent $1\%Pt/SiO_2$ catalyst.

Since the reaction of methyl hexanoate is sequential, the key to catalyst stability is metal function that resists again coking. As seen above, pure Pt fails in maintaining its initial activity. Addition of Sn into Pt/SiO_2 improves the ester activity in the way that conversion of the ester into coupling products is somehow facilitated and importantly the deoxygenation reactions of these intermediates into hydrocarbons survives longer. First, it is possibly the Sn species that facilitate the adsorption of the ester on the alloy compared to pure platinum. Marinelli et al. and other researchers have suggested the preferred adsorption mode of some functional groups (i.e. aldehyde, ketone, carboxylic acids) starts with interaction of carbonyl oxygen with cationic Sn. [54] In fact, he claimed that addition of Sn into Pt/SiO_2 decrease the adsorption energies of crotonaldehyde and

other similar compounds compared to Pt. [55] Some also claimed that the adsorption of oxygenates containing carbonyl group with metal surfaces is initiated by carbonyl oxygen-metal bond. [12] Compared to silica support, the interaction between the ester and Sn cations is significantly enhanced, leading to higher condensation activity on Sn domains. Second, as confirmed by chemisorptions, TPR, and XPS results, Pt-Sn alloys have been formed on 1%Pt-1.3%Sn/SiO_2. It could be possible that the Sn species, in close contact with Pt, transfer carbon deposits from Pt into the support in the same fashion as dehydrogenation reactions.[26] Some researchers also suggested that the role of Sn is to titrate the highly active and coke-forming defect sites of pure Pt. [56] Some researchers also believed that addition of Sn to Pt has both electronic and geometric effects. [57] Introduction of Sn causes rupture of ensembles of Pt active sites, which leads the suppression of the structure sensitive reactions such as coking. Sn also electronically modifies the Pt surface in such way that the adsorption energy of dehydrogenated species decreases compared to monometallic Pt. Thus, the amount of coke deposited on spent bimetallic catalyst is slightly lower than spent monometallic Pt catalyst. Besides carbon deposit, CO can act like one of the poison sources as well. Some investigators have reported that the poisoning effect of CO is not as pronounced with the alloy catalyst because Pt-Sn alloy does not adsorb CO. [55] Even though the introduction of Sn breaks Pt active ensembles, which are required for deoxygenation reactions; the stability of the pure Pt catalyst is significantly improved.

If the addition of Sn into pure Pt catalyst positively impacts the catalyst stability, the introduction of K into Pt-Sn leads to the optimal catalyst performances with desirable stability and overall methyl ester activity. In many other works, potassium is added into

Pt-Sn catalyst to neutralize some unwanted acid sites, which causes cracking and undesirable reactions. [58] In fact, the XPS data has suggested that more chloride retained on the K-doped catalysts than non-potassium catalysts. Chloride is associated mostly with potassium to form potassium chloride. However, there is no direct correlation of chloride concentration with the methyl ester activity observed. It is the activity of potassium that causes dramatic changes. In particular, potassium helps to segregate Sn out of the Pt-Sn alloy and possibly creates new domains (i.e. KOH or K_2SnO_x) for methyl ester adsorption. The high condensation activities on K-related species are confirmed by the results of 1%Pt-0.5%Sn/SiO_2 and 1.3%Sn-0.5%K/SiO_2 catalysts. It could be possible that formation of carboxylate species or intermediates during condensation reactions is greatly facilitated on alkaline oxide surface such as potassium. The effect of potassium here can be compared with the identical effect of Zn on copper catalysts in formation of heavy ketones as feeding various alcohols. [59] Although the contribution of Sn in coupling reactions is appreciable, the impact of potassium somehow outweighs that of Sn. At the end, the catalyst design comes to the optimization of suitable Pt-Sn-K molar ratios so that Sn-K domains are active for condensation production and Pt-Sn alloys are able to maintain high deoxygenation activity into hydrocarbons. That means varying potassium loadings has tremendous impacts on activity and coking tendency of the catalysts. In fact, increase in potassium concentration leads to higher accumulation of coupling products and consequently greater amounts of carbon residuals on spent catalysts. If the cokes on 1%Pt/SiO_2 and 1%Pt-1.3%Sn/SiO_2 catalysts are relatively uniform, reflective by sharp high-oxidation-temperature peaks, cokes deposited on the combinational Pt-Sn-K/SiO_2 catalysts are relatively disperse. Additionally, the carbonaceous residuals accumulate into

greater quantities on the latter. Cokes on the K-doped catalysts contain fragments possibly attributed to silica support, Sn-K, and Pt. The contribution from Sn-K domains outnumbers the other two. It is most likely that these carbon deposits on K-doped catalysts are associated with segregated SnO_x or KOH domains, where the coupling reaction of methyl ester molecules occurs vigorously.

The addition of Sn and K into Pt/SiO_2 not only affects the overall catalyst performance but also greatly shapes the distribution of the dominant hydrocarbon products, C_5 compounds. In another word, the doping of these two metals has directly influenced two side reactions: alkene-to-alkane hydrogenation and double-bond isomerization. On the pure platinum catalyst, ensembles of active sites are available for double-bond isomerization. However, this catalyst cokes quickly, which provides the source of hydrogen for hydrogenation of C_5 alkenes to alkane. For these reasons, the ratios of C_5 alkene/alkane and alpha/internal C_5 alkenes are lowest with the pure platinum catalyst. The introductions of Sn and K have several simultaneous effects: rupturing ensembles of Pt sites, enhancing the coverage of condensation compounds on the surfaces, and consolidating the catalyst stability. Breaking active ensembles and populating surfaces with oxygenates might suppress double-bond isomerization activity. However, the fact that deactivation is better controlled leads to reduction in hydrogen available for alkene-to-alkane hydrogenation reactions.

5. Supporting Reactions: Reaction of 6-Undecanone and Reaction of Methyl Hexanoate in the Presence of Toluene

5.1 Reactions of 6-undecanone over silica-supported Pt catalysts

Since 6-undecanone was observed as the dominant condensation product in the reaction of methyl hexanoate over silica-supported Pt catalysts, the conversion of this symmetrical ketone plays an important role in the reaction complex of the original ester. It is proposed that the symmetrical ketone serves as an intermediate product in the conversion of the original ester to final C_5 and C_6 hydrocarbons. To evaluate this hypothesis, the reactions of 6-undecanone were carried over Pt catalysts under hydrogen and inert atmospheres. The production distribution from the reaction of 6-undecanoneon 1%Pt/SiO_2 catalyst with hydrogen is presented in figure A-4.17. It is clearly seen that 6- undecanone is highly active since the complete conversion of 6-undecanone can be achieved at relatively low W/F (0.05 h). The main products are C_5 and C_6 hydrocarbons, in which the saturated alkanes are dominant. Other two groups of products include C_{11} hydrocarbons and cracking products. The C_{11} group consists of a distribution of C_{11} hydrocarbon alkane and alkenes. These products could be originated from the hydrogenation reaction of the ketone to alcohol followed by either dehydration or C-O hydrogenolysis reactions. This hydro-deoxygenation reaction of 6-undecanone could be catalyzed by Pt metal or by bifunctional catalyst. The bifunctional catalyst involves the hydrogenation activity on metal functionality and dehydration activity on acid functionality, which could come from the support. The cracking products include a range of smaller ketones (i.e decanone) and light hydrocarbons. These compounds are resulted from the de-alkylation reactions of 6-undecanone and C_5 and C_6 hydrocarbon products. In contrast to the high reactivity of 6-undecanone with hydrogen, the activity of 6-undecanone on 1%Pt /SiO_2 catalyst under inert atmosphere is rather low as seen in figure A-4.18. In fact, the catalyst shows very high activity (nearly 100% conversion) in the initial period of reaction. However, it

quickly deactivates to around 15% conversion after 1 hour of reaction. Together with this decrease in conversion, the selectivity of decomposition hydrocarbons also decreases.

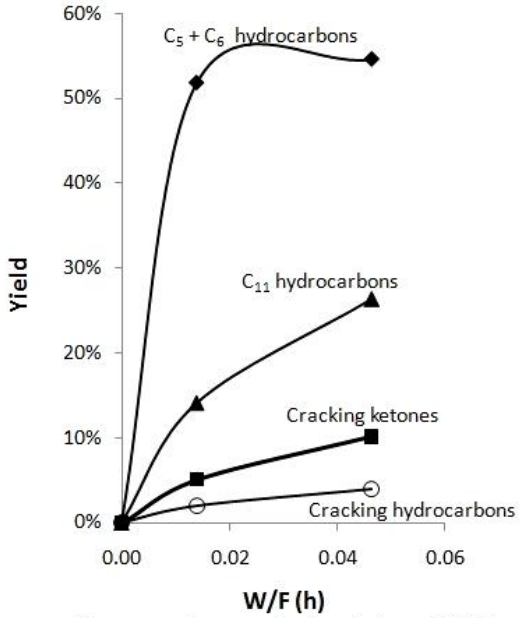

Figure A-4.17: Overall conversion and selectivity of different products from reaction of 6-undecanone on 1%Pt/SiO_2 catalyst under hydrogen. Reaction conditions: TOS = 1h, T = 653K, P = 0.1MPa

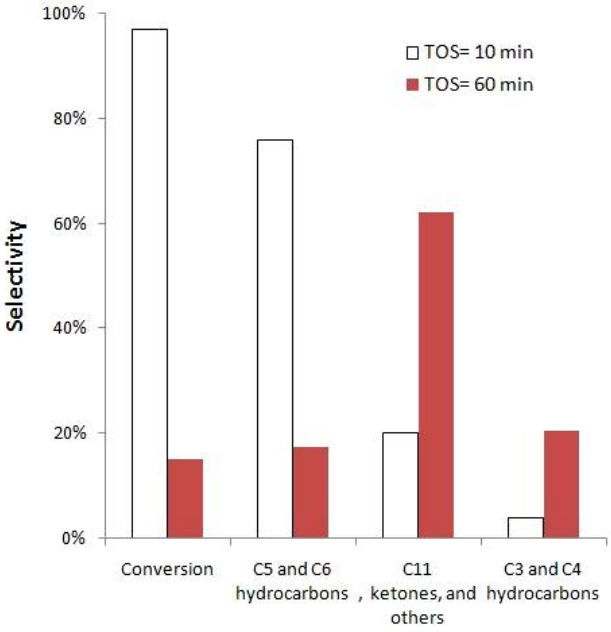

Figure A-4.18: Overall conversion and selectivity of different products from reaction of 6-undecanone on 1%Pt/SiO_2 catalyst under helium at various time on stream. Reaction conditions: W/F = 3.7h, T = 653K, P = 0.1MPa

Conversely, the contribution from group of C_{11} hydrocarbons, cracking ketones, and other products increases. The main contribution in this group comes from the other products, which are mostly dehydrogenated and aromatic-like isomers of 6-undecanone. It could be possible that the dehydrogenation of 6-undecanone followed by ring closure reactions is favored under inert atmosphere, leading to stable products that cannot be decomposed into lighter C_5 and C_6 hydrocarbons. Also, these stable oxygenates might be one of the causes for the quick deactivation of pure Pt catalyst. The temperature-programmed oxidation profile of 1%Pt/SiO_2 in figure A-4.19 depicts the oxidation of two types of residuals. The low-temperature peak could be accounted for the oxygen-containing coke, which can come from the above strongly-bounded oxygenates from 6-undecanone. The refractory portion of coke could come from the highly dehydrogenated hydrocarbons, which are decomposition products (hydrocarbons) of the original ketone. It is worth pointing out the oxidation profile of pure Pt here is different from that in the reaction of methyl hexanoate, in which mostly refractory type of coke is detected. It could be possible that in the 6-undecanone reaction, decomposition, cracking, and dehydrogenation/ring-closure reactions of ketone all occur on Pt active sites. Meanwhile, Pt mostly catalyzes the deoxygenation reactions of various oxygenate to hydrocarbons in the reaction of methyl hexanoate. Consequently, highly-dehydrogenated hydrocarbon products are the main cause for pure Pt catalyst deactivation in the latter reaction.

The deactivation is, however, not as severe for 1%Pt-1.3%Sn-0.5%K/SiO_2 catalyst compared to pure Pt catalyst. As exhibited in Figure A-4.20, at the same W/F, this catalyst also shows high initial activity. After one hour of time on stream, the conversion drops to 75% instead of 15% on Pt/SiO_2 catalyst. Nevertheless, changes in

product distribution pattern are similar as pure Pt catalyst. The longer the course of reaction is, the higher amount of stable oxygenates is detected. Figure A-4.21 shows the overall product composition of 6-undecanone with increasing W/F. All of the data points are taken at one hour time on stream. Therefore, the C_{11} hydrocarbons, cracking, and other products become dominant instead of C_5 and C_6 hydrocarbons. In fact, at low W/F, C_{11} hydrocarbons and smaller ketones are more populated compared to the stable isomers of 6-undecanone. At higher W/F, 6-undecanone only gets converted into other stable oxygenates and C_5 and C_6 compounds crack into lighter hydrocarbons. Consequently, the stable isomers of 6-undecanone outnumber C_{11} hydrocarbons and cracked ketones. As supporting evidence, Di-cosimo et al. has also reported the formation of aromatic-like oxygenates from condensation products of acetone.[60] It could be possible that the metal sites (i.e. Pt or Pt-Sn) that are active for decomposition, cracking, and dehydrogenation/ring-closure of the original ketone are deactivated quickly. Literature suggested that the dehydrogenation reaction can proceed on small ensembles of surface Pt,[61] therefore; the deactivated catalyst is still able to catalyze the dehydrogenation reaction of 6-undecanone. This also explains why a maximum in yield of C_5 and C_6 hydrocarbons at medium W/F is observed. This is in good agreement with the fact that the temperature-programmed oxidation profile of 1%Pt-1.3%Sn-0.5%K/SiO_2 catalyst shows a significantly higher amount of carbon residual compared to that of 1%Pt/SiO_2 catalyst. The larger contribution to carbon residual on spent 1%Pt-1.3%Sn-0.5%K/SiO_2 comes from the oxygen-containing condensate. The formation of these species might occur on metal active sites, leading to suppression of the most structure sensitive reaction such as ketone decomposition reaction to hydrocarbons. This is very likely since 6-

undecanone bears two long alkyl chain lengths, which could increase the possibility of forming carbon-metal bond compared to oxygen-metal bond. Co-feeding 6-undecanone with other methyl esters (i.e. methyl butyrate and methyl hexanoate) did not help facilitating the conversion of this ketone. The adsorption competition created by co-feeding toluene and 6-undecanone (molar ratio 25:1) did not alter the activity of the ketone as well. The fact that 6-undecanone is seen to be produced and converted totally in the reaction of methyl ester suggests that decomposition reaction of this compound is facilitated by hydrogen. As mentioned above, hydrogen is also detected as one of the light gases released from methyl ester reaction. It could be possible that hydrogen inhibits the dehydrogenation route of the ketone so that much less dehydrogenated oxygenate is produced from the ketone. Consequently, the metal function of the catalyst is kept active for the decomposition reaction to hydrocarbons.

5.2 Reaction of methyl hexanoate over 1%Pt-1.3%Sn-0.5%K/SiO_2 catalyst in the presence of toluene

In the reaction complex of methyl hexanoate, the condensation activity of this ester appears to be relatively high at low W/F or high coverage of the feed on the catalyst surface. This is reflective by the dominating percentage of condensation products at low conversion of methyl hexanoate. To further verify the formation of these products, experiments of co-feeding methyl hexanoate with toluene were carried in both continuous flow and pulse modes. In addition, Pt-Sn-K catalyst was chosen as a representative catalyst. In the purpose of creating competitive adsorption between toluene and methyl ester on the surface, a high molar ratio (toluene:ester = 25:1) was chosen. The conversion of pure ester is also adjusted to be relatively low so that the

condensation species become dominating products. As displayed in figure A-4.22, the overall conversion of methyl hexanoate is lower in the presence of toluene due to its competitive adsorption. The selectivity of final C_5 and C_6 products is significantly higher with the mixed feed. Conversely, greater amount of condensation products is seen with pure methyl hexanoate feed. Without the co-adsorption of toluene on the catalyst surface, the ester might be able to come close to more form condensation products. When toluene competes for same active sites, methyl hexanoate converts more into final hydrocarbon products via direct decarboxylation/decarbonylation reactions. The results from continuous flow mode are further confirmed by the pulse studies. Figure A-4.23 shows the evolutions of different products from pulsing methyl hexanoate over 1%Pt-1.3%Sn-0.5%K/SiO_2 catalyst recorded by the mass spectroscopy. Among other products (i.e. C_5 hydrocarbons), the formation of 6-undecanone is clearly visualized. However, when pulsing a mixture of toluene and methyl hexanoate (25:1) over the same catalyst, no sign of heavy ketone is observed as seen in figure A-4.24. Similar to the results seen with the reaction in flow mode, the methyl hexanoate here converts directly to hydrocarbons and light gas.

6. Proposed Reaction Schemes for Methyl Ester Conversions on Silica-Supported Pt Catalysts

As previously mentioned, under hydrogen atmosphere, the reaction of methyl octanoate over 1% Pt/Al_2O_3 yields mostly C_7 hydrocarbons via decarboxylation and decarbonylation routes. C_7 compounds can come from various oxygenates, including the original ester, derived acids, aldehyde, and alcohol.

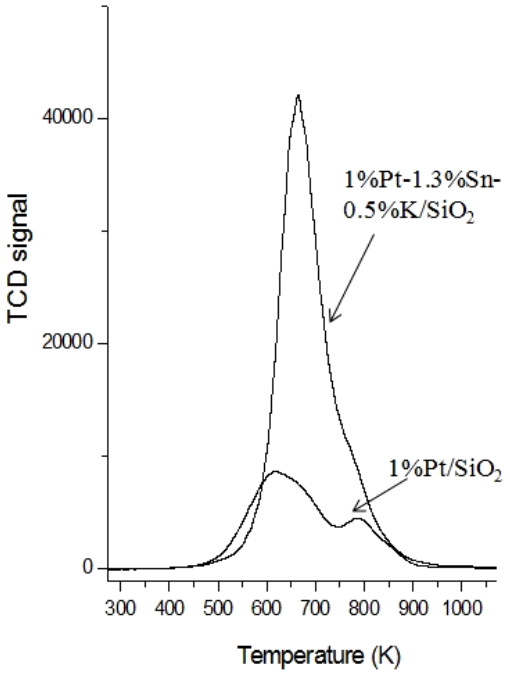

Figure A-4.19: Temperature programmed oxidation of spent $1\%Pt/SiO_2$ and $1\%Pt\text{-}1.3\%\text{-}0.5\%K/SiO_2$ catalysts in the reaction of 6-undecanone under helium. Reaction conditions: W/F = 3.7h, T = 653K, P = 0.1MPa

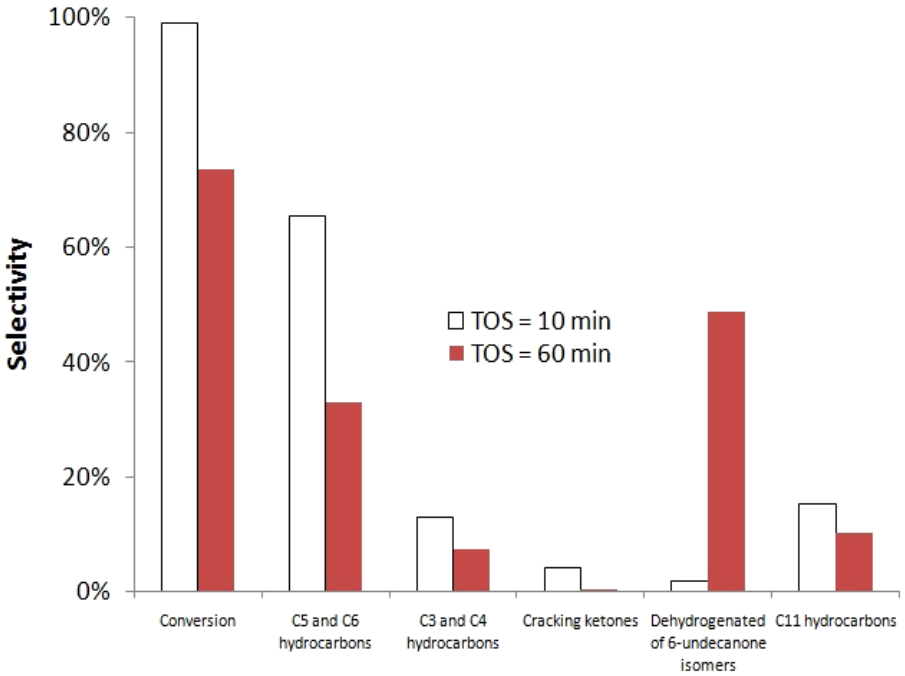

Figure A-4.20: Overall conversion and selectivity of different products from reaction of 6-undecanone on $1\%Pt\text{-}1.3\%\text{-}0.5\%K/SiO_2$ catalyst under helium at various time on stream. Reaction conditions: W/F = 3.7h, T = 653K, P = 0.1MPa

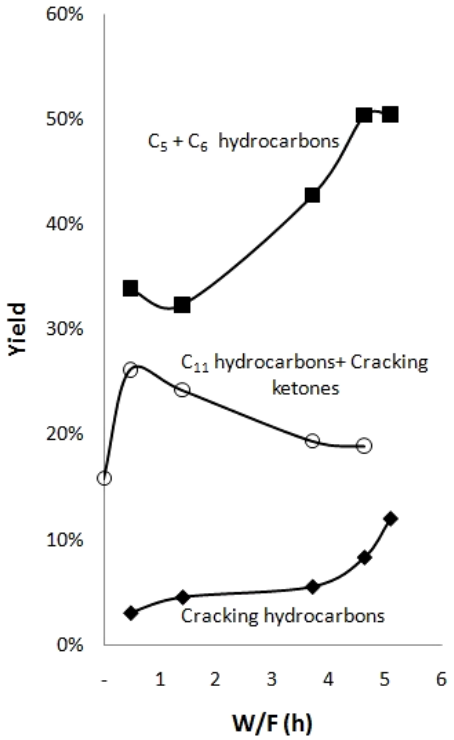

Figure A-4.21: Product distribution from reaction of 6-undecanone on 1%Pt-1.3%-0.5%K/SiO_2 catalyst under helium at various time on stream. Reaction conditions: T = 653K, P = 0.1MPa

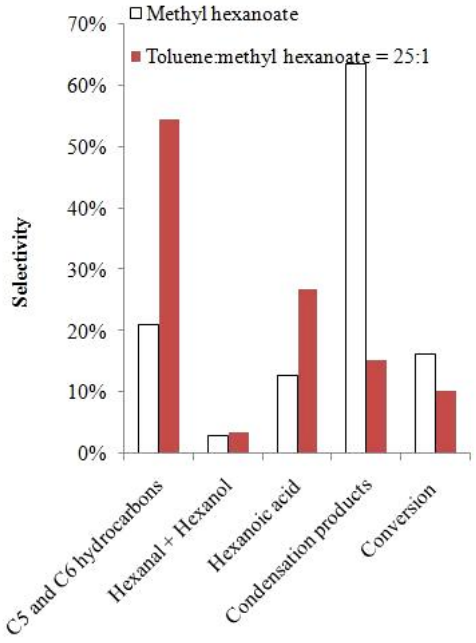

Figure A-4.22: Product distribution from reaction of methyl hexanoate and mixture of toluene and methyl hexanoate (molar ratio 25:1) on 1%Pt-1.3%-0.5%K/SiO_2 catalyst under helium. Reaction conditions: T = 653K, P = 0.1MPa

Figure A-4.23: Evolution of different products from pulsing methyl hexanoate over 1%Pt-1.3%-0.5%K/SiO_2 catalyst bed under helium. Reaction conditions: T = 653K, P = 0.1MPa

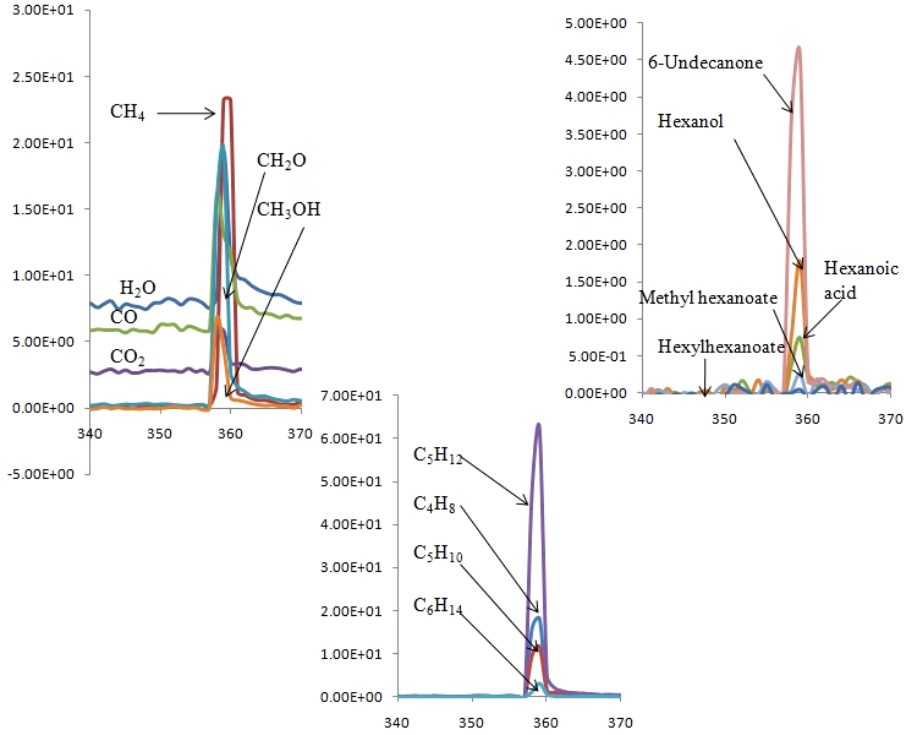

Figure A-4.24: Evolution of different products from pulsing mixture of toluene and methyl hexanoate (25:1) over 1%Pt-1.3%-0.5%K/SiO_2 catalyst bed under helium. Reaction conditions: T = 653K, P = 0.1MPa

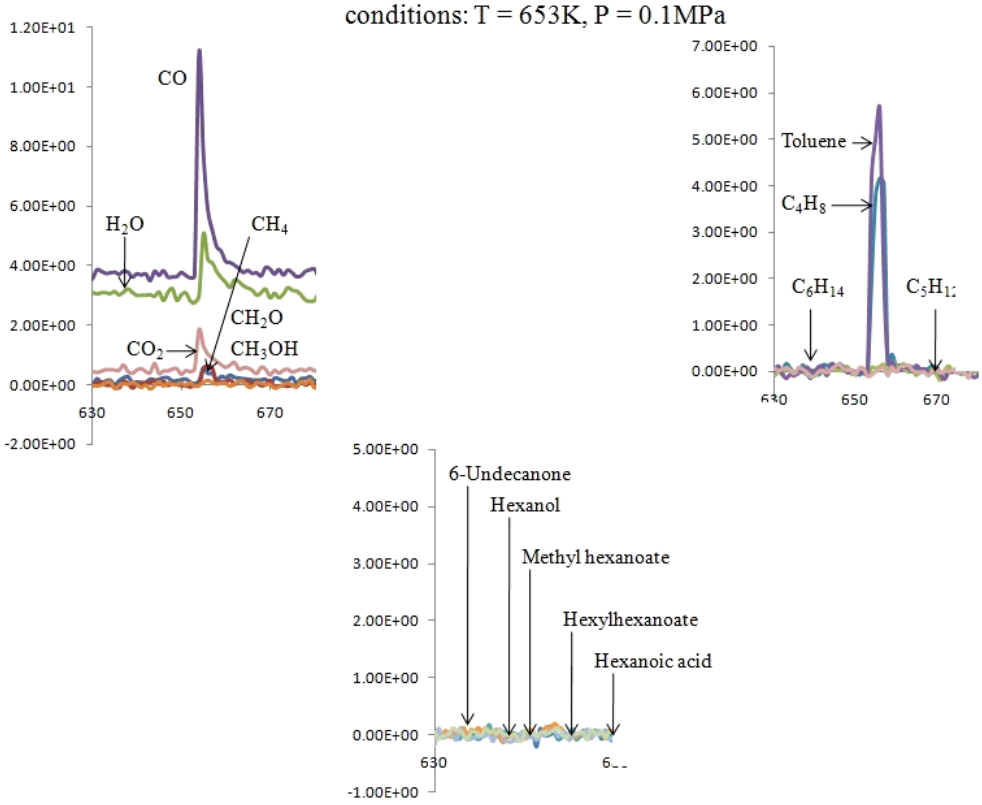

Since the presence of hydrogen suppresses ketonization reaction on support (i.e. alumina or silica), most of the activity of the ester occurs on Pt surface. Although on Pt surface, η^1 is reported to be the dominant species for adsorbed aldehyde or alcohol, η^2/η^1 ratio increases with hydrogen adsorbed on the surface. Same trend has been observed with modification of Pt (111) surface with potassium ion. Both adsorbed hydrogen atoms [62] and potassium ions decrease the metal work function, which promotes the population of η^2 species. η^1 Species desorbs molecularly. The deoxygenation reaction of aldehyde and alcohol most likely undergoes η^2 intermediate, which will further decompose via acyl intermediate. Different from aldehyde and alcohol, the first interaction between the carboxylic acid molecules with the noble metal (i.e. Pd) surface might occur via bonding with carboxylate or η^1 species as mentioned in chapter I. In fact, the carboxylate mode is energetically favored than the η^1 configuration. However, the adsorption configuration of ester on metal surface might be different from that of carboxylic acid. It is reported that the dissociation of methyl ester (i.e. methyl benzoate) on metal oxides proceeds via alkoxide C-O bond cleavage to form RCO and OCH_3 portions. The dissociation to release CH_3^+ fragment would be unfavorable due to the instability of primary carbon cation. However, on metal surface (i.e. Pt), two C-O cleavages to form RCO and RCOO species are possible since both carboxylic acids and alcohol/aldehyde are observed as reaction intermediates under hydrogen condition. In one case, the two adsorbed species, RCO and OCH_3, can either undergo hydrogenation or decomposition reactions depending on the reaction conditions. In the reaction of methyl octanoate over supported Pt catalysts in hydrogen, the dominant products are C_7 hydrocarbons, thus; it is likely that RCO intermediate forms the acyl species, which will undergo decarbonylation reaction to

produce C_7 hydrocarbon products. In other case, the carboxylate intermediate (ROO) could undergo decarboxylation to form corresponding hydrocarbon and CO_2 as well. Besides carboxylic acid and alcohol/aldehyde as observed intermediates, heavy ketone is considered as one of the intermediates since it is formed and converted to hydrocarbons. However, its production is minimal due to the fact that the presence of hydrogen is known to inhibit the formation of heavy ketone because hydrogen in fact promotes other reaction routes. The formation of ketone is known to occur on various oxides. In case of Pt/SiO_2 catalyst, the ketonization reaction might happen on silica support via coordinatively unsaturated sites. The ketone consequently undergoes decomposition reaction via η^1 species or oxametallacycles species. The detailed reaction mechanism of methyl esters in hydrogen atmosphere is exhibited in figure A-4.25.

Without hydrogen, the product distribution has changed significantly in the reaction of methyl hexanoate over Pt/SiO_2 catalyst. After 1 hour of reaction, most of the activity goes to condensation instead of deoxygenation. The adsorbed configuration of ester on Pt surface might be similar to the previous reactions with hydrogen. However, monometallic Pt cannot stand the deactivation causing by deposition of highly dehydrogenated compounds derived from olefin products. Therefore, decarboxylation and decarbonylation reactions of the ester on Pt surface last shortly. In fact, under hydrogen-deficient atmosphere, condensation and ketonization reactions on oxide surface, silica, are enhanced. The ketone is quickly transformed into hydrocarbons on clean Pt ensembles. However, those active sites are covered with coke rapidly due to low-coke-tolerance characteristic of pure platinum catalyst. This explains why the hydrocarbon yield remains lows on deactivated Pt/SiO_2.

The addition of Sn and K certainly promotes the adsorption of ester via interaction of either Sn or K cations with carbonyl oxygen atoms. In addition, K species (i.e. KOH) and Sn species (i.e. SnO_x) are active catalysts for ketonization of carboxylic acids and esters. The ketonization of methyl hexanoate over K species might via decomposition of surface potassium carboxylates, which commonly happened with alkaline metals. For a transition metal like Sn, the affinity for oxygen is relatively high, therefore; Sn component in the Pt-Sn-K catalyst could attract the adsorption of methyl esters in the form of carboxylates. Formation of ketones on Sn oxide surfaces can occur either via ketene-like intermediate or bimolecular carboxylate mechanism. It is possible that from fraction of reduced Sn atoms might be able to catalyze deoxygenation reaction. It is certain that most of the deoxygenation activity happens on Pt or Pt-Sn ensembles, where coke tolerance is much improved. Therefore, Pt-Sn-K/SiO_2 catalyst converts methyl hexanoate more effectively than pure Pt/SiO_2.

7. Conclusion

There are several main points withdrawn from this work.

- The reactions of methyl hexanoate over supported Pt catalysts without hydrogen precede via different reaction pathways. Since the transformation of the ester to final hydrocarbon products via condensation intermediates is dominant, the performance of all tested catalysts will be analyzed under the light of this pathway.

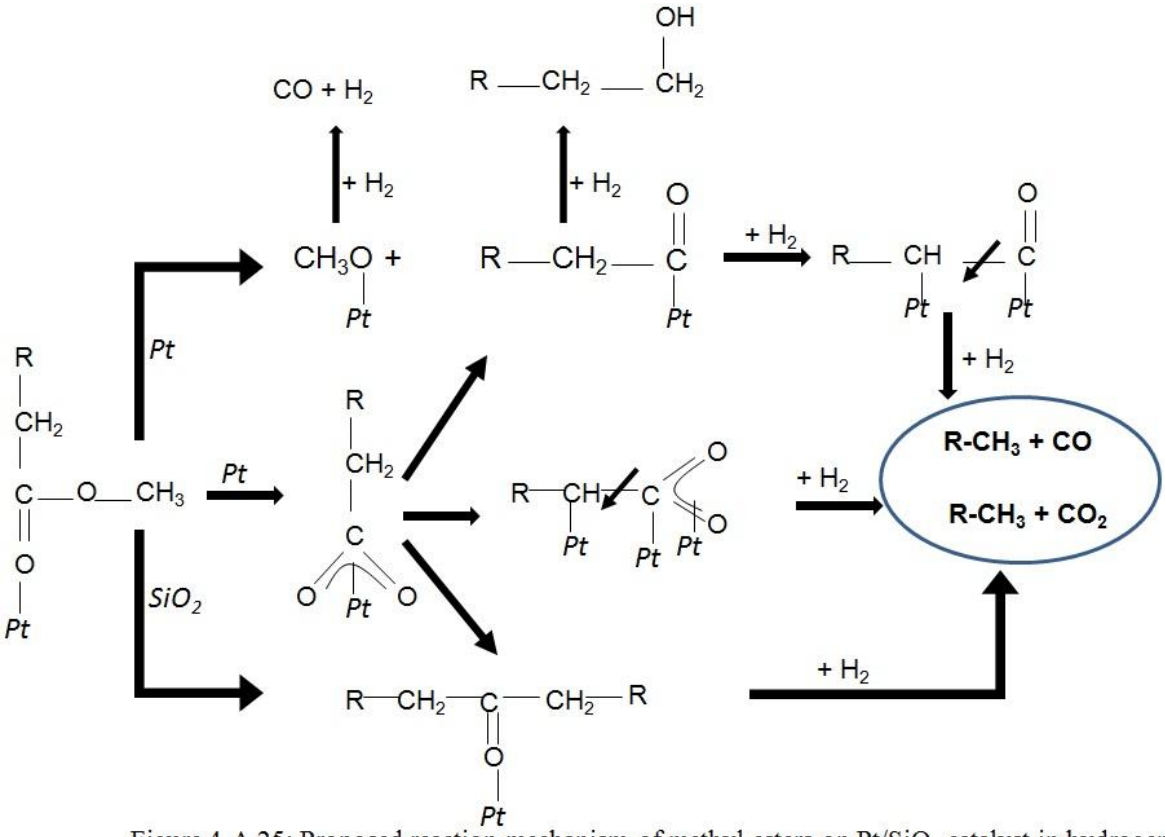

Figure 4-A.25: Proposed reaction mechanism of methyl esters on Pt/SiO_2 catalyst in hydrogen

- Both carboxylic acid and alcohol/aldehyde intermediates completely convert into hydrocarbons without hydrogen. However, the decomposition of 6-undecanone is strongly facilitated in the presence of hydrogen compared to helium. In order to achieve the complete conversion of this intermediate during methyl hexanoate reaction, the hydrogen source could be supplied from other side reactions such as coking.
- As a support, silica still shows a low level of conversion of methyl hexanoate, in which condensation products dominate. It could be possible that silica decomposes the methyl ester into carboxylate species, which either couple to form these condensation products or oligomerize to form "oxygenate" type of condensate on silica.
- 1% Pt/SiO_2 is an active catalyst in the reaction of methyl hexanoate. Pt active sites are required in decomposing the heavy products into C_5 and C_6 hydrocarbons. However, pure platinum catalyst deactivates quickly due to the strongly adsorbed dehydrogenated species. This is accordingly reflected by the oxidation profile of the spent Pt catalyst. The dehydrogenation reactions might in turn provide a source of hydrogen, which helps to clean and maintain the activity of silica support. That is why the activity of deactivated $1\%Pt/SiO_2$ catalyst is considerably higher than that of silica.
- Addition of Sn into Pt/SiO_2 catalyst shows a substantial improvement in catalyst stability. It is the Pt-Sn alloys, which are more coke tolerant than pure Pt, that retain the conversion of the condensation products to hydrocarbons.

- Further enhancement is observed with introduction of potassium. The combinational Pt-Sn-K catalysts comprise of two important functions. These are: Sn-K oxide species condensating the original ester and Pt-Sn alloys converting condensation intermediates into final hydrocarbon products. The balance of these two functions helps to maintain the stability of the catalyst. In details, the additions of both Sn and K have several simultaneous effects. Firstly, the Pt ensembles are ruptured owing to Sn and K coverage and formation of Pt-Sn alloy. Secondly, potassium enhances the segregation of Sn out of Pt-Sn alloy. Adsorption energy of the ester is reduced on Pt-Sn alloy due to the facilitated interaction of the ester molecule with cationic Sn species. Among all tested Pt-Sn-K catalysts, 1%Pt-1.3%Sn-0.5%K/SiO_2 exhibits the highest activity and stability in reaction of methyl hexanoate. When excess potassium (loading 1.5 %) is used, a great deal of coupling accumulation occurs, which results in rapid coking of the catalyst.

8. References

[1] DOE Report "Top Value Added Chemicals from Biomass Volume I—Results of Screening for Potential Candidates from Sugars and Synthesis Gas", August 2004

[2] Mavrikakis, M., and Barteau, M. A., *J. Mol. Catal. A: Chem.* **131,** 135 (1998)

[3] Benziger, J.B., and Madix, R. J., *J. Catal*. **65**, 49 (1980)

[4] Davis, J. L, and Barteau, M.A., *Surf. Sci.* **256**, 50 (1991)

[5] Doornkamp, C., and Ponec, V. *J. Mol. Catal. A: Chem.* **162**, 19 (2000)

[6] Peng, X.D., and Barteau, M.A., *Catal. Let.* **7**, 395 (1990)

[7] Pallassana, V., and Neurock, M., *J. Catal.* **209**, 289 (2002)

[8] Brands, D. S., Poels, E. K., and Bliek, A., *Appl. Catal. A: Gen.* **184**, 279 (1999)

[9] Agarwal, A. K., Cant, N. W., Wainwright, M. S., and Trimm, D. L., *J. Mol. Catal.* **43**, 79 (1987)

[10] Rachmady, W., and Vannice, M. A., *J. Catal.* **192**, 322 (2000)

[11] De Lange, M.W., Thesis, University of Twente, 2000.

[12] Rachmady, W., and Vannice, M. A., *J. Catal.* **207**, 317 (2002)

[13] Sakata, Y., Tol-Koutstaal, C. A. V., and Ponec, V., *J. Catal.* **169,** 13 (1997)

[14] Pestman, R., Van Duijne, A., Pieterse, J.A.Z., and Ponec , V., *J. Mol. Catal. A: Chem.* **103**, 175 (1995)

[15] Kim, K. S., and Barteau, M.A., *J. Catal.* **12**, 353 (1990)

[16] Pestman, R., Koster, R. M., Van Duijne, A., Pieterse, J.A.Z., and Ponec , V., *J. Catal.* **168**, 265 (1997)

[17] Maier, W. F., Roth, W., Thies, I., and Rague Schleyer P. v., *Chem. Ber.* **115**, 808 (1982)

[18] Claus, P., Lucas, M., and Lucke, B., *Appl. Catal. A: Gen.*, **79**, l (1991)

[19] Da Rocha Filho, G. N., Brodzki, D., and Djega-Mariadassou, G., *Fuel* **72** 543 (1993)

[20] Gusmao, J., Brodzki, D., Djega-Mariadassou, G., and Frety, R., *Catal. Tod.* **5**, 533 (1989)

[21] Snare, M., Kubickova, I., Maki-Arvela, P., Eranen, K., Murzin, D.Y., *Chem. Ind.* **115,** 415 (2005)

[22] Snare, M., Kubickova, I., Maeki-Arvela, P., Eraenen, K., Murzin, D.Y., *Ind. Eng. Chem. Res.* **45,** 5708 (2006)

[23] Klimkiewicz, R., and Teterycz, H., *React. Kinet. Catal. Lett.* **75,** 165 (2002)

[24] Glinski, M., and Kijenski, J., *React. Kinet. Catal. Lett.* **69**, 123 (2000)

[25] Do, P. T., Chiappero, M., Lobban, L. L., and Resasco, D. E, *Cat. Let.* **130**, 9 (2009)

[26] Cortright, R.D., and Dumesic, J. A., *J. Catal.* **148**, 771 (1994)

[27] Cortright, R.D., and Dumesic, J. A., *J. Catal.* **157**, 576 (1995)

[28] Hill, J. M., Cortright, R.D., and Dumesic, J.A., *Appl. Catal. A: General* **168** 9 (1998)

[29] Brinkmeyer, F. M., and Rohr, D. F., U.S. Patent 4,866,211 (1987)

[30] Li, Y.X., Kladunde, K. J., and Davis, B. H., *J. Catal.* **128**, 1 (1991)

[31] Meitzner, G., Via, G. H., Lytle, F.W., Fung, S.C., and Sinfelt, J. H., *J. Phys. Chem.* **92**, 2925 (1988)

[32] Imai, T., and Hung, C.W., U.S. Patent 4430517 (1983)

[33] Cortright, R. D., and Dumesic, J. A., *Appl. Catal. A* **129**, 101 (1995)

[34] Stagg, S.M., Querini, C. A., Alvarez, W. E., and Resasco, D. E., *J. Catal.* **168**, 75 (1997)

[35] Verbeek, H., and Sachtler, W. M. H., *J. Catal.* **42**, 257 (1976)

[36] Rodrıguez, D., Sanchez, J., and Arteaga G., *J. Mol. Catal. A: Chem.* **228**, 309 (2005)

[37] Llorca J., Delapiscina P. R., Fierro J. L. G., Sales J., and Homs, N., *J. Catal.* **156**, 139 (1995)

[38] Ramallo-Lpez, J. M., Santori, G. F., Giovanetti, L., Casella, M. L., Ferretti, O. A., and Requejo, F. G., *J. Phys. Chem. B.* **107**, 11441 (2003)

[39] Aika, K., Shimazaki, K., Hattori, Y., Ohya, A., Ohshima, S., Shirota, K., and Ozaki, A., *J. Catal.* **92**, 296 (1985)

[40] Handy, B. E., Dumesic, J. A., Sherwood, R. D., and Baker, R. T. K., *J. Catal.* **124**, 160 (1990)

[41] Sooknoi, T., Danuthai, T., Lobban, L. L., Mallinson, R. G., and Resasco, D. E., *J. Catal.* **258**, 199 (2008)

[42] Bjørn Donnis, B., Egeberg, R. G., Blom, P., Knudsen, K. G., Top Catal **52**, 229 (2009)

[43] Snarea, M., Kubičkováa, I., Mäki-Arvelaa, P., Chichovaa, D., Eränena, K., and Murzin, D.Y., *Fuel* **87**, 933 (2008)

[44] Van Druten, G.M.R., and Aksu, L., and Ponec, V. *Appl. Catal. A: Gen*. **149**, 181 (1997)

[45] Yoon, C., Yang, M. X., and Somorjai, G. A., *J. Catal.* **176** 35 (1998)

[46] Foger, K., and Anderson, J. R., *J. Catal.* **54**, 318 (1978)

[47] King, S. T., and Strojny, E. J., *J. Catal.* **76**, 214 (1982)

[48] Vansant, E.F., Van Der Voort, P., and Vrancken, K.C**.,** *Stud. Surf. Sci. Catal.* , **93** (1995)

[49] Davis, J.L., and Barteau, M. A., *Surf. Sci.* **235**, 235 (1990)

[50] Davis, J.L., and Barteau, M. A., *Surf. Sci.* **208,** 383 (1989)

[51] Anderson, J. R., *Adv. Catal.* **30**, 1 (1973)

[52] Cadus, L. E., Gorriz, O. F., and Rivarola, J. B., *Ind. Eng. Chem. Res.* **29**, 1143 (1990)

[53] Fiedorow, R., Przystajko, W., and Sopa, M., *J. Catal.* **68**, 33 (1981)

[54] Ponec , V., *Appl. Catal. A: Gen.* **149,** 27 (1997)

[55] Marinelli, T. B. L W., and Ponec, V. *J. Catal.* **156**, 51 (1995)

[56] Park,Y.K., Ribeiro,F. H., and Somorjai, G. A, *J. Catal.* **178,** 66 (1998)

[57] Shen, J., Hill, J. M., Watwe, R. M., Spiewak, B. E., Dumesic, J. A., *J. Phys. Chem. B* **103**, 3923 (1999)

[58] Park, Y. K., Ribeiro, F. H., and Somorjai, G. A., *J. Catal.* **178**, 66 (1998)

[59] Elliott, D. J., and Pennella, F., *J. Catal.* **119**, 359 (1989)

[60] Di Cosimo, J. I., D´ıez, V. K., Xu, M., Iglesia, E. , and Apestegu, C. R *J. Catal.* **178**, 499 (1998)

[61] Biloen, P., Dautzenberg, F. M., and Sachtler, W. M. H., *J. Catal.* **50**, 77 (1977)

[62] Christmann, K., and Ertl, G., *Surf. Sci.* **60**, 365 (1976)

CHAPTER V: REACTIONS OF METHYL DODECANOATE AND TRIACETIN

1. Reactions of Methyl Dodecanoate

In the previous section, reactions of probe molecules (methyl octanoate and methyl hexanoate) are tested over a range of supported Pt catalysts. The basic reaction chemistry is analyzed and different product formation pathways are proposed. That information becomes a useful tool to explore the following reactions of a real fatty acid methyl ester: methyl dodecanoate or methyl laurate. Conversions of two molecules share the common groups of liquid products including: cracking products, decarboxylation/decarbonylation hydrocarbons, hydrogenation hydrocarbons, 1-oxygen-containing products and condensation/heavy products. There are also some light gases and oxygenates such as CO, CO_2, CH_4, formaldehyde, and methanol. The light gas analysis has recorded that CO is dominant. Having C_{12} methyl ester as a feed, C_{11} and C_{12} hydrocarbons are major products. Since the objectives of this reaction is to maximize the total alkene yields and activity and stability of the catalysts and minimize the cracking these C_{11} and C_{12} alkenes are desirable. In turn, light hydrocarbons, dienes, aromatics, and heavies become undesirable. To achieve the above targets, the reactions are mostly carried out in plug flow reactor and under inert gas (i.e. nitrogen). The operating pressure and temperature are 3.4 MPa and 653 K, respectively. The products are collected in liquid during the course of reaction. As seen in the preceding section, rapid catalyst deactivation is a major problem with inert gas reaction. Therefore, hydrogen partial pressure is strictly controlled here in order to optimize both catalyst lifetime and total

alkene yields. The tested catalysts include: 1%Pd/Al_2O_3, 1%Pt/Al_2O_3, 1%Pt-0.5%Sn/SiO_2, 1%Pt-1.3%Sn/SiO_2, and 1%Pt-1.3%Sn-0.5%K/SiO_2.

1.1 Conversion of methyl dodecanoate over 1%Pd/Al_2O_3 and 1%Pt/Al_2O_3 catalysts

Besides platinum, palladium is a good catalyst for conversion of carboxylic acids and alkyl esters. Maeir et al. has first claimed the high activity of Pd/SiO_2 catalyst in decarboxylation of hexanoic acid in vapor phase.[1] Recently, it has been reported by Murzin et al. that among all tested catalysts, 5%Pd/C turns out as the most effective catalyst in reaction of stearic acid and ethyl stearate in liquid phase. [2-3]For that reason, both Pt and Pd supported on alumina are first tested for the reaction of methyl laurate. Table A-5.1 tabulates the average conversion of methyl laurate over 1%Pd/Al_2O_3 and 1%Pt/Al_2O_3 under nitrogen flow and after 4 hour time-on-stream. At the same W/F, Pt catalyst results in higher accumulated conversion than that of Pd catalyst (38% versus 24%). Although both catalysts produce mostly C_{11} hydrocarbons, greater amount of heavy products are observed with Pt/Al_2O_3. When 5% of hydrogen in argon replaces nitrogen, the activity of platinum catalyst is much improved. The average conversion after four hour reaction increases to almost 100%. Together with activity improvement, the amount of heavy products is reduced. This result is in a good agreement with the reaction of methyl octanoate over Pt/Al_2O_3 in helium versus in hydrogen. Hydrogen helps to limit the condensation reactions. In addition, hydrogen might help to desorb the surface-adsorbed species that are potential coking precursors. However, the NMR analysis has confirmed the greater percent of saturated C_{11} hydrocarbons is present in the liquid products from this reaction.

Catalyst	**1%Pt/Al_2O_3**	**1%Pd/Al_2O_3**	**1%Pt/Al_2O_3**
W/F (h)	0.3	0.3	0.3
Reduction pressure (M Pa)	3.4	3.4	3.4
Reduction temp (K)	653	653	653
Reduction time (h)	2	2	2
Gas (mL/min)	400 of N_2	400 of N_2	400 of 5% H_2 in Argon
Average Conversion (0 to 4 h TOS)	**38.2%**	**24.4%**	**94.9%**
Cracking	2.6%	2.9%	9.1%
C_{11} olefins/parafin	27.9%	13.6%	82.2%
C_{11} dienes + aromatics	0.4%	0.5%	0.5%
C_{12} olefins/parafin	0.3%	0.5%	1.2%
C_{12} dienes + aromatics	0.4%	0.2%	0.7%
C_{12} alcohol/aldehyde	0.2%	2.0%	0.1%
C_{12} feed and dehydrogenated feed	61.8%	75.6%	5.1%
C_{12} acid	2.7%	3.3%	0.3%
Heavies	4.1%	1.4%	0.8%

Table A-5.1: Product distribution of reactions of methyl dodecanoate over different supported Pt and Pd catalysts

Catalyst	**1%Pt-1.3%Sn/SiO_2**	**1% Pt-0.5%Sn/SiO_2**	**1%Pt/Al_2O_3**	**1%Pt-1.3%Sn-0.5 %K/SiO_2**
Average conversion (0 to 2.5 h TOS)	**24.8%**	**46.0%**	**79.9%**	**50.0%**
Cracking	14.2%	8.4%	0.5%	2.6%
C_{11} olefins	3.3%	24.9%	67.0%	33.2%
C_{11} dienes + aromatics	0.5%	1.2%	3.6%	2.2%
C_{12} olefins	2.2%	3.5%	6.7%	3.9%
C_{12} dienes + aromatics	1.9%	1.7%	0.7%	1.8%
C_{12} alcohol	0.3%	1.4%	0.8%	1.6%
C_{12} feed and dehydrogenated feed	75.2%	54.0%	20.1%	49.8%
C_{12} acid	1.7%	3.1%	0.5%	3.5%
Heavies	0.7%	1.7%	0.1%	1.3%
Average conversion (2.5 to 5 h TOS)	**26.3%**	**17.1%**	**32.8%**	**37.0%**
Cracking	16.4%	3.2%	0.7%	2.7%
C_{11} olefins	1.9%	7.5%	25.9%	20.8%
C_{11} dienes + aromatics	0.6%	0.2%	1.3%	2.2%
C_{12} olefins	2.8%	1.0%	2.3%	2.2%
C_{12} dienes + aromatics	0.7%	1.9%	0.2%	2.4%
C_{12} alcohol	0.2%	0.9%	0.8%	1.0%
C_{12} feed and dehydrogenated feed	73.7%	82.9%	67.2%	63.2%
C_{12} acid	1.4%	0.5%	1.3%	2.9%
Heavies	0.9%	1.9%	0.4%	2.6%
Conversion Ratio	**0.06**	**0.63**	**0.59**	**0.26**

Table A-5.2: Product distribution of reactions of methyl dodecanoate on Pt/Al_2O_3, $Pt\text{-}Sn/SiO_2$, and $Pt\text{-}Sn\text{-}K/SiO_2$ catalysts at T = 653 K, W/F = 0.46 h, Gas rate = 400 mL/min of nitrogen

In summary, the first reaction attempt has shown that 1%Pt/Al_2O_3 is a better catalyst compared with 1%Pd/Al_2O_3. Increasing partial pressure of hydrogen creates a positive impact on the overall catalyst activity but hurts the selectivity of alkenes by hydrogenating those alkenes into saturated hydrocarbons.

1.2 Conversion of methyl dodecanonate over Pt-Sn-K/SiO_2 catalysts

Since the presence of hydrogen in the gas flow impairs total alkene selectivity, the inert atmosphere is still preferred. However, the major problem with inert gas is quick catalyst deactivation. As seen in table A-5.2, the conversion drop, which measures the percent difference in average conversion after 2.5 hour and 5 hour time on stream, is 60% for 1%Pt/Al_2O_3 at W/F of 0.46 hour. When 0.5 % Sn is added into Pt, the catalyst activity drops due to Pt active site covered by Sn. Besides, the stability of the catalyst is not significantly improved. When greater amount of Sn (1.3%Sn) is doped, the catalyst stability is greatly enhanced. At the same W/F, the conversion drop is almost negligible for the bimetallic catalyst (6%). Pure Pt catalyst is more active at the beginning of the reaction since the initial average conversion for Pt/Al_2O_3 is 3 time higher than that of the Pt-Sn catalyst (80% versus 25%). This high activity drops quickly with time due to low coking resistance of pure platinum catalyst. The adsorption strength of olefinic coke precursors is reduced on Sn-modified Pt catalyst as seen in many other works.[4] Therefore, the catalyst surface is kept cleaned for the conversion of methyl laurate.

The noticeable drawback of this bimetallic catalyst is excessive cracking. Cracking products include low-molecular hydrocarbons and methyl esters. Since the original feed composes of a long carbon backbone, most of the cracking activity occurs along that backbone. These products make up about 50% product selectivity. Lowering

the reaction temperature by 50 K (from 653 K to 623 K) does not result in reduction in cracking activity. It is the acidity, which originates from residual precursor chlorine on the catalyst, causing this undesirable cracking. According to the above results, even though the reduction step has removed majority of precursor chlorine, there is still some chlorine remaining on the reduced 1%Pt-1.3%Sn/SiO_2 surface reported by XPS results. Others researchers also observed intensive cracking with alumina-supported Pt-Sn catalysts prepared by chloride precursors in dehydrogenation reactions of normal alkanes.[5] To neutralize the undesirable acid sites, alkaline metals (i.e. potassium) are added. In fact, the study of butane dehydrogenation on silica-supported Pt-Sn-K has shown that the selectivity of iso-butene is enhanced while the cracking selectivity is greatly suppressed. Table A-5.2 displays that addition of 0.5%K does help to minimize the cracking; however; the catalyst stability is significantly impaired (conversion drop equal to 26%). This is an expected result since many researchers has reported that the presence of potassium partially ruptures the interaction between Pt and Sn. Since the molar ratio of Pt: Sn: K is 1:2:2.5, part of the potassium forms KCl and the rest interacts more closely with Sn. Therefore, some of the Sn contributing to the alloy phase is segregated. This alternates the compositions and status of Pt-Sn alloy, which is responsible for high coking resistance of the bimetallic Pt-Sn catalyst.

In summary, both 1% Pt/Al_2O_3 and 1% Pd/Al_2O_3 appears as effective catalysts for methyl laurate conversions under inert gas medium. The dominant products are C_{11} hydrocarbons, which consists of mostly alkenes. Although the former produces greater amount of heavy products, it is more active than the latter. This higher activity might be attributed to the higher dispersion of Pt catalyst. The stability of the pure Pt catalyst is

significantly improved with the addition of 1.3%Sn, making Pt:Sn molar ratio equal to 1:2. Nevertheless, this bimetallic catalyst produces excessive cracking of both original ester and hydrocarbon products due to the presence of acidity associated with remaining chlorine from precursors. To neutralize those acid sites, 0.5%K is added into Pt-Sn catalyst. On 1%Pt-1.3%Sn-0.5%K/SiO_2, the cracking activity is well controlled. However, the stability is impaired owing to alloy Sn segregated by potassium. In addition to the catalyst composition, there are several operating parameters one could vary to obtain the optimal catalyst stability and total alkene yields such as: reduction time (4.5 hour versus 2 hour), reduction temperature (723 K versus 653 K), and potassium loading (1.5% versus 0.5%). It is important to notice that the conversion drop is a function of initial conversion as well. It will be more accurate if the catalyst comparison is done at the same level of initial conversions.

2. Reactions of Triacetin

Previously the conversions of methyl esters into chemical and fuel products have been shown. It is learned that supported noble metal catalysts (i.e. Pt and Pd) are active and selective for deoxygenation of methyl esters into hydrocarbons. In fact, methyl esters are originally derived from triglyceride compounds. Additionally, both the former and the latter share the same functional group (-COO-), which is commonly present in the mixture of compounds in renewable sources. The chemistry of ester functional group in methyl esters is well evaluated in the previous sections. However, the details of reactions of –COO- group in triglyceride are unknown. Therefore, this section will give more insights on the conversion of a model triglyceride compound, triglyceride of acetic acid or triacetin, on supported metal catalysts.

Before analyzing the effect of different catalysts on the products of triacetin, it will be informative to introduce the possible products evolved during the reaction of triacetine. Besides the light gases such as CO_2, CH_4, CO, transformation of triacetin over supported metal catalysts with hydrogen yields several light gaseous compounds, and two main groups of liquid products :namely glycerides and light oxygenates. The liquid product formations are shown in figure A-5.1. The light gas detection was confirmed with the mass spectroscopy in figure A-5.2. The glycerides include mono- and di-glycerides. The position of the ester functional group could vary, leading to a number of mono- and di-glycerides. The glycerides come from the truncation of one or two ester groups from triacetin. The light oxygenates compose of derived compounds from acetic acid such as alkyl acetates, acetic acid, and acetaldehyde. These compounds not only result from the conversion of the ester group but also come from breaking C-C bonds of the 3-C chain. Figure A-5.3 illustrates the presence of the two groups of compounds in gas chromatogram. The light oxygenates come out before the glycerides. In the same study, using triglycerides of fatty acids as model feeds, although Murzin et al. proposed mono- and di-glycerides as reaction intermediates he was not be able to detect them. [6]In the same line, Kubicka et al. showed that the intermediates from triglyceride reactions were not seen due to their high activity.[7] This difference clearly marks the advantage of using a short triglyceride like triacetin as a model triglyceride compound, in which all of the possible reaction intermediates are able to be monitored.

The reactions of triacetin were carried over three supported metal catalysts: 1%Pt/γ-Al_2O_3, 1%Pt-1.3%Sn-0.5%K/SiO_2, and 10%Cu/SiO_2. As stated above, the reaction on Pt catalyst yields two types of products. Their contributions also change with

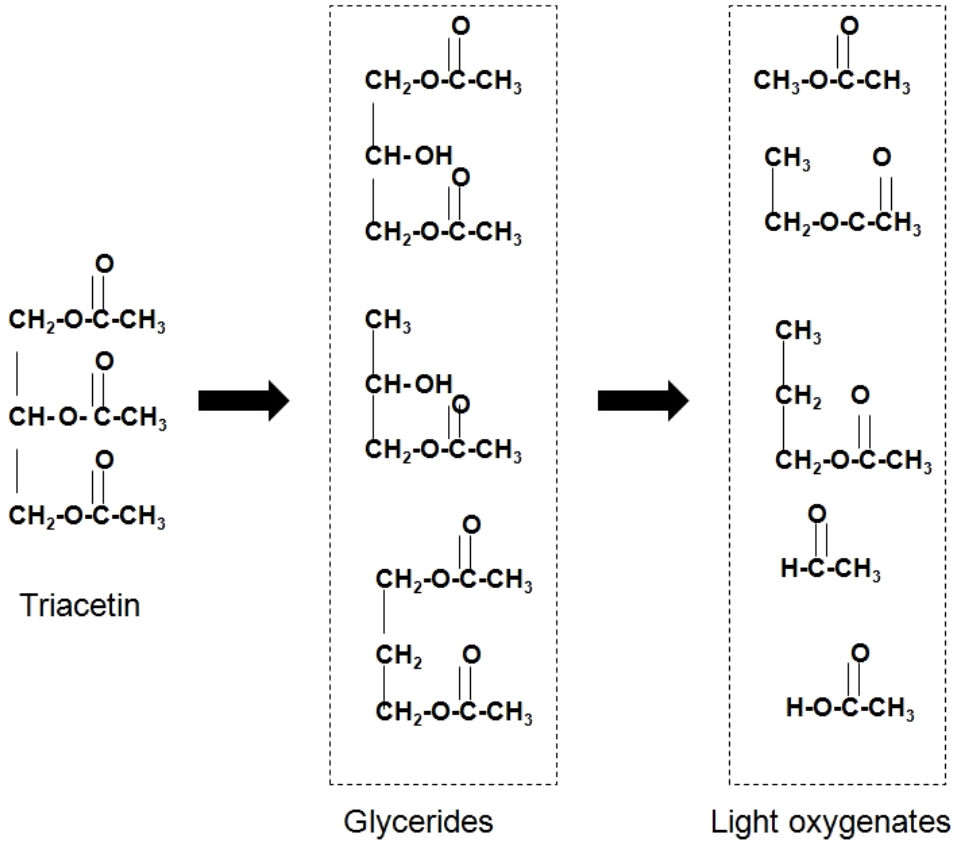

Figure A-5.1: Proposed reaction scheme of triacetin on supported noble metal catalysts in hydrogen

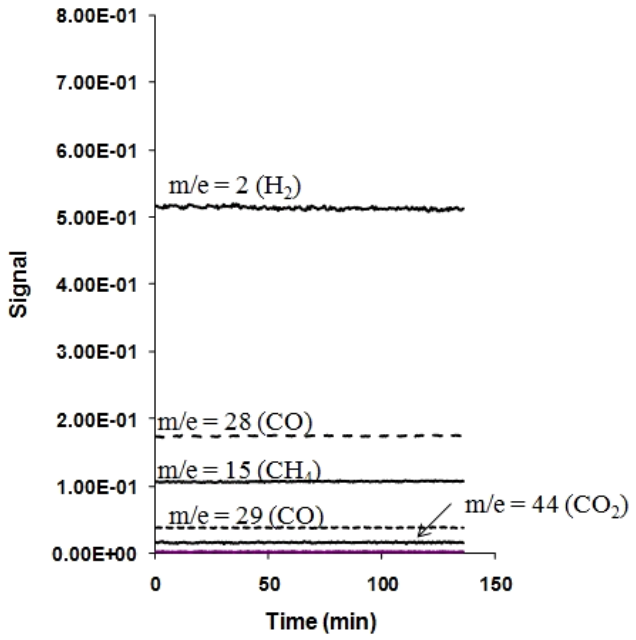

Figure A-5.2: Mass spectroscopy result of light gases produced in reactions of triacetin over supported metal catalysts

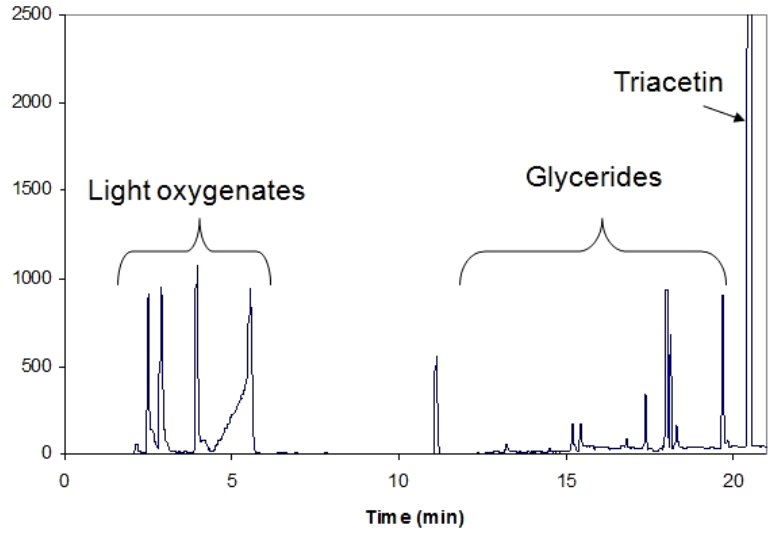

Figure A-5.3: Typical chromatogram of products in reactions of triacetine over supported noble metal catalysts

1%Pt/γ-Al_2O_3 catalyst T= 653 K, P = 3.4MPa Gas flow = 200 mL/min of H_2		
Compounds	**Yield (%)**	
Methanol	3.5%	12.8%
Acetaldehyde	3.8%	21.9%
Ethanol	4.0%	9.0%
Methyl acetate	2.1%	2.2%
Acetic acid	11.4%	26.2%
Ethyl acetate	1.4%	1.0%
Propyl acetate	2.0%	12.1%
Other	0.5%	2.0%
Other	0.5%	0.6%
1,2-Propanediol, 1-acetate	1.0%	1.2%
1,2-Propanediol, 1,2-diacetate	2.6%	0.5%
1,3-Propanediol, 1,3-diacetate	1.8%	0.6%
1,3-Propanediol, 1-acetate	0.6%	1.1%
1,2,3-Propanetriol, 1,2-diacetate	0.1%	0.6%
1,2,3-Propanetriol, 1-acetate	2.8%	0.7%
1,2,3-Propanetriol, 1,3-diacetate	0.1%	0.4%
Triacetine	61.7%	7.1%
Conversion	**38.3%**	**92.9%**
Total selectivity of light oxygenates	**74.1%**	**91.9%**
Total selectivity of glycerides	**25.9%**	**8.1%**

Table A-5.3: Selectivity of two main groups of products from reactions of triacetin over 1% Pt/Al_2O_3 catalyst

1%Pt-1.3%-0.5%K/SiO_2 catalyst T = 653 K, P = 3.4M Pa Gas flow = 200 mL/min of H_2 or H_2 in Argon		
Liquid Phase Analysis	**H_2/Feed Ratio**	
Compounds	**100**	**2.5**
Methanol	5.3%	18.2%
Acetaldehyde	15.1%	0.0%
Ethanol	12.8%	0.4%
Methyl acetate	7.2%	3.1%
Acetic acid	26.1%	7.8%
Ethyl acetate	1.7%	3.9%
Propyl acetate	5.2%	2.2%
Other	0.0%	2.6%
Other	0.0%	1.3%
1,2-Propanediol, 1-acetate	2.7%	1.5%
1,2-Propanediol, 1,2-diacetate	1.6%	2.8%
1,3-Propanediol, 1,3-diacetate	1.5%	2.1%
1,3-Propanediol, 1-acetate	4.6%	1.1%
1,2,3-Propanetriol, 1,2-diacetate	0.5%	0.8%
1,2,3-Propanetriol, 1-acetate	2.0%	0.9%
1,2,3-Propanetriol, 1,3-diacetate	1.9%	2.1%
Triacetine	11.8%	49.3%
Conversion	**88.2%**	**50.7%**

Table A- 5.4: Selectivity of two main groups of products from reactions of triacetin over Pt-Sn-K/SiO_2 catalyst

10% Cu/SiO_2 catalyst T = 653 K, P = 3.4 M Pa Gas flow = 200 mL/min H_2		
Compounds	**Yield (%)**	**Selectivity (%)**
Methanol	1.1%	2.9%
Acetaldehyde	2.5%	6.7%
Ethanol	6.3%	17.0%
Methyl acetate	11.5%	30.7%
Acetic acid	7.3%	19.5%
Ethyl acetate	0.5%	1.5%
Propyl acetate	0.7%	1.9%
Other	1.1%	2.9%
1,2-Propanediol, 1-acetate	1.4%	3.7%
1,2-Propanediol, 1,2-diacetate	0.6%	1.6%
1,3-Propanediol, 1,3-diacetate	0.4%	1.1%
1,3-Propanediol, 1-acetate	1.5%	4.1%
1,2,3-Propanetriol, 1,2-diacetate	0.4%	1.1%
1,2,3-Propanetriol, 1-acetate	0.6%	1.7%
1,2,3-Propanetriol, 1,3-diacetate	1.3%	3.5%
Triacetine	62.6%	
Conversion	37.4%	

Table A-5.5: Selectivity of two main groups of products from reactions of triacetin over Cu/SiO_2 catalyst

conversion. In details, the selectivity of light oxygenates increases and that of glyceride decreases with increasing conversion as reported in table A-5.3. This could reflect the role of glycerides as intermediates in conversion of triacetin to light oxygenate compounds. At low conversion, the intermediates dominate. As the conversion increases, the glycerides get further transformed into light oxygenates. In fact, Murzin et al. proposed a similar pathway for the conversion of fatty acid triglycerides. He attributed the negligible concentration of mono- and di-glycerides in the product mixture to the high activity of these compounds. [8] Once they are formed, they quickly react to lighter products.

The trend observed with the pure Pt catalyst also works with other tested catalysts. In addition, the role of hydrogen partial pressure was studied in the reaction of triacetin over 1%Pt-1.3%Sn-0.5%K/SiO_2 catalyst. In fact, as shown in table A-5.4, higher hydrogen concentration leads to higher conversion. When pure hydrogen is used, acetic acid appears as a dominant product. However, at lower hydrogen concentration, methanol becomes as the dominant product although contribution from acetic acid is still considerable. When table A-5.5 shows that copper catalyst replaces Pt-Sn-K catalyst, methyl acetate dominates. This is a surprising result since the formation of methyl acetate involves C-C cleavage, which is not normally expected on copper catalysts. Further investigation is needed in order to clarify the role of each metal in the conversion of triacetin.

3. References

[1] Maier W.F., Bergmann, K., Bleicher, W., and Schleyer, P.V.R., *Tetrahedron Letters*, **22**, 4227 (1981)

[2] Snare, M., Kubickova, I., Maki-Arvela, P., Eranen, K., Murzin, D.Y., *Chem. Ind.* **115,** 415 (2005)

[3] Snare, M., Kubickova, I., Maeki-Arvela, P., Eraenen, K., Murzin, D.Y., *Ind. Eng. Chem. Res*. **45**, 5708 (2006)

[4] Cortright, R.D., and Dumesic, J. A., *J. Catal.* **148**, 771 (1994)

[5] Imai, T., and Hung, C.W., U.S. Patent 4430517 (1983)

[6] Snarea, M., Kubičkováa, I., Mäki-Arvelaa, P., Chichovaa, D., Eränena, K., and Murzin, D.Y., *Fuel* **87**, 933 (2008)

[7] Simacek, P., Kubicka, D., Sebor, G., and Pospisil, M., *Fuel* **88**, 456 (2009)

[8] Snare, M., Kubickova, I.,Maeki-Arvela, P., Eraenen, K., Waerna, J., and Murzin, D. Yu., *Chem.Eng. J.* **134**, 29 (2007)

CHAPTER VI: TRICKLE-BED REACTOR AND MONOLITH CATALYSTS

In the previous sections, it is seen that the combinational Pt-Sn-K catalysts show the highest stability and selectivity toward alpha alkene products in the reactions of methyl esters. It is also found that the higher potassium loading results in higher alpha/internal ratio. In other words, the high K concentration strongly inhibits the alpha-to-internal double-bond isomerization reactions at the same conversions. To further improve the selectivity of alpha alkenes, the combination Pt-Sn-K will be deposited into metal foam catalyst. The apparent advantage of the monolith system (in this case Inconel metal foam was used instead of monolith) is that the initial products are able to desorb quickly into the gas phase, consequently limiting the double-bond isomerization reactions.

1. Scanning Electron Microscopy (SEM) Images of the Metal Foam Substrate

In order to increase the catalyst surface area, carbon fibers were grown on the metal foam base. The details of carbon fiber production experiments are described in chapter II. Figure A-6.1 displays the SEM images of carbon fibers growth on two substrates: fresh metal foam and HCl-treated metal foam. It is clearly seen that the fibers produced on treated foam are longer and more uniform than that on fresh foam. This could be due to the HCl treatment, in which metal surfaces become rougher, consequently leading to more active sites to grow carbon fibers.

2. Reactions of Methyl Dodecanoate on Pt-Sn-K on Metal Foam

All reactions were operated in trickle-bed conditions. The liquid products were collected and analyzed. The GC and NMR analysis were used to calculate contribution of alpha alkenes regard to internal alkene products. A representative product distribution of

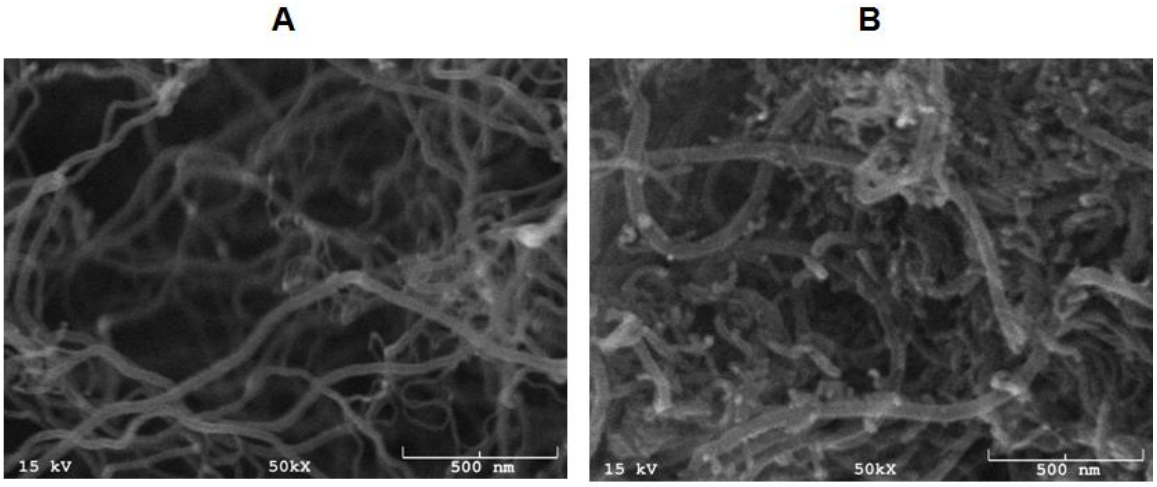

Figure A-6.1: SEM images of carbon fiber produced on metal foam treated with HCl solution (A) and fresh foam (B)

Compounds	**Yield (%)**	**Selectivity (%)**
C_{10} olefins	0.10%	0.50%
Total C_{11} olefins	23.60%	84.50%
Total C_{12} olefins	2.00%	7.00%
Others	0.20%	0.70%
C_{12} aldehyde	0.60%	2.00%
C_{12} alcohol	0.20%	0.60%
Feed	72.00%	
Acid	1.00%	3.70%
Heavy	0.30%	1.00%
Conversion	**28.0%**	

Table A-6.1: Production distribution in methyl dodecanoate reactions over Pt-Sn-K coated on fresh metal foam catalyst at TOS = 2.5 hour

T = 653 K, P = 2.72 M Pa					
TOS (h)	1	2.5	4	5.5	6.5
Conversion (%)	32.5	28	26.1	24	21.1
C_{11} selectivity (%)	79.3	84.5	76.5	76.8	81
alpha/internal	0.5	0.5	0.48	0.49	0.48

Table A-6.2: Alpha C_{11} olefin selectivity in methyl dodecanoate reaction over Pt-Sn-K coated on fresh metal foam catalyst at various time on stream

T = 653 K, P = 2.72 M Pa				
TOS (h)	1.5	3	4.5	5.5
Conversion (%)	35.7	30	24.8	21.4
C_{11} selectivity (%)	72.2	70.7	66.5	62.8
alpha/internal	0.42	0.44	0.48	0.56
T = 653 K, P = 1.36 M Pa				
Conversion (%)	36.6	31.2	27.3	23.2
C_{11} selectivity (%)	88.6	87.7	86.4	85.9
alpha/internal	0.45	0.43	0.42	0.41

Table A-6.3: Alpha C_{11} olefin selectivity in methyl dodecanoate reaction over Pt-Sn-K coated on HCl-treated metal foam catalyst at various time on stream

methyl laurate was summarized in Table A-6.1. Without hydrogen, this catalyst is highly selective for decarboxylation/decarbonylation reactions, reflecting by the dominant C_{11} alkene products (>80% selectivity). C_{12} hydrocarbons and oxygenates contribute in a small portion. Having that in mind, it is informative to explore the effect of different treatments and catalyst deactivation on the selectivity of desirable alpha alkenes. Table A-6.2 shows the conversion of methyl laurate on untreated foam as time on stream increases. Over the course of 6.5 hours, the conversion level drops from 32% to 21%.C_{11} alkenes stay as dominant products throughout the time. However, as the catalyst deactivates, contribution of alpha alkenes regard to internal alkenes does not significantly improve. When the metal substrate is treated with HCl, it is seen that the initial conversions at after one hour on stream are slightly higher as seen in table A-6.3. Although the significant improvement in alpha/internal ratio is not observed, the effect of operating pressure is apparent here. The C_{11} hydrocarbons appear less dominant at higher pressure compared to that at lower pressure. Consequently, the selectivity of condensation products increases with pressure. Here it is clearly seen that as the catalyst deactivates, the ratio of alpha/internal increases from 0.42 to 0.56. In contrast, lower operating pressure leads to higher C_{11} hydrocarbon selectivity and also lower alpha/internal ratio. In short, although the elevated pressure causes a faster catalyst deactivation and greater condensation accumulation, it helps to enhance the selectivity of alpha alkenes or inhibit the double-bond isomerization reactions. The relative low alpha/internal ratio observed here might be attributed to the poor liquid distribution, in which thick layers of liquid feed may prevent the fast desorption of C_{11} alkenes into the gas phase. To further optimize alpha alkene selectivity, a better liquid distribution system

is recommended so that the true trickle-bed conditions are obtained. In addition, the elevated pressure is preferred.

CHAPTER VII: SUMMARY

Nowadays the demand for uses of renewable feed stocks for production of chemical and fuels rapidly increase due to the phase-out of fossil sources. The work presented in this dissertation focuses on the conversion of methyl esters and triglycerides into hydrocarbons, which can be used as chemicals and fuels. The main drive for this work comes from the fact that both methyl esters and triglycerides are derived products from various renewable sources such as vegetable oils and biomass. In addition, obtained knowledge on the reaction chemistry of these compounds will be a useful tool for upgrading sustainable bio-oils, which will replace fossil materials in many applications. In fact, the desirable hydrocarbons can be achieved through the deoxygenation reactions of the feeds. In order to optimize the yield and selectivity of the hydrocarbons, the first step is to establish and verify the reaction mechanisms, in which all possible reaction pathways leading to formation of hydrocarbons are identified. Second, the effects of various parameters on the deoxygenation reactions also need to be examined. The important parameters include pressure, temperature, hydrogen partial pressure, and reactor configuration. Certainly, one cannot exclude the important role of catalysts. The variation of these parameter will be implemented in the reactions used several probe molecules such as methyl hexanoate, methyl octanoate, methyl dodecanone, and triacetin. The results from these works can be summarized into several main highlights:

- The reactions of methyl esters on supported metal catalysts can be operative in a number of main pathways, which include hydrogenation/hydrogenolysis, decarboxylation/decarbonylation, and ketonization. The estimated activation energies follow this order: hydrogenation < decarboxylation/decarbonyaltion <

ketonization. While decarboxylation/decarbonylation reactions are known to be operative regardless of hydrogen, hydro-deoxygenation reactions require the presence of hydrogen. In fact, hydrogen participates in the latter reactions and activates the catalysts. Conversely, the presence of hydrogen is known to suppress the ketonization reaction in the way that it promotes other reactions such as deoxygenation and hydrogenation. Thus, at highly elevated temperature (i.e. 653 K), the ketonization still occurs at a small extent in hydrogen. The hydro-deoxygenation reactions can occur on either metals (i.e. Pt, Pd, and Cu) or reducible metal oxides (i.e. TiO_2 and SnO_2). It is the oxygen vacancy created in the reductive atmosphere that catalyzes the oxygen-removing reaction on metal oxides. Compared to hydro-deoxygenation reactions, the decarboxylation/decarbonylation reactions are more structure sensitive. The latter require a larger ensemble of active sites and are often seen to be operative on noble metal catalysts. The reducible oxides can catalyze the decarboxylation/decarbonylation reactions to a relatively small extent yet. While the two above reactions occur on both metal and metal oxide surfaces, the ketonization reactions are only detected to happen on oxide catalysts. Even stable SiO_2 and Al_2O_3 surfaces are capable of catalyzing the ketonization reactions via coordinatively unsaturated sites after being dehydroxylated.

- Carboxylate species can be claimed as surface species when carboxylic acids adsorb on metal and metal oxide surfaces. Upon heating, these species can desorb or undergo reactions to form other oxygenates or hydrocarbons. Differently, the dissociation of methyl esters on metal oxides is accompanied by the deposition of

methoxide fragment onto the surface. Although the initial adsorption mode of methyl esters on metal surfaces is controversial, it could be possible that the adsorption configuration varies from one metal to another and depends on the gas condition.

- Supported Pt catalysts are active for conversion of methyl esters into hydrocarbons in hydrogen. Complete deoxygenation of the esters can be obtained at sufficiently high W/F. Depending on the particular supports, the hydrocarbon distribution will vary. For instance, on alumina-supported Pt catalyst, decarboxylated/decarbonylated hydrocarbons are entirely dominant. Meanwhile on titania-supported Pt catalyst, hydrogenated hydrocarbons appear in considerable amounts.
- Further enhancement in hydrogenation activity is observed when copper is used instead of platinum. Cu catalyst is less active than Pt catalyst in the reaction of methyl esters; therefore; the former requires higher reaction temperature and total hydrogen pressure.
- The hydrocarbons produced from the reaction of methyl esters are linear; therefore, they are not good candidates for fuel molecules due to their high cloud points. This initiates an additional isomerization reaction of linear to branched hydrocarbons following the deoxygenation reaction. Bifunctional Pt on acidic support catalysts (i.e. zeolites, solid acids) are seen as effective catalysts for isomerization of long-chain alkanes. However, high degree of branching can only be obtained if the complete deoxygenation of the esters is achieved. Therefore,

two reactors in series, in which deoxygenation reactor is followed by isomerization reactor, turn out as the optimal setup.

- Although the decarbonylation/decarboxylation reaction of methyl esters does not require hydrogen, the pure platinum catalyst (i.e. Pt/SiO_2) without hydrogen deactivates quickly due to the strongly adsorbed dehydrogenated species. The reactions of methyl hexanoate here proceed via different reaction pathways involving alcohols/aldehydes, carboxylic acids, and condensation products as intermediates. Among those pathways, transformation of the esters to final hydrocarbon products via condensation intermediates is dominant. Additional experiments have shown that the deoxygenation activities of corresponding alcohols/aldehydes and carboxylic acids without hydrogen are high. Meanwhile, without hydrogen, the major condensation species, symmetrical ketones, are not able to undergo complete decomposition to hydrocarbons without hydrogen. Without hydrogen, the dehydrogenation pathway of heavy ketone is dominant due to the length of alkyl chains. It could be possible that these compounds react with hydrogen generated during the methyl ester reactions to form hydrocarbons. Addition of Sn into Pt/SiO_2 catalyst shows a substantial improvement in catalyst stability. It is the Pt-Sn alloys, which are more coke tolerant than pure Pt, that retain the conversion of the condensation products to hydrocarbons. Further enhancement is observed with introduction of potassium. The combinational Pt-Sn-K catalysts comprise of two important functionalities. These are: the coupling reactions of the esters occur on Sn-K oxide species and Pt-Sn alloys convert condensation intermediates into final hydrocarbon products. The balance of these

two functions helps to maintain the stability of the catalyst. In details, the additions of both Sn and K have several simultaneous effects. Firstly, the Pt ensembles are ruptured owing to Sn and K coverage and formation of Pt-Sn alloy. Secondly, potassium enhances the segregation of Sn out of Pt-Sn alloy. Among all tested Pt-Sn-K catalysts, 1%Pt-1.3%Sn-0.5%K/SiO_2 exhibits the highest activity and stability in reaction of methyl hexanoate. Reactions of methyl esters on this catalyst release H_2, CO_2, CH_4, and CO. These gas compositions not only depend on the sole reaction of methyl esters but also rely on the other side reactions such as water gas shift, coke formation, and light oxygenate decomposition.

- Besides model methyl ester compounds, a simple triglyceride, triacetin, was also tested to gain insights on the reaction of a triglyceride molecule. On supported Pt catalyst, triacetin converts into two main groups of liquid products: namely glycerides and light oxygenates. The glycerides include mono- and di-glycerides. The glycerides come from the truncation of ester groups from triacetin. The light oxygenates compose of derived compounds from acetic acid such as alkyl acetates, acetic acid, and acetaldehyde. The reaction results reveal that glycerides act like intermediates in conversion of triacetin to light oxygenate compounds. At low conversion, the intermediates dominate. As the conversion increases, the glycerides get further transformed into light oxygenates.

PART B: REACTIONS OF NAPHTHENIC COMPOUNDS ON SUPPORTED IRIDIUM CATALYST

CHAPTER I: INTRODUCTION

1. Introduction

In the United States, legislations have recently imposed more stringent environmental regulations on petroleum fuels, especially sulfur and polynuclear aromatic hydrocarbon (PAH) contents. Reduction of sulfur leads to reduction in NOx emission and particulate matter (PM) in exhaust gases. Environmental Protection Agency (EPA) has set an upper limit for sulfur content in diesel fuel to 15 ppm, which begins to be effective in mid-2006.[1] Aromatics (i.e. benzene, toluene, naphthalene…) are carcinogenic and produce PM or soot in jet, diesel and gasoline engines.[2] In jet fuel, high tendency to form soot of aromatics is associated with low smoke point. In diesel fuel, presence of PAHs lowers the cetane number (CN) or cetane index (CI), which determines ignition quality of fuel. In near future, EPA might set the CI of 40 and maximum aromatics content of 35 volume standards for nonroad, locomotive and marine diesel fuel.[3] During gasoline production, aromatics are added to increase the octane number. High concentration of aromatics in gasoline also affects cloud point in cold start. Therefore, reduction of aromatic content, together with olefin content, T50 and T90, is an important part of California phase 3 reformulated gasoline specifications. [4] The contents of benzene and total aromatics are now 0.8% and 25 % volume, respectively.

Cetane number is an important property of diesel fuel. Low-CN fuels cause poor ignition quality, knocking… and so on. Aromatics have lowest CNs and normal paraffin have the highest CN. Cetane values of normal paraffins also increase with number of carbon atom in the molecules. CNs of naphthenic compounds and iso-paraffin fall in between those of aromatics and normal paraffins. Moreover, increasing degree of

branching decreases the CN. [5]Naphthalene, which has a CN of 1, is a common aromatic compound in diesel range. Figure B-1.1 shows the reaction pathway to convert naphthalene to n-decane, which results in CN increase from 1 to 77. It is clearly seen that, in order to convert naphthalene into high-CN molecules, complete hydrogenation is required prior to selective ring opening (SRO). SRO indicates that ring opening only occurs at substituted carbon center to create straight-carbon-chain paraffins. [6]

In a similar fashion, octane number (ON) is a key parameter in determining the quality of gasoline. High ON means high resistance of fuel against knocking. In combustion engine, a compressed mixture of fuel and air is introduced. Due to thermal stability of each molecule and the ensuing radicals, some molecules tend to burn sooner than others, which cause knocking[7]. There are two types of ON: research octane number (RON) and motor octane number (MON). The reported ON is an average of two above values. ONs are based on a scale on which isooctane is 100 (minimal knock) and heptane is 0 (bad knock). In general, aromatics (i.e. benzene, toluene…) and iso-paraffins have high ONs. For iso-paraffins, branching is desirable, because it increases ONs, which is in contrast to CN. Therefore, normal paraffins are undesirable. To achieve the goal of making gasoline more environmentally friendly, while keeping the its ON high, aromatics need to be converted to iso-paraffins with substantially high ON.

In addition to CN and ON, the smoke point (SP), which is the maximum smoke-free laminar diffusion flame height, has been employed widely to evaluate the tendency to form soot of different fuels. This tool was first applied for kerosenes, later diesel and then jet engine fuels.[8-9] Many researchers have tried to relate smoke points and molecular structures of hydrocarbon compounds. It was found that the inverse of smoke point, or

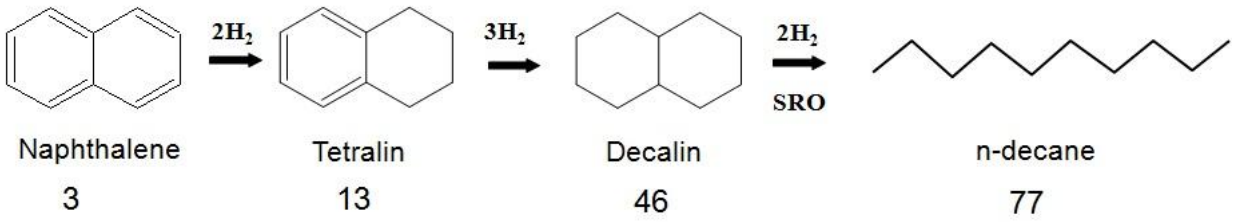

Figure B-1.1. Sequential Cetane Number improvement of naphthalene by hydrogenation and selective ring opening

potential to form soot, increases from normal alkanes to branched alkanes to alkylbenzenes and finally naphthalenes.[10-11] Since smoke points vary with experimental conditions, the concept of threshold soot index (TSI), which is calculated from the height of smoke and experimental constants, can be used to compare soot tendency of different fuel molecules.[12]

As stated above, molecular structures of hydrocarbon compounds greatly affect properties of various fuels. Molecules used in diesel engine require long-chain paraffins to obtain high CN. Meanwhile, branching iso-paraffins are desirable for gasoline engine. In this present work, a useful tool to estimate CN, ON and TSI values of individual hydrocarbons was developed. This prediction tool is operated by a neural network using a set of CN, ON and TSI experimental value databases and descriptors predicted by QSAR. Consequently, the predicted CN and ON values were used as an important criteria to select the most appropriate strategies or reaction pathways to improve CN for diesel and ON for gasoline. Catalytic results were then carried out to demonstrate the practical applications of the theoretical concepts.

The catalytic strategy to reduce the aromatic content in diesel and gasoline fuels has been proposed as hydrogenation reaction of the aromatic rings followed by ring contraction and ring opening reactions. The ring contraction reaction of 6-membered ring to 5-membered ring is necessary because the rate of opening 5-membered ring is known

to be much faster than that of 6-membered ring. In the scope of this research, selective ring opening of fully-hydrogenated naphthenic compounds, were chosen as representative molecules both in diesel and gasoline ranges. Ring opening reaction will be studied on supported Iridium catalyst, which is known for its high ring opening activity. By changing the support of the iridium catalyst, different ring opening product distributions are obtained in which, different ring cleavage positions are observed, leading to a great influence on CN or ON of alkane products. In details, the Ir/SiO_2 catalyst is selectively breaking unsubstituted C-C bond cleavages, which results in products with high degree of branching or higher ONs. In contrast, Ir/Al_2O_3 catalyst appears as the most active and selective toward this type of ring opening to break C-C bond at substituted positions, which could produce products with lower ONs or higher CNs than the original feed. The addition of K and Ni has changed both activity and selectivity of Ir catalysts. Particularly, the incorporations of Ni and K to Ir/Al_2O_3 catalyst at a certain ratios could inhibit the cleavage of C-C bond at substituted positions and undesirable secondary hydrogenolysis, resulting in an increase in ONs of product mixtures. Catalyst variation is not the only parameter that has been studied in the ring opening reactions. In fact, model feed molecules has been also altered. A series of alkyl cyclohexanes with varying alkyl chain lengths and their relative positions were studied on Ir/Al_2O_3 catalyst. From these results, common trends in the ring opening product distribution were observed. Since the selective ring opening reaction for fuel upgrading is proposed to occur in the mixture of hydrocarbon pools, including aromatics, the ring opening reaction was studied in the presence of aromatics as well.

2. References

[1] Cooper, B. D. *Appl . Catal. A-Gen.,* **137**, 203(1996)

[2] Barry, E.G., McCabe, L.J., Gerke, D.H., Perez, J.M., SAE-Paper, 852078, pp 11-33

[3] In "Summary and Analysis of Comments: Control of Emissions from on Road Diesel Engines", EPA 420-R-04-008, May 2004

[4] In "Regulation of Fuel and Fuel Additives: Extension of California Enforcement Exemptions for Reformulated Gasoline to California Phase 3 Gasoline". EPA, Federal Register **70**, 75914 (2005)

[5] Wilson, M., Fisher, I., and Kriz, J. *Ind. Eng. Chem. Prod. Res. De.,***25**, 505(1986)

[6] Santana, R.C., Do, P.T., Alvarez, W.E., Taylor, J.D., Sughrue, E.L., and Resasco., D.E., *Fuel,* **85**, 643 (2006)

[7] Ghosh, P., Hickey, K. J., Jaffe, S. B., *Ind. Eng. Chem. Res.* **45**, 337 (2006)

[8] Gulder, O. L. ,*Combust. Flame.,* **78**, 179(1989)

[9] Olson, D. B., Pickens, J. C., Gill, R. J., *Combust. Flame.,* **62**, 43(1985)

[10] Hunt Jr, R. A., *J. Ind. Eng. Chem* **45** , 602 (1953)

[11] Schalla, R. L., and McDonald, G. E., *J. Ind. Eng. Chem.* **45** , 1497 (1953)

[12] Calcote, H. F., and Manos, D. M., *Combust. Flame.,* **49**, 289 (1983)

CHAPTER II: EXPERIMENTAL SETUP

1. Catalyst Preparation

The gamma-alumina (γ-Al_2O_3, HP-140 from Sasol) and silica (HiSil-210; PPG) were used as supported for catalyst prepared. All catalysts were prepared by co-impregnation method with aqueous solutions of $IrCl_3.3H_2O$ (Alfa-Aesar), $NiCl_2.xH_2O$ (Alfa-Aesar), and K_2CO_3 (Alfar-Aesar). The concentration of the precursor solution was adjusted to the desired metal loading. In this study 0.9 wt.% Ir was prepared for monometallic catalyst on Al_2O_3 and SiO_2 supported. For Ir-Ni bimetallic catalyst, 0.3, and 0.1 wt.% Ni were co-impregnated with 0.9 wt.% Ir on Al_2O_3 supported to obtain Ni:Ir molar ratio equal to 1, and 0.3, respectively. For Ir-K catalyst, 0.5 wt.% K on Al_2O_3 to obtain K:Ir molar ratio equal to 2.5. After the impregnation the samples was kept at ambient temperature for 4 hours, and then dried at 383 K overnight, and finally calcined in air at 573 K for Ir and Ir-K catalysts and at 673 K for Ir-Ni catalysts.

2. Catalyst Characterization

2.1 Chemisorption of carbon monoxide

The chemisorption experiments were used to estimate the metal dispersion on the catalyst. The CO uptake measurements were performed in a 1/4" flow reactor made of quartz, containing 0.1 g catalyst. Before exposing to CO, the samples were reduced in-situ under 50 ml/min of H_2 at 723 K or 603 K for 1 hour, and purged in flowing He for 0.5 hour and then cooled down to room temperature. The stream was continuously monitored online by a mass spectrometer. Calibrated pulses of 250 µl of 5%CO in He were sent over the catalyst be every 5 min, until the areas of the m/e=28 peak stopped increased, which indicated that the saturation adsorption capacity had been reached. The

total amount of CO taken-up by the sample was calculated by quantifying the area of the peak with the total number of CO moles present in the 250 µl loop filled with 5%CO in He.

2.2 Temperature programmed reduction (TPR)

The TPR experiments were carried out in a 1/4" quartz tube coupled to a TCD detector. A sample of 50 mg was heated with heating rate 10 K /min up to 1173 K in a flow of 20 mL/min of 5.2% H_2 in Ar mixture. Water produced during the reduction was removed using a cold trap with frozen acetone. The TPR profile was monitored continuously with an online TCD detector.

3. Catalytic Activity Measurement

The ring opening reactions of all tested naphthenic and paraffinic compounds were carried out at 1/2" O.D. fixed bed stainless steel reactor equipped with a thermowell to insert the thermocouple into the center of the catalysts bed to keep isothermally. The catalytic activity was conducted in gas phase reaction at total pressure of 3.4 MPa, 603 K, H_2/HC molar ratio of 30. The Ir-Ni and Ir-K catalysts were first reduced under flowing H_2 at 3.4 MPa, 723 K for 1.5 hour. All other catalysts were reduced at 3.4MPa, 603 K for 1.5 hour. After the pretreatment, the reactor was cooled downed down in flowing H_2. Then, the liquid reactant was introduced in the reactor using Isco LC-500 high-pressure syringe pump. The product were collected as liquid in a dry-ice in acetone bath (temperature is 197 K to capture all the products) and were analyze by Hewlett Packard 5890 Plus GC and Shimadzu GC-MS-P500.

CHAPTER III: RING OPENING OF 1,3-DIMETHYLCYCLOHEXANE ON IRIDIUM CATALYSTS: MODIFICATION OF PRODUCT DISTRIBUTION BY ADDITION OF NI AND K TO IMPROVE FUEL PROPERTIES

1. Introduction

Due to environmental concerns, the United State legislatures have called for the reduction of aromatic contents in both gasoline and diesel fuels.[1-2] The concept of SRO of saturated naphthenic compounds, following deep hydrogenation of aromatics, was primarily introduced to improve the cetane number of diesel fuel.[3-5] Products with highly linear carbon chain, i.e. normal paraffins, are desirable due to their high CNs. On the other hand, iso-paraffins with high degree of branching are preferred in gasoline fuel since they have high ONs. The loss of molecular weight of hydrocarbons during RO is undesirable because the presence of hydrocarbons with low molecular weight results in high Reid vapor pressure (RVP), which is strictly regulated to be less than 50 kPa in the summer time for gasoline mixtures in most parts of the United States. As first pointed out by Gault et al. and others, ring opening of naphthenic compounds over metal catalysts can proceed via different mechanisms such as: dicarbene, adsorbed olefin or metallocyclobutane.[6-8] Recently, McVicker et al. reported the high ring opening activity of Ir catalysts on six-member ring naphthenics. [9]They observed that dicarbene mode is strongly favorable on Ir catalysts. In the line with this study, it has been found that the preference of C–C bond opening at substituted or unsubstituted positions depends not only on the nature of the reactant but also on the type support of iridium catalyst used. The addition of methyl substituents facilitates the rate of ring opening of C_6 rings, as well

as contributes positively to the ring opening at sterically hindered C–C bonds. Iridium on alumina has shown to be the most selective toward the ring opening at substituted carbon center.[10] Dicarbene mode typically occurs on silica-supported Ir catalyst, which has low dispersion. In consequence, this catalyst may be desirable for producing high ON products.

Although Ir/SiO_2 is a suitable catalyst for ON improvement, its low activity due to low dispersion is a concern. The desirable catalyst for increasing ON should have exhibit the high activity of Ir/Al_2O_3 and selectivity of Ir/SiO_2. One possible solution is to modify the Ir catalysts by adding the second metal. Inhibition of interaction between Ir and alumina can be done by using Ni as the additional metal. It is well known that Ni interacts strongly with alumina, forming surface nickel aluminate-like species in the sub-monolayer regime.[11] Additionally, Ni interacts with noble metals such as Ir, Ru and Pt to form alloys.[12-13] Recently, it has been reported that Ni modifies the electronic property of Rh and protects Rh from sulfur poisoning.[14] Another metal worth considering is potassium. It is well known that the presence of K alter both the catalytic activity and selectivity of unmodified catalysts due to geometric and electronic effects.[15-16] Potassium is known to prevent the carbon formation in methane reforming reaction. Recently, it was reported by some researchers that electron alteration to the metal by K^+ or K^0 may provide the increasing of strength of hydrogen chemisorption.[15 -16]

In this current work, the direct focus is on ON enhancement of alumina and silica catalysts by analyzing clearly high octane number products. The effect of addition of Ni and K on supported Ir catalysts in ring opening of 1,3-dimethylcyclohexane (1,3DMCH) will be reported. In the light of ON enhancement, the product distributions of modified

catalysts will be compared with those of pure iridium catalysts. Finally, the impact of Ni and K will be evaluated in term of ON improvement and Reid vapor pressure of product mixtures.

2. **Catalyst Characterization Analysis**

The CO chemisorption of mono and bimetallic catalysts was summarizes in table B-3.1. The CO/Ir ratio on pure Ir supported on Al_2O_3 is higher than that on SiO_2 which indicated smaller Ir cluster on SiO_2 supported. [10]On alumina support, the addition of Ni and K resulted in the decreasing of CO adsorption. It could due to the fact that the addition of second metal or promoter might partially cover active site.

The temperature-programmed reduction profiles of the Ir-Ni/Al_2O_3 and pure Ir catalysts were illustrated in figure B-3.1. TPR profile of 0.9%Ir/SiO_2 catalyst observed a shoulder peak at 453 K and main peak at 563 K. The two hydrogen-consumption step was attributed to the reduction of different nano-aggregate state of Ir oxide species on silica surface or two morphologically different particles of iridium oxide.[17-18] For 0.9%Ir/Al_2O_3 catalyst one peak was observed, from around 393 K to around 593 K with maximum at 473 K, corresponding to the reduction of Ir oxide to metal Ir. [19-20]For Ni/Al_2O_3 catalyst two peaks was observed, the first one at around 573 K and, the second broad peak at temperature higher than 673 K. The first was corresponding to the reduction of Ni oxide while the second peak may due to the reduction of highly dispersion of Ni oxide and/or the reduction of Ni aluminate, respectively.[21-23]The first peak of all Ir-Ni/Al_2O_3 catalysts was present in the intermediate between those of corresponding reduction temperature of the oxide of monometallic Ir and Ni catalyst. This suggests the shift of reduction of Ir oxide to higher temperature due to strong

Table B-3.1:Compositions and metal dispersions of the Ir-containing catalysts.

Catalyst	%wt.Ni or K	Ni/Ir or K/Ir molar ratio	CO (μmol/g)	CO/M [(a)]
0.9 %Ir/Al_2O_3	-	-	43.8	0.94
0.9 %Ir-0.1 %Ni/Al_2O_3	0.1	0.3	41.6	0.70
0.9%Ir-0.3%Ni/Al_2O_3	0.3	1.0	38.0	0.40
0.9%Ir-0.5%K/Al_2O_3	0.5	2.5	35.0	0.75
0.9%Ir/SiO_2	-	-	14.9	0.32

[(a)] M is Ir or Ni

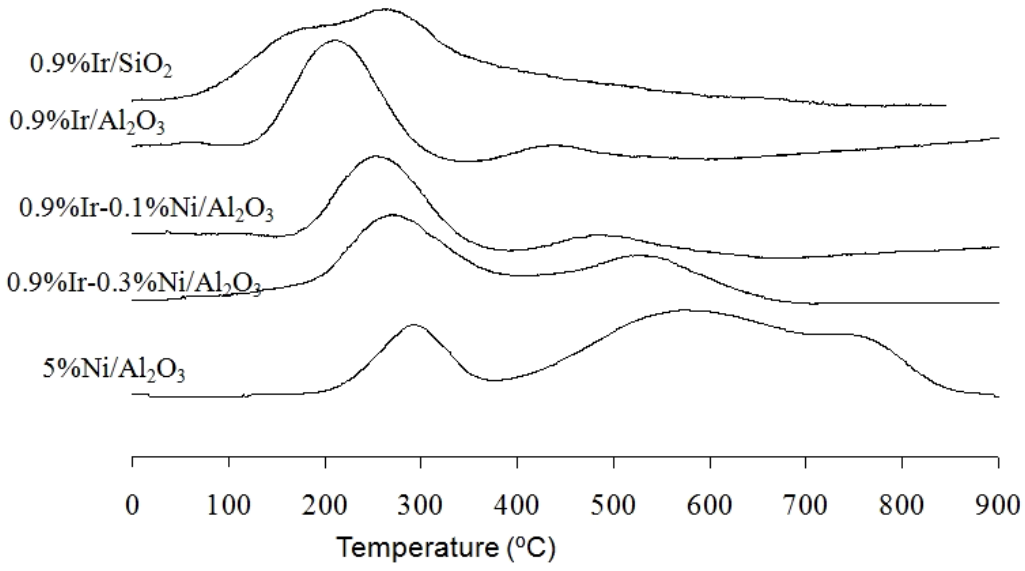

Figure B-3.1: Temperature programmed reduction of different support Ir, Ni and Ir-Ni catalysts.

interaction between Ir and Ni metal. In addition, the addition of Ni may migrate inside the support o form nickel aluminate.

3. **Catalytic Activity Analysis**

3.1 Hydrogenolysis reactions on Ir/Al_2O_3 and Ir/SiO_2 catalysts

The first hydrogenolysis reaction is the ring opening of 1,3DMCH. As seen in scheme B-3.1, the RO reaction yields three primary products: 2-methylheptane ($2MC_7$), 4-methylheptane ($4MC_7$) and 2,4-dimethylhexane ($2,4DMC_6$). These primary products then crack to form other RO molecules with lower carbon numbers such as: 2,4-dimethylpentane ($2,4DMC_5$), 2-methylhexane ($2MC_6$), 3-methylhexane ($3MC_6$), 2-methylpentane ($2MC_5$), 3-methylpentane ($3MC_5$), 2-methylbutane ($2MC_4$), iso-butane (iso-C_4), n-butane (n-C_4) and so on. Figure B-3.2 shows the ON and vapor pressure (VP) of all RO products. Among those products, only five molecules, $2,4DMC_6$, $2,4DMC_5$, $2MC_5$, $3MC_5$ and $2MC_4$, have ON higher than that of the original feed, which is 63. Therefore, sum of yield of these five products, which are denoted as HON products, should be maximized. Although the ON of $2MC_4$ is 90, its high vapor pressure makes it an undesirable product. The evolution of sum of yield of the other four HON products was followed as a function of W/F for $0.9\%Ir/Al_2O_3$ and $0.9\%Ir/SiO_2$ catalysts (see figure B-3.3). At low W/F, $0.9\ \%Ir/Al_2O_3$ catalyst yields the higher amount of HON products than $0.9\%Ir/SiO_2$ catalyst. This is due to the higher activity of alumina-supported Ir catalyst as mentioned in previous work. As the W/F increases, the molecules with higher carbon number continue to break to lighter products ($<C_5$), which results in a decrease in the sum of yield of HON products for both catalysts. However, the maximum amount of HON products is slightly higher on silica catalyst than on alumina catalyst.

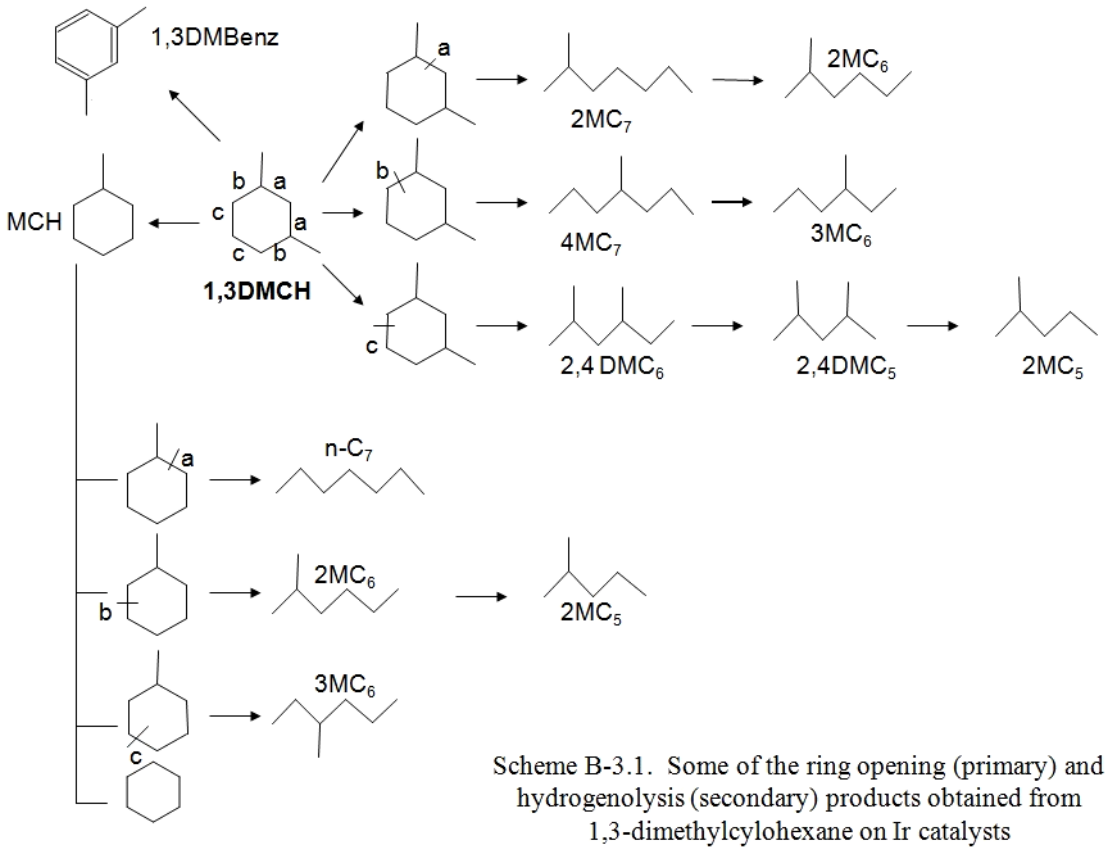

Scheme B-3.1. Some of the ring opening (primary) and hydrogenolysis (secondary) products obtained from 1,3-dimethylcylohexane on Ir catalysts

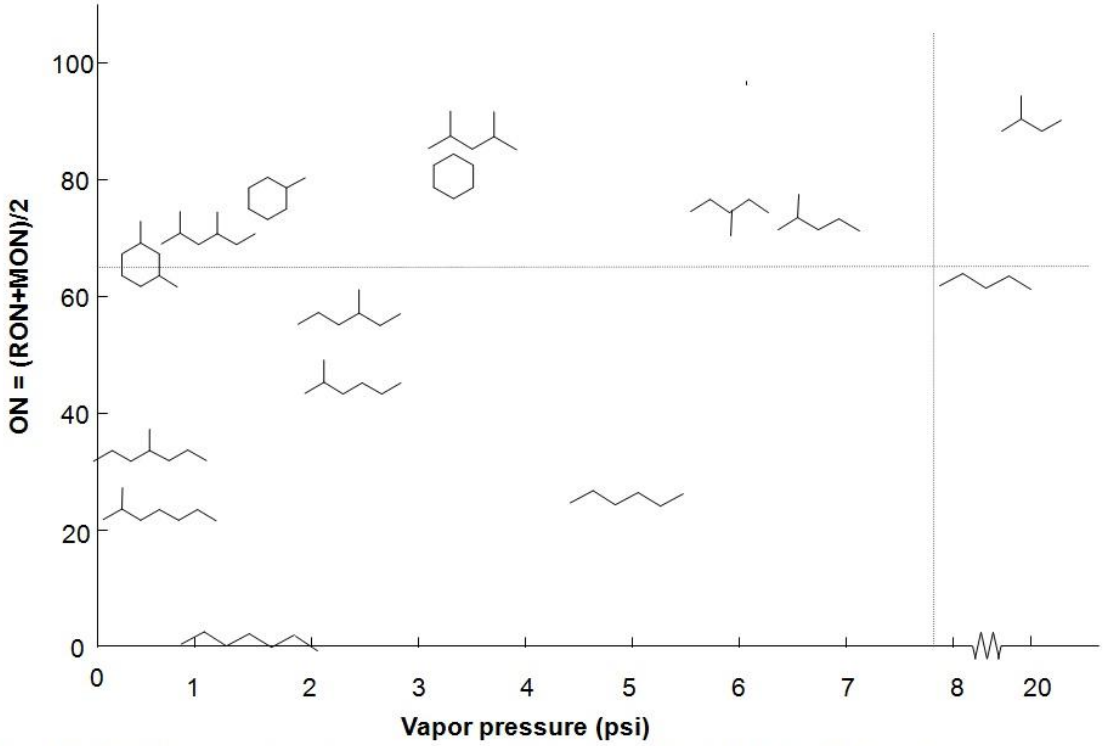

Figure B-3.2: Octane number and vapor pressure of typical products of 1,3-dimethylcyclohexane ring opening.

Since the hydrogenolysis reaction of primary and secondary products to lighter molecules is important in ON improvement, the second hydrogenolysis reactions of $2MC_7$ and $2,4DMC_6$ were tested individually to understand the effect of support and molecular structure on the product distributions. Figure B-3.4 and B-3.5 show the product cracking pattern of these two hydrocarbons on 0.9 %Ir/Al_2O_3 and 0.9%Ir/SiO_2 catalysts. To understand the intrinsic selectivity of different C-C bond position cleavages, the reaction conversion was kept low (< 5%). Hydrogenolysis reactions of $2,4DMC_6$ and $2MC_7$ yield 6 and 7 major products, respectively, which corresponds to different C-C bonds in the molecules. In the reaction of $2,4DMC_6$, there are three groups of bond cleavages such as primary-secondary (C1-C2), primary-tertiary (C1-C3) and secondary-tertiary (C2-C3). In the reaction of $2MC_7$, four groups of bond are ruptured: C1-C2, C1-C3, C2-C3 and secondary-secondary (C2-C2). The selectivity of various groups was compared with the statistical value. Several comments are drawn here. First of all, on 0.9%Ir/SiO_2 catalyst, breaking of both C1-C2 and C2-C2 bonds in two molecules, which can be originated from dicarbene mode, is dominant compared to that of bonds involving tertiary carbon. In the reaction of $2,4DMC_6$, 2,4-dimethylpentane ($2,4DMC_5$) is the primary product resulting from C1-C2 bond rupture. $2,4DMC_5$ makes up 75% of the total hydrogenolysis products on 0.9%Ir/SiO_2 catalyst, and only 35% on 0.9 %Ir/Al_2O_3 catalyst. In the reaction of $2MC_7$, on silica catalyst, five dicarbene products make up almost 90 % of the total products. Second, 0.9 %Ir/Al_2O_3 catalyst is more selective toward breaking sterically hindered C-C bonds than 0.9%Ir/SiO_2 catalyst. As seen in figure B-3.4 and figure B-3.5, percents of C1-C3 and C2-C3 bond cleavages are all higher on alumina than on silica catalyst. The conclusion drawn from the hydrogenolysis

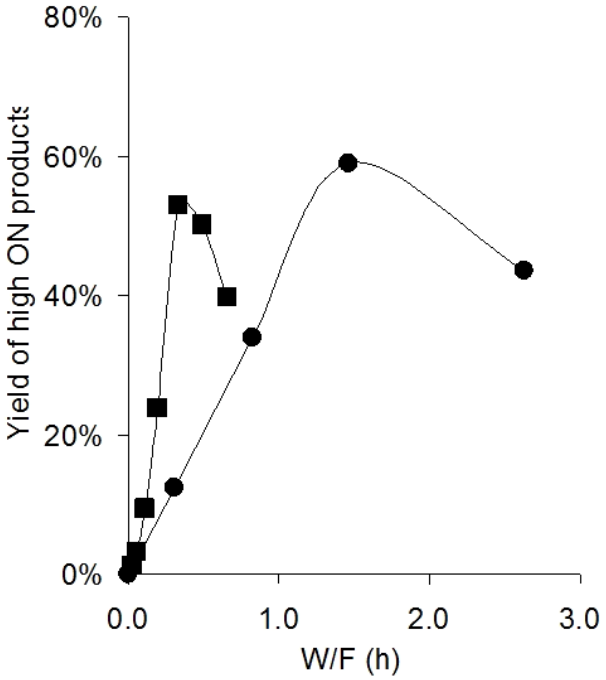

Figure B-3.3: Yield of high Octane number products (2,4DMC$_6$, 2,4DMC$_5$, 2MC$_5$, 3MC$_5$) from ring opening of 1,3-dimethylcyclohexane. Reaction was conducted at 603 K and 3.4 MPa. Hydrogen and hydrocarbon ratio was kept at 30. ■, 0.9 %Ir/Al_2O_3; ●, 0.9%Ir/SiO_2

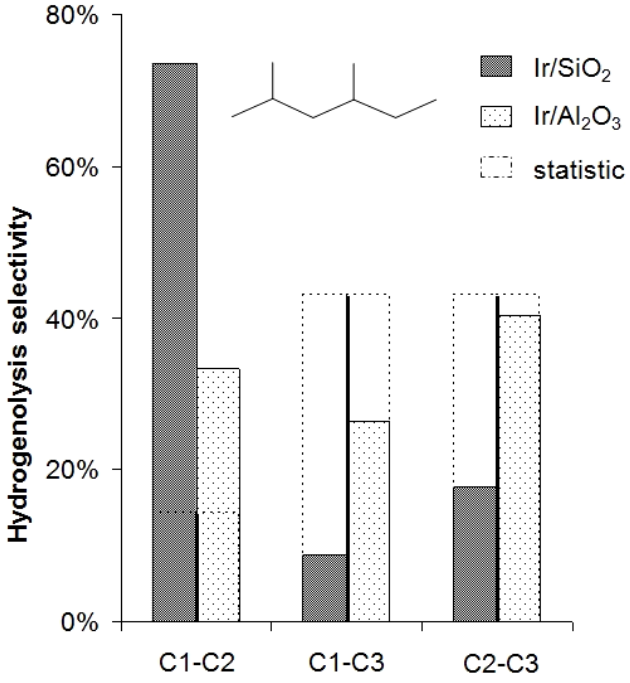

Figure B-3.4: Selectivities of hydrogenolysis of 2,4DMC$_6$ at different C-C bond positions. Reaction was conducted at 603 K and 3.4 MPa. Hydrogen and hydrocarbon ratio was kept at 30, W/F=0.008 h on 0.9 %Ir/Al_2O_3 and 0.025 h on 0.9%Ir/SiO_2. Products 2,4DMC$_5$ (from C1-C2); 3MC$_6$ and 2MC$_6$ (from C1-C3); 2MC$_5$, iso-C$_4$, and iso-C$_5$ (from C2-C3).

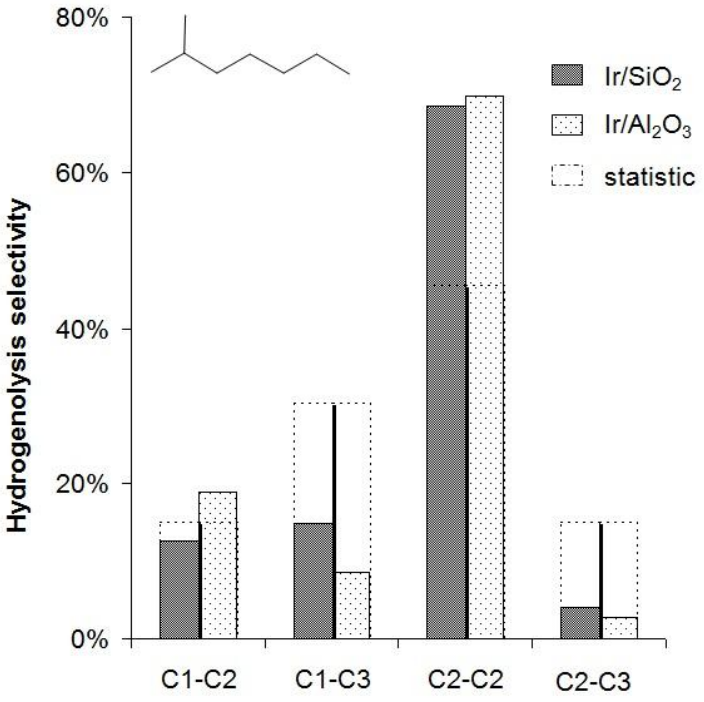

Figure B-3.5: Selectivities of hydrogenolysis of $2MC_7$ at different C-C bond positions. Reaction was conducted at 603 K and 3.4MPa. Hydrogen and hydrocarbon ratio was kept at 30, W/F = 0.008 h on 0.9 %Ir/Al_2O_3 and 0.025 h on 0.9%Ir/SiO_2. Products 2MC6 (from C1-C2); n-C7 (from C1-C3); 2MC5, 2MC4, iso-C4, and n-C4 (from C2-C2); n-C5 (from C2-C3).

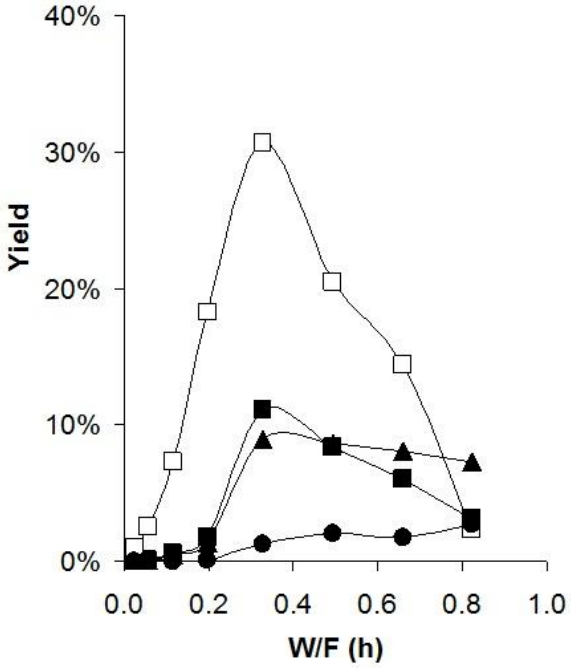

Figure B-3.6a: Yield of high Octane number products from ring opening of 1,3-dimethylcyclohexane over 0.9%Ir/Al_2O_3 catalyst. Reaction was conducted at 603 K and 3.4 MPa. Hydrogen and hydrocarbon ratio was kept at 30. □, 2,4DMC_6; ■ , 2,4DMC_5; ▲, $2MC_5$; ●, $3MC_5$.

of these two acyclic compounds is similar to the one previously drawn from the ring opening of cyclic compounds: 1,2- and 1,3-dimethylcyclohexane. 0.9%Ir/Al_2O_3 catalyst is selective toward substituted C-C bond cleavages, at the meantime; 0.9%Ir/SiO_2 catalyst is selective toward breaking unsubstituted C-C bonds. Last, only on silica catalyst, primary-secondary bond is preferentially broken in 2,4DMC_6 reaction, where no secondary-secondary bond is present. However, for both catalysts, the latter has a higher preference than the former in 2MC_7 reaction, where two types of bonds are available. 75% of total primary products from 2,4DMC_6 ends up as 2,4DMC_5. The statistical percent of breaking this bond is only 14 %. On the other hand, 2-methylhexane (2MC_6), which results from C1-C2 bond cleavage, contributes to only 15 % of the total primary products from 2MC_7. Compared to statistical value of 43 %, four products in the reaction of 2MC_7 such as 2MC_5, 2MC_4, iso-C_4, and n-C_4 constitute 70% in the total primary products for both 0.9%Ir/Al_2O_3 and 0.9%Ir/SiO_2 catalysts.

The cracking patterns of 2,4DMC_6 and 2MC_7 on 0.9%Ir/Al_2O_3 and 0.9%Ir/SiO_2 catalysts gives some light to the evolutions of individual HON products in the ring opening reaction of 1,3DMCH. Figure B-3.6a and figure B-3.6b presents the yields of four HON products on alumina and silica catalysts, respectively. At low W/F, 2,4DMC_6 is present in the highest amount among four products. However, as conversion proceeds, it gets cracked to products with lower carbon number such as 2,4DMC_5, 2MC_5 and so on. Because 2,4DMC_5 is the secondary product, it increases with conversion at a slower rate than 2,4DMC_6. At high conversion, it follows the same trend as 2,4DMC_6. The difference between two catalysts is that the formation rate of 2,4DMC_5 is faster on alumina than on silica. The maximum yield of 2,4DMC_5, the product with the highest ON of 85, is 22%

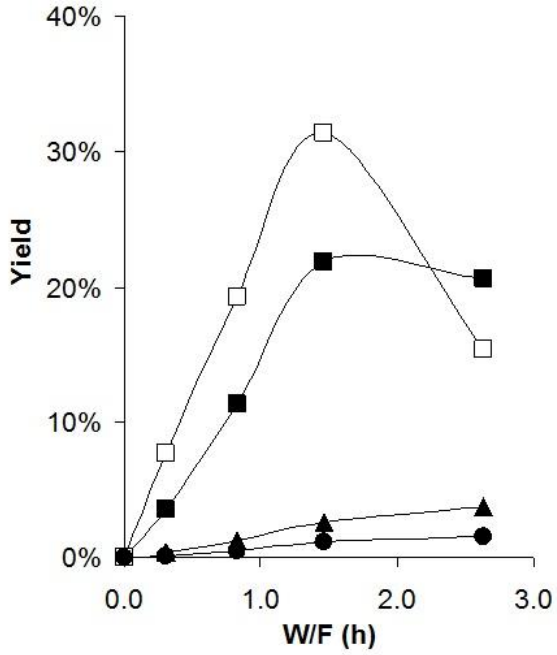

Figure B-3.6b: Yield of high Octane number products from ring opening of 1,3-dimethylcyclohexane over 0.9%Ir/SiO_2 catalyst. Reaction was conducted at 603 K and 3.4 MPa. Hydrogen and hydrocarbon ratio was kept at 30. □, 2,4DMC$_6$; ■ , 2,4DMC$_5$; ▲, 2MC$_5$; ●, 3MC$_5$.

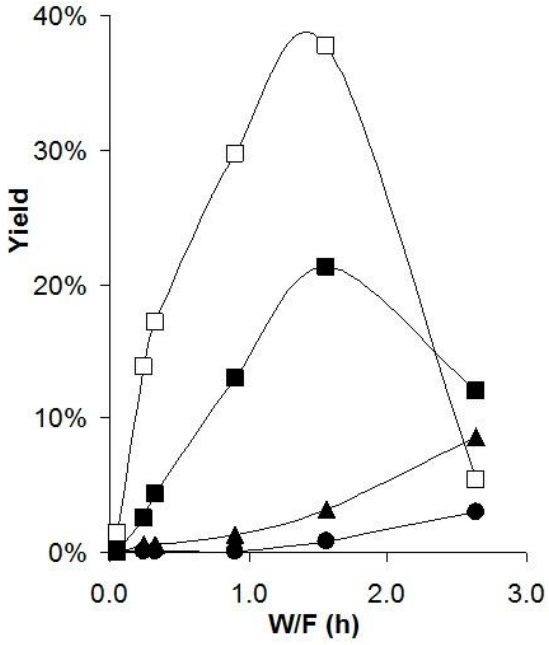

Figure B-3.6c: Yield of high Octane number products from ring opening of 1,3-dimethylcyclohexane over 0.9%Ir-0.1%Ni/Al_2O_3 catalyst. Reaction conducted at 603 K and 3.4 MPa; H_2/hydrocarbon ratio 30. □, 2,4DMC$_6$; ■ , 2,4DMC$_5$; ▲, 2MC$_5$; ●, 3MC$_5$.

on silica catalyst and only 10 % on alumina catalyst. Additionally, the cracking product $2MC_5$ gets converted on 0.9 %Ir/Al_2O_3 catalyst as the W/F increases. At the meantime, on silica catalyst, both two cracking products $2MC_5$ and $3MC_5$ keep increasing even at substantially high W/F. This is in agreement with the observations in the reactions of acyclic compounds. In the $2,4DMC_6$ reaction, 0.9%Ir/SiO_2 has a much higher tendency to form $2,4DMC_5$ via C1-C2 cleavage than 0.9%Ir/Al_2O_3 (see figure B-3.4). Alternatively, alumina catalyst is more active than silica catalyst; therefore, once $2,4DMC_5$ and $2MC_5$ are formed they get converted to cracking products immediately. This causes the difference in $2,4DMC_5$ and $2MC_5$ profiles on 0.9 %Ir/Al_2O_3 and 0.9%Ir/SiO_2 catalysts in figure B-3.6a and figure B-3.6b. Excessive cracking of HON products at high W/F is also the main reason causing a decrease in yield of HON products on alumina catalyst (see figure B-3.3).

3.2 The effect of Ni and K on pure Ir catalysts.

To take advantage of the high activity of alumina catalyst and to avoid excessive cracking of HON products, modifying both the support and iridium metal by adding a second metal is a potential option. The high activity of 0.9%Ir/Al_2O_3 catalyst is originated from the high hydrogenolysis activity of Ir and the high dispersion of this catalyst. Also, alumina interacts strongly with iridium metal, which in turn increases the dispersion of the metal on the support surface. It is well known that Ni is capable of blocking the interaction between the first metal with supports by forming surface nickel aluminate-like species in the sub-monolayer regime.[11] Additionally, alloys between Ni and noble metals are widely reported. In this present work, we have tested two Ir-Ni catalysts with varying molar ratios (Ir: Ni = 3:1 and 1:1). It turns out that the percent of

Ni on 0.9%Ir-0.3%Ni/Al_2O_3 catalyst is relatively high; therefore, Ni characteristic strongly dominates the selectivity of the catalyst. As mentioned in the literature, here the de-methylation product is dominant, not the ring opening products. [24-25] As a consequence, only the activity of 0.9%Ir-0.1%Ni/Al_2O_3 catalyst is reported here. Figure B-3.6c depicts the evolution of four HON products as a function of W/F. Compared with 0.9%Ir/Al_2O_3 catalyst, the activity of 0.9%Ir-0.1%Ni/Al_2O_3 is lower. However, there are gains in the yields of both 2,4DMC_6 and 2,4DMC_5 when Ni is added into 0.9%Ir/Al_2O_3. Although the yield of 2MC_5 for 0.9%Ir-0.1%Ni/Al_2O_3 is less than for 0.9%Ir/Al_2O_3, no decrease in yield is observed with this molecule even at high W/F. This is due to the fact that undesirable cracking and high activity of 0.9%Ir/Al_2O_3 catalyst is inhibited by the introduction of Ni. Together with the chemisorption and TPR data, it can be concluded that Ni interacts with alumina to form aluminate species during the calcinations step, which prevents Ir from spreading on alumina surface. Consequently, 0.9%Ir-0.1%Ni/Al_2O_3 catalyst is not as dispersed as 0.9%Ir/Al_2O_3 catalyst. It is also likely that Ir and Ni forms alloy, which changes the activity and selectivity of monometallic Ir on alumina. In the previous work, it is attributed the formation of metallocyclobutane intermediate, which is required to break substituted C-C bonds, to special Ir sites adjacent to alumina surface. The interaction of Ni with Ir and alumina might block some of those special sites; therefore, 0.9%Ir-0.1%Ni/Al_2O_3 tends to behave like a dicarbene catalyst. It produces a higher yield of 2,4DMC_6, a dicarbene RO product, than both 0.9%Ir/Al_2O_3 and 0.9%Ir/SiO_2 catalysts.

Beside Ni, another metal worth considering is potassium. It is well known that the presence of K alter both the catalytic activity and selectivity of unmodified catalysts

due to geometric and electronic effects. Potassium might help to lower the activity and cracking ability of alumina catalyst and increase the low activity of silica catalyst while maintaining its selectivity. One potassium-doped Ir catalysts reported here is 0.9%Ir-0.5%K/Al_2O_3 (molar ratio Ir:K = 1:2.5). The molar ratio between Ir and K on alumia is chosen as 2.5 in order to keep high activity of 0.9%Ir/Al_2O_3 catalyst. When compared figure B-3.6a and figure B-3.6d, it is clearly seen that the activity of the two catalysts is similar even though the dispersion of 0.9%Ir-0.5%K/Al_2O_3 is lower than that of 0.9%Ir/Al_2O_3. The obvious difference between two catalysts is that 0.9%Ir-0.5%K/Al_2O_3 is able to maintain the increasing yields of both 2,4DMC_5 and 2MC_5 even when a decrease in yield of 2,4DMC_6 is observed. This is a positive contribution of potassium to 0.9%Ir/Al_2O_3 catalyst because 2,4DMC_5 and 2MC_5 all have ONs higher than that of 2,4DMC_6.

When potassium is introduced into 0.9%Ir/SiO_2 catalyst, a positive contribution is also recognized in term of catalyst dispersion. CO chemisorption data shows that potassium-doped Ir on silica is more dispersed than solely iridium on silica. This is an interesting result because one would expect a decrease in dispersion due to the covering Ir sites by potassium. In fact, we have found that potassium on silica assists Ir from sintering. A more detailed discussion of this phenomenon can be found in another publication. The fact that the activity of the K-doped catalyst did not increase with the dispersion data cannot be explained at this moment. Further investigation is needed. The increasing dispersion of K-doped catalyst makes it behave like alumina catalyst. Together with the high yield of 2,4DMC_6 seen in figure B-3.6e, yields of substituted RO products such as 2MC_7 and 4MC_7 are also higher than those on the unmodified silica catalyst,

which is not shown here. In addition, K-doped silica catalyst produces a substantially lower amount of 2,4DMC$_5$, a RO product with the highest ON. An increase in substituted RO products with low ONs and a decrease in high ON products would jeopardize the ON improvement of ring opening product mixture.

3.3 Octane number of product mixtures and Ried vapor pressure

One way to evaluate the octane number enhancement of each catalyst is to compute the octane number of the product mixtures. Models for prediction of ON of hydrocarbon mixtures were proposed by many researchers. Recently, Ghosh et al. has recommended a model that can predict the octane number within a standard error of 1 number for both RON and MON.[26] The inputs are ONs and molar compositions of individual compounds. Parameters used in the model are interaction coefficients for each type of molecules, which are alkanes and naphthenes in this case. The naphthenes are cis and trans isomers of the feed left unreacted. The alkanes include RO products from C_5 to C_8. By using this model, octane numbers of product mixtures are calculated at different W/F for five catalysts: 0.9%Ir/Al_2O_3, 0.9%Ir/SiO_2, 0.9%Ir-0.1%Ni/Al_2O_3, and 0.9%Ir-0.5%K/Al_2O_3 (see figure B-3.8). Four catalysts follow three distinct trends. First, K-doped silica catalyst has shown a continuously decreasing octane number at all W/F. Being more dispersed than 0.9%Ir/SiO_2, this catalyst produces a substantial amount of substituted RO products (i.e 2MC$_7$ and 4MC$_7$) and their de-methylation products (i.e. 2MC$_6$ and 3MC$_6$), which bear low octane numbers. Additionally, the low yield of high ON products (i.e. 2,4DMC$_5$ and 2MC$_4$) shown figure B-3.7 cannot offset the negative impact of these low ON compounds.

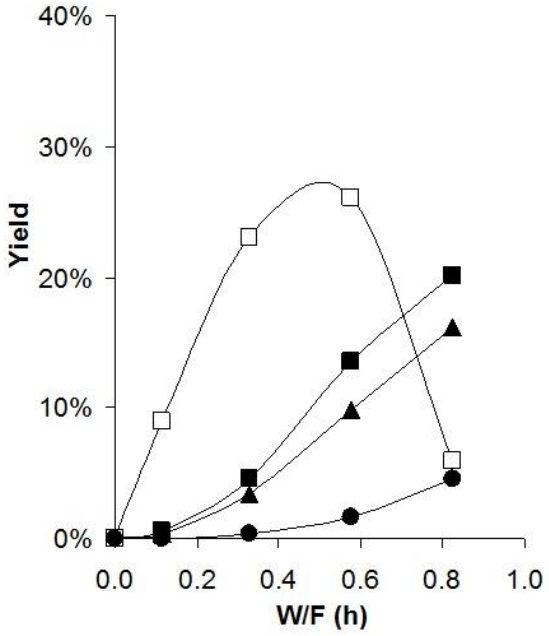

Figure B-3.6d: Yield of high Octane number products from ring opening of 1,3-dimethylcyclohexane over 0.9%Ir-0.5%K/Al_2O_3 catalyst. Reaction conducted at 603 K and 3.4 MPa; H_2/hydrocarbon ratio 30. □, 2,4DMC$_6$; ■ , 2,4DMC$_5$; ▲, 2MC$_5$; ●, 3MC$_5$.

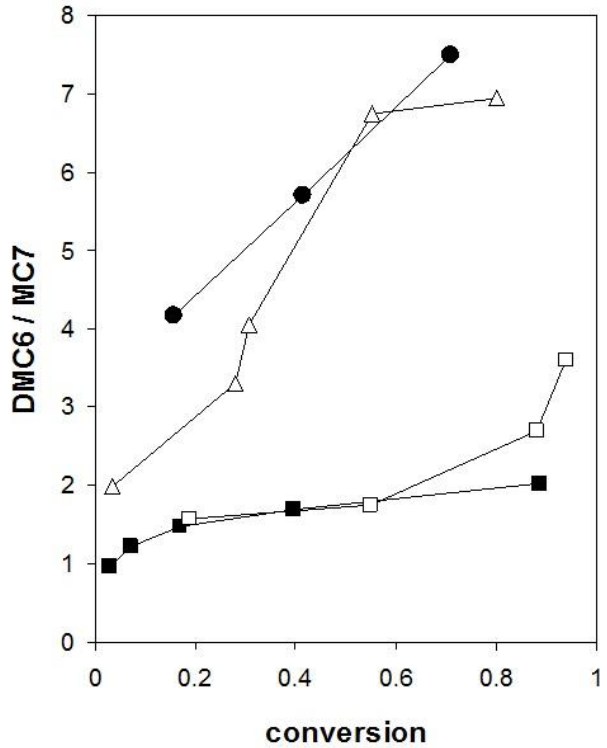

Figure B-3.7: Ratio of di-branched to mono-branched C_8 products from 1,3-dimethylcyclohexane ring opening as a function of total conversion. Reaction conducted at 603 K and 3.4 MPa; H_2/hydrocarbon ratio 30. Catalysts: ■, 0.9% Ir/Al_2O_3; ●, 0.9%Ir/SiO_2; △ 0.9 %Ir-0.1 %Ni/Al_2O_3; □, 0.9%Ir-0.5%K/Al_2O_3

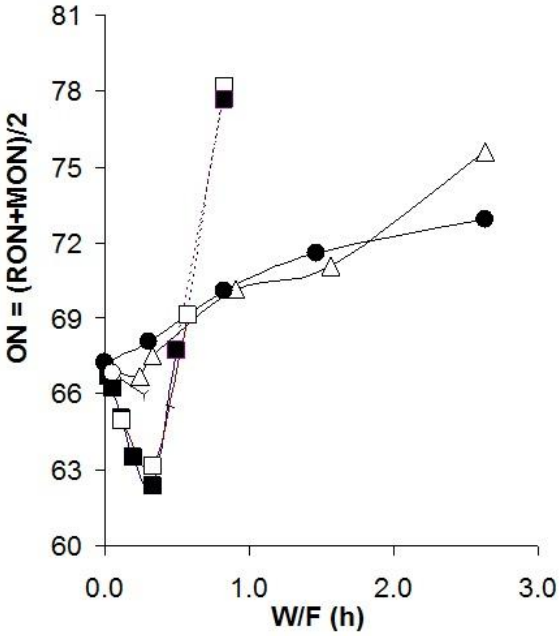

Figure B-3.8: Octane number of product mixture from ring opening of 1,3-dimethycyclohexane. Reaction was conducted at 603 K and 3.4 MPa. Hydrogen to hydrocarbon ratio was kept at 30. ■, 0.9%Ir/Al_2O_3; ●, 0.9%Ir/SiO_2; △ 0.9 %Ir-0.1 %Ni/Al_2O_3; □, 0.9%Ir-0.5%K/Al_2O_3

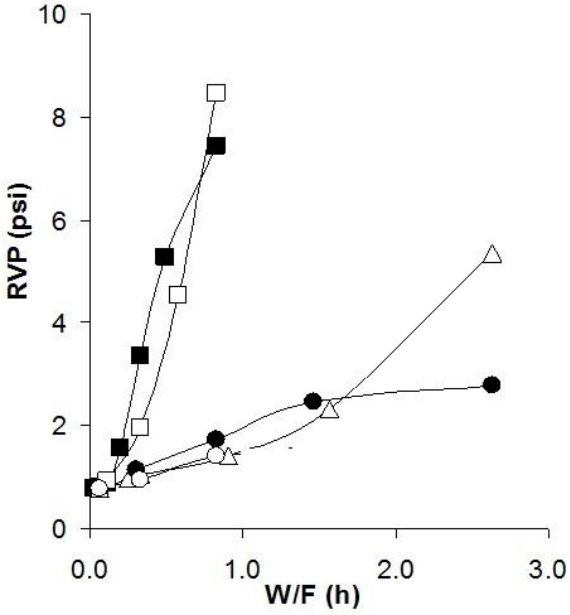

Figure B-3.9: Reid vapor pressure (RVP) of product mixture from ring opening of 1,3-dimethylcyclohexane. Reaction was conducted at 603 K and 3.4 MPa. Hydrogen to hydrocarbon ratio was kept at 30. ■, 0.9%Ir/Al_2O_3; ●, 0.9%Ir/SiO_2; △ 0.9 %Ir-0.1 %Ni/Al_2O_3; □, 0.9%Ir-0.5%K/Al_2O_3

Second, octane number is jeopardized at low W/F and drastically increases as the catalyst bed gets longer for 0.9%Ir/Al_2O_3 and 0.9%Ir-0.5%K/Al_2O_3 catalysts. Of four catalysts, these two catalysts are most selective producing substituted RO products (i.e. $2MC_7$ and $4MC_7$). At low W/F, these methylheptanes are not able undergo secondary hydrogenolysis to lighter products with high ON such as methylpentanes and methylbutane. Therefore, as seen in figure B-3.7, the yield of C_5 products is relatively small. Although 0.9%Ir/Al_2O_3 and 0.9%Ir-0.5%K/Al_2O_3 catalysts form considerable amounts of RO dicarbene products $2,4DMC_6$; conversion of $2,4DMC_6$ to $2,4DMC_5$, which is the highest ON product among compounds with acceptable vapor pressures, is not favored on these catalysts. It is the tendency of 0.9%Ir/Al_2O_3 and 0.9%Ir-0.5%K/Al_2O_3 catalysts to form more low-octane-number and less high-octane-number products causes a considerable loss in ON at low W/F. As the catalyst bed gets longer, the increasing ON mainly comes from the contribution of large quantities of methylpentanes and methylbutane, which are resulted from de-alkylation of primary RO products. From the hydrogenolysis of $2,4DMC_6$, it is clearly seen that 0.9%Ir/Al_2O_3 catalyst breaks not only C1-C2 bonds but also more sterically hindered C1-C3 and C2-C3 bonds. The intensive cracking ability of 0.9%Ir/Al_2O_3 catalyst is also observed in $2MC_7$ reaction, where C2-C2 bonds are ruptured. Consequently, the major products from $2MC_7$ are $2MC_5$ and $2MC_4$. Adding K into alumina catalyst modifies catalyst dispersion; however, excessive cracking ability of 0.9%Ir/Al_2O_3 catalyst has not been controlled completely.

In contrast, cracking of primary RO products is quite moderate on 0.9%Ir/SiO_2 and 0.9%Ir-0.1%Ni/Al_2O_3 catalysts. While 0.9%Ir/Al_2O_3 catalyzes all of the C-C bond

scissions in 2,4DMC$_6$ molecule, 0.9%Ir/SiO$_2$ only prefers to cleave C1-C2 bond to form 2,4DMC$_5$. Plus, on silica catalyst, bond involving tertiary carbon in the latter molecule is preserved from excessive cracking. The incorporation of Ni into alumina catalyst at a certain ratio also suppresses undesirable hydrogenolysis of the primary RO products due to presence of Ni-aluminate and Ir-Ni alloy. As a sequence, the maximum yield of 2,4DMC$_5$ is much higher on 0.9%Ir/SiO$_2$ and 0.9%Ir-0.1%Ni/Al$_2$O$_3$ catalysts than on alumina catalyst. The yield of C$_5$ products in figure B-3.7 is reversed. Besides, these catalysts are more selective toward dicarbene RO mode, therefore, the ratios of 2,4DMC$_6$ over sum of 2MC$_7$ and 4MC$_7$ are much higher for both 0.9%Ir/SiO$_2$ and 0.9%Ir-0.1%Ni/Al$_2$O$_3$ catalysts. Particularly, being more active than 0.9%Ir/SiO$_2$ catalyst, 0.9%Ir-0.1%Ni/Al$_2$O$_3$ catalyst even produces a greater deal of 2,4DMC$_6$ at a comparable W/F. All of these results are supportive in explaining the increasing ON with W/F for both 0.9%Ir/SiO$_2$ and 0.9%Ir-0.1%Ni/Al$_2$O$_3$ catalysts in figure B-3.8. A sharp jump at high W/F for Ni-doped alumina catalyst is an experimental error associated with temperature raise inside the catalyst bed, where excessive cracking might occur.

Besides the octane number analysis, Reid vapor pressure (RVP) of product mixture is an important criterion which should be taken into consideration. If the vapor pressure is too high, a vapor lock can happen and prevent the flow of gasoline. Conversely, if it is too low, it is difficult to start the engine in cold weather. Gasoline contains a portion of high-volatility fractions such as C$_4$, C$_5$ hydrocarbons and so on. These fractions have a major influence on vapor pressure. Figure B-3.9 displays Reid vapor pressure of liquid product mixtures calculated from Pro II software as a function of W/F for four catalysts. In the liquid product mixtures, C$_5$ alkanes are the easiest

compounds to vaporize, therefore, these compounds are responsible for raising the RVP. From figure B-3.9, it is clearly seen that the RVP of each catalyst follows the similar trend as yield of C_5 products in figure B-3.7. At a comparable W/F, higher Reid vapor pressures are witnessed with 0.9%Ir/Al_2O_3 and 0.9%Ir-0.5%K/Al_2O_3, two catalysts with higher hydrogenolysis activity. In parallel with the high RVP, the ON enhancement is also greater on these two catalysts than on 0.9%Ir/SiO_2 and 0.9%Ir-0.1%Ni/Al_2O_3 catalysts. Depending on the practical applications where high or low vapor pressure is required, the two former catalysts would be more favored than the latter catalysts or vice versa.

4. Conclusion

The addition of K to the Ir/Al_2O_3 catalyst results in decreased secondary hydrogenolysis, but does not affect the ratio of substituted to unsubstituted ring opening. As a result, the increase in octane number is not much different from that obtained on the Ir/Al_2O_3 catalyst. By contrast, the addition of Ni to Ir/Al_2O_3 catalyst at appropriate molar ratios suppresses the cleavage of C-C bond at substituted positions, thus making the alumina supported catalyst behave more like a silica-supported catalyst, giving a product with improved octane number and moderate vapor pressure.

5. References

[1] Petzny, W.J., and Halsig, C. P., Proceedings of the DGMK Conference on The Future Role of Aromatics in Refining and Petrochemistry, Erlangen, Germany, October 13–15, 7 (1999)

[2] Owen, K., and Coley, T., Automotive Fuels Reference Book, 2nd ed., Soc. Autom. Engin. Inc., Warrendale, PA, (1995)

[3] Kubiˇcka, D., Kumar, N., Arvela, P.M., Tiitta, M., Niemi, V., Karhu, H., Salmi, T., and Murzin, D.Y., *J. Catal.* **227**, 313 (2004)

[4] Arribas, M.A., Concepci´on, P., and Mart´ınez, A., *Appl. Catal. A* **267**, 111 (2004)

[5] Santana, R.C., Do, P.T., Santikunaporn, M., Alvarez, W.E., Taylor, J.D., Sughrue, E.L., and Resasco, D.E., *Fuel* **85**, 643 (2006)

[6] Gault, F.G. ,*Adv. Catal.*, **30**, 1 (1981)

[7] Boudart, M., and Ptak, L.D., *J. Catal.* **16**, 90 (1970)

[8] Sinfelt, J.H., *Catal. Rev.* **3**, 175 (1969)

[9] McVicker, G.B., Daage, M., Touvelle, M.S., Hudson, C.W., Klein, D.P., Baird, W.C., Cook, B.R., Chen, J.G., Hantzer, S., Vaughan, D.E.W., Ellis, E.S., and Feeley, O.C., *J. Catal.* **210**, 137 (2002)

[10] Do Phuong, T., Alvarez, W.E., and Resasco, D.E., *J. Catal.* **238**, 477 (2006)

[11] Osaki, T., Horiuchi, T., Sugiyama, T., Suzuki, K., and Mori, T. *Catal. Lett.* **52,** 171 (1998)

[12] Boissel, V., Tahir, S., and Koh, C.A., *Appl. Catal. B* **64**, 234 (2006)

[13] Abbas, T., and Khawaja, F.A. ,*Solid State Commun.* **49**, 641 (1984)

[14] Strohm, J. J., Zheng, J., and Song, C. *J. Catal.* **238**, 309 (2006)

[15] Balandin, A. A., Eley, D. D., Frankenburg, W. G., Komarewsky, V. I., and Weisz, P. B., *Adv. Catal.* **10**, 96 (1958)

[16] Dowden. D. A., *J. Chem. Soc. London* 242 (1950)

[17] Foger, K., and Jaeger, H., *J. Catal.* **70**, 53 (1981)

[18] Wogerbauer, C., Maciejewski, M., Baiker, A., and Gobel, U., *J. Catal.* **201**,113 (2001)

[19] Huang, Y.J., Fung, S.C., Gates, W.E., and McVicker, G.B., *J. Catal.* **118**, 192 (1989)

[20] Subramanian, S., and Schwarz, J.A., *Appl. Catal. A* **74**, 65 (1991)

[21] Osaki, T., Horiuchi, T., Sugiyama, T., Suzuki, K., and Mori, T., *Catal. Lett.* **52**, 71 (1998)

[22] Zieliliski, J., *J. Mol. Catal.* **83**, 197 (1993)

[23] Wang, J., Dong, L., Hu, Y., Zheng, G., Hu, Z., and Chen, Y., *J. Catal.* **204**, 274 (2001)

[24] Leclercq, G., Leclercq, L., Bouleau, L.M., Pietrzyk, S., and Maurel, R., *J. Catal.* **88**, 8 (1984)

[25] Du, H., Fairbridge, C., Yang, H., and Ring, Z., Appl. *Catal. A* **294**, 1 (2005)

[26] Ghosh, P., Hickey, K.J., and Jaffe, S.B., *Ind. Eng. Chem. Res.* **45**, 337 (2006)

CHAPTER IV: RING OPENING OF VARIOUS NAPHTHENIC COMPOUNDS ON SUPPORTED IRIDIUM

Before introducing the new reaction results, it is worth mentioning the previous hypothesis, which could be used to interpret some of the new findings. From the study of ring opening reactions of 1,2-dimethylcyclohexane and 1,3-dimethylcyclohexane, it was found that the preference of C–C bond opening at substituted or unsubstituted positions of the 6-membered rings depends on both the nature of the reactant and the type of catalyst used. The presence of methyl substituents enhances the rate of ring opening of C6 rings, as well as contributes positively to the ring opening at sterically hindered C–C bonds, which are close to the substituents. It could be that the metallocycles intermediates, which involve the interactions of metal center with substituent groups and lead to steric C-C cleavages, are facilitated. Iridium on alumina has shown to be the most selective toward the ring opening at substituted carbon center. This preference on alumina-supported catalysts is associated with a support effect rather than to an effect of metal dispersion, although alumina catalysts of different metal dispersions show a higher selectivity than that obtained on any of the silica catalysts. Dicarbene mode, which is associated with breaking unsubstituted C-C bonds, typically occurs on silica-supported Ir catalyst, which has low dispersion.

1. Ring Opening Reactions of 1-Ethyl-3-Methylcyclohexane on Supported Iridium Catalysts

In the previous chapters, the effects of supports and promoters in the iridium catalyst have been explored. Here, the variations in reactant molecular structures on the

ring opening reactions on alumina and silica-supported Ir catalysts will be analyzed. The first molecule employed is 1-ethyl-3-methylcyclohexane. Since the substituent positions of this molecule and 1,3-dimethylcyclohexane are similar, the results of the former will be analyzed in comparison with the results from the latter. Figure B-4.1 shows the ratio of substituted/dicarbene C-C cleavages for two reactant molecules on 0.9%Ir/SiO_2 and 0.9%Ir/Al_2O_3 catalysts. As stated before, the interaction between iridium and alumina support enhances to steric C-C ruptures, consequently leading to higher absolute substituted/dicarbene ratios for both reactants on alumina compared to silica. [1]However, it is interesting to note that the ratios on two catalysts are also higher for 1-ethyl-3-methylcyclohexane. In fact, the ethyl group seems to create more steric hindrance compared to the methyl group, which might cause limited excess to the substituted C-C bonds. Therefore, it could be possible that the formation of metallocycle intermediates is promoted by the presence of the ethyl group. In the reaction of 1,3-dimethylcyclohexane, 4-membered ring between Ir metal center with three carbon atoms, one of whose is the methyl carbon, was proposed to be responsible for breaking substituted C-C bonds. Instead of forming 4-membered cycle intermediate, the ethyl substituent might create 5-membered cycle that in turn could be more stable that the 4-membered ring. This result is in good agreement with the de-alkylation product distributions. At relatively low conversions, in which the secondary cracking is minimized, the breaking of C-C bonds closet to the ring is observed greater on ethyl group compared to that on methyl group. In other words, the de-ethylation/de-methylation ratio is always higher than unity as shown in Table B-4.1 .It is the preferred metallocycle associated with ethyl substituent that leads to the higher possibility of breaking around this substituent. This preference occurs on

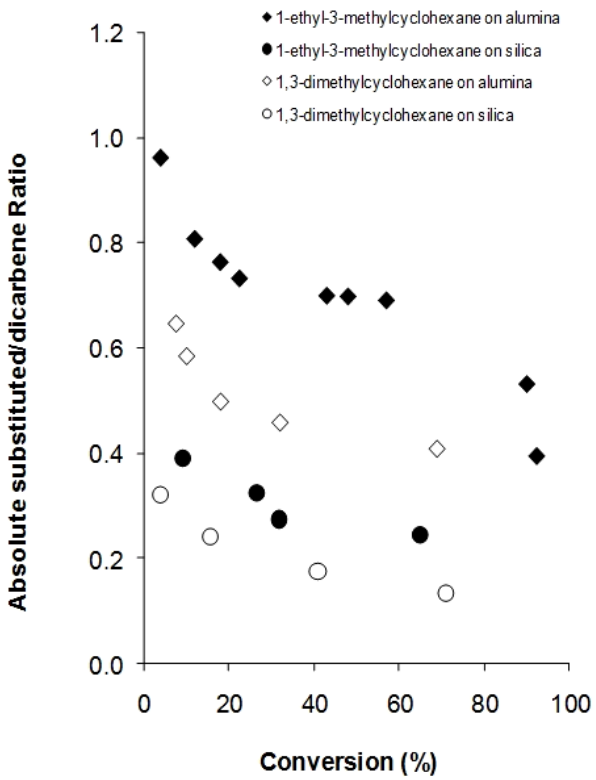

Figure B-4.1: The ratio of substituted/dicarbene ring opening products for 1-ethyl-3-methylcyclohexane and 1,3-dimethylcyclohexane reactions on 0.9% Ir/Al_2O_3 and 0.9% Ir/SiO_2 catalysts. The reaction was carried at 603 K and 3.4 M Pa.

Conversion	Yields of de-alkylation products		Diethylation/dimethylation
	Ethylcyclohexane	Methylcyclohexane	
4.3 %	0.07%	0.18%	2.45
12.0 %	0.22%	0.39%	1.82
18.0 %	0.32%	0.58%	1.81
20.4 %	0.30%	0.60%	2.02

Table B-4.1: De-alkylation products from the reaction of 1-ethyl-3-methylcyclohexane on 0.9% Ir/Al_2O_3 catalyst. The reaction was carried at 603 K and 3.4 M Pa.

both alumina and silica catalysts. Additionally, the activation energy for this intermediate formation is higher than the dicarbene, therefore; the higher substituted/dicarbene ratio is observed at higher reaction temperature (603 K compared to 553 K). As depicted in figure B-4.1, since the dicarbene mode is greatly dominant on silica support, higher percent of substituted C-C bond ruptures is recorded on alumina at 553 K than on silica at 603 K. In fact, the dicarbene intermediate involves the adsorptions of unsubstituted carbons such as primary and secondary carbons. Therefore, breaking of two secondary-secondary C-C bonds of the ring can be attributed to the dicarbene intermediate. It could be also possible that it is the dicarbene transition state that is responsible for breaking primary-secondary C-C bond on the ethyl substituent. Since the formation of two carbon-metal sigma bonds on the ethyl group is hindered either by the presence of the ring or by the favorable metallocyle intermediate, the chance of breaking this primary-secondary C-C bond is lower than the other two secondary-secondary C-C bonds. This is reflected by the lower selectivity of dimethylcyclohexane compared to 3-ethyl-5-methylhexane and 3,5-dimethylheptane shown in table B-4.2. The presence of ethyl group also hinders the cleavage of unsubstituted C-C bond adjacent to this group compared to the bond adjacent to methyl group. In other words, 3-ethyl-5-methylhexane is always populated than 3,5-dimethylheptane.

In summary, increase in the carbon chain length of substituent has several effects in the ring opening reactions of substituted cyclohexane molecules on iridium catalysts. The presence of ethyl group enhances the ring opening at substituted C-C bonds compared to methyl group. This could be due to the ease of forming 5-membered intermediate ring in respect with 4-membered ring. In addition, the presence of the

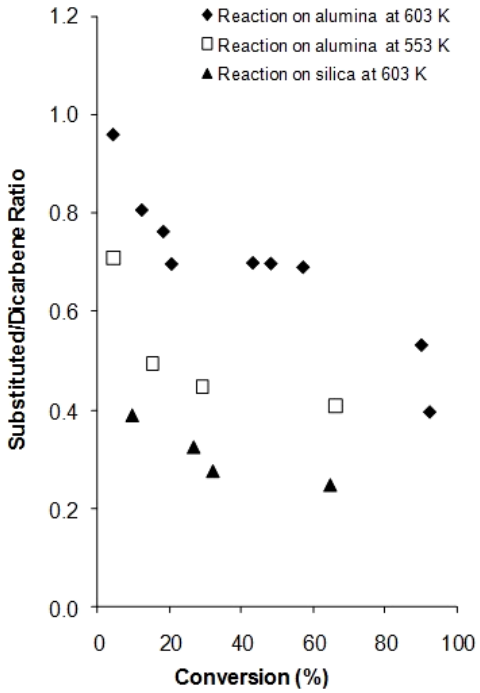

Figure B-4. 2: The ratio of substituted/dicarbene ring opening products for 1-ethyl-3-methylcyclohexane reactions on 0.9% Ir/Al_2O_3 and 0.9% Ir/SiO_2 catalysts. The reaction was carried at 603 K and 553 K and 3.4 M Pa.

	Selectivity of dicarbene products		
Conversion	1,3-dimethylcylcohexane	3-ethyl-5-methylhexane	3,5-dimethylheptane
4.3 %	9.67%	15.29%	13.00%
12.0%	10.49%	18.45%	15.82%
18.0%	11.76%	18.61%	16.75%

Table B-4.2: Selectivity of dicarbene products from the reaction of 1-ethyl-3-methylcyclohexane on 0.9% Ir/Al_2O_3 catalyst. The reaction was carried at 603 K and 3.4 M Pa.

bulkier ethyl group limits the formation of dicarbene intermediates between secondary-secondary carbons or primary-secondary carbons. This substituent effects are hold true for both alumina and silica supported catalysts.

2. Ring Opening Reactions of Other Alkylcyclohexanes on Alumina-Supported Iridium Catalyst

The interesting findings from ring opening reaction of 1-ethyl-3-methylcyclohexane have prompted the author to study the reactions of other naphthenic molecules on iridium catalysts. Table B-4.3 shows the product distributions from the ring opening reaction of different alkylcyclohexanes on 0.9%Ir/Al_2O_3 catalyst. The alkyl chain includes methyl, ethyl, propyl, isopropyl, butyl, tert-butyl, and isobutyl groups. The relative arrangements among the substituents also vary. Various normalized ratios were calculated by taking the experimental results divided by the statistical values.

First, the ratio of substituted/dicarbene C-C bond cleavages was reported for all the tested molecules, except 1,3,5-trimethylcyclohexane, which contains no secondary-secondary C-C bond. Table B-4.3 shows the increasing contribution of substituted C-C bond rupture as one moves from methyl to ethyl to propyl substituents, while keeping the same relative position between two substituents. For instance, the substituted/dicarbene ratio is 0.85 for 1,2-dimethylcyclohexane, 1.95 for 1-ethyl-2-methylcyclohexane, and 2.20 for 1-methyl-2-propylcyclohexane. As stated before, this could be due to the ease of forming metallocyle intermediate, which might be facilitated by the increasing size of the ring. The 6-membered ring intermediate with propyl group could be more stable than that with 5 members from ethyl group due to the reducing ring strain. In addition to the size of

Normalized ratio	1,3-dimethyl cyclohexane	1,2-dimethyl cyclohexane	1,4-dimethyl cyclohexane	1-ethyl-2-methyl cyclohexane	1-ethyl-3-methyl cyclohexane	1-methyl-2-propyl cyclohexane
Substituted/dicarbene	0.52	0.85	0.25	1.95	1.10	2.20
Sec-tertiary/tertiary-tertiary	0	0.38	0	0.23	0	0.12
De-alkylation/Ring opening	0.30	0.30	0.33	0.56	1.00	0.77
Dealkylation: Secondary-tertiary/primary-secondary	0	0	0	2.08	1.67	4.64
Dealkylation: Secondary-secondary/primary-secondary	0	0	0	0	0	0.65

Table B-4.3: Product distribution of ring opening reactions of different naphthenic compounds on $0.9\%Ir/Al_2O_3$ catalyst

Normalized ratio	ethylcyclohexane	propylcyclohexane	butylcyclohexane	tert-butylcyclohexane	isopropylcyclohexane	methylcyclohexane
Substituted/dicarbene	0.36	0.30	0.36	0.30	0.81	0.30
Sec-tertiary/tertiary-tertiary	0	0	0	0	0	0
De-alkylation/Ring opening	0.30	0.64	0.53	0.56	0.30	0.30
Dealkylation: Secondary-tertiary/primary-secondary	2.5	12.5	5.93	0	0	0
Dealkylation: Secondary-secondary/primary-secondary	0	2.4	9.50	0	0	0

Table B-4.3: Product distribution of ring opening reactions of different naphthenic compounds on $0.9\%Ir/Al_2O_3$ catalyst

Normalized ratio	1,2,4-trimethyl cyclohexane	1,3,5-trimethyl cyclohexane	4-methylheptane	2-methylheptane	2,4-dimethylhexane
Substituted/dicarbene	1.06	0	0	0	0
Secondary-tertiary/tertiary-tertiary	0.48	0	0	0	0
De-alkylation/Ring opening	0.30	0.66	0	0	0
Dealkylation: Secondary-tertiary/primary-secondary	0	0	3.10	7.00	0.27
Dealkylation: Secondary-secondary/primary-secondary	0	0	4.40	8.63	0

Table B-4.3: Product distribution of ring opening reactions of different naphthenic compounds on $0.9\%Ir/Al_2O_3$ catalyst

the substituents, the relative closeness between two groups has some impacts on the chances of breaking at the substituted carbon position. Dimethylcylcohexane molecules set as a typical example. The substituted/dicarbene ratio is highest when two methyl groups are in ortho position. Conversely, the ratio is lowest when the groups are in para position. The same trend is observed with 1-ethyl-2-methylcyclohexane and 1-ethyl-3-methylcyclohexane. Together with this, the products resulting from breaking tertiary-tertiary C-C bond are the most dominant ones among the products resulting from substituted C-C cleavages. This is a surprising result because the tertiary-tertiary C-C bonds are thought to be the most sterically hindered. In contrast to the clear impact of alkyl chain length on the substituted/dicarbene ratio observed with di-substituted cyclohexane molecules, table B-4.3 records no obvious trend for mono-substituted 6-membered rings. As one moves from methyl to butyl groups, the ratio remains around 0.30. The only high ratio is randomly observed with isopropylcyclohexane (0.81). It is also worth mentioning that the ratio for mono-substituted compounds is lower than that for di-substituted compounds. This confirms the important contribution from the number of substituent in breaking sterically hindered C-C bonds. The more substituent the molecules have the greater possibility of breaking substituted C-C bond was seen. For example, the substituted/dicarbene ratio calculated for one of the tri-substituted cyclohexanes in table B-4.3, 1,2,4-trimethylcyclohexane, is 1.06, which is higher than that for all other di-methyl substituted cyclohexanes. However, the fact that this ratio is lower than that for di-substituted cyclohexanes containing ethyl and propyl groups leads to another conclusion. That is: the role of alkyl chain length outweighs the role of number of substituents although they both greatly influence the chances of ring opening

at substituted C-C bonds. The longer the chain length also results in the greater possibility of rupturing the most sterically hindered C-C bond, tertiary-tertiary C-C bond. In fact, as depicted in table B-4.3, the secondary-tertiary/tertiary-tertiary C-C bond cleavage is lowest for 1-methyl-2-propylcyclohexane and highest for 1,2-dimethylcyclohexane. When the number of substituent increases from 2 to 3, the above ratio increases (0.38 for 1,2-dimethylcyclohexane and 0.48 for 1,2,4-trimethylcyclohexane). This means that the introduction of more substituents lessens the change of breaking the most inaccessible tertiary-tertiary C-C bond.

Alumina-supported iridium catalyst is very active for ring opening reactions of 1-ring naphthenic molecules. Increasing both quantity and chain length of the substituents of the naphthenic rings enhances the possibility of rupturing the sterically hindered C-C bonds. However, the long alkyl groups also cause undesirable dealkylation reactions, in which the number of carbons is not preserved. Table B-4.3 tabulates the dealkylation/ring opening ratio for all tested naphthenic compounds. The overall trend is that the dealkylation activity increases with the chain length of the substituents. For instances, this ratio is 0.3 for 1,3-dimethylcylohexane and 1.0 for 1-ethyl-3-methylcyclohexane. Together with that, the substituented C-C bonds closest to the ring, secondary-tertiary C-C bonds, is preferentially broken than the C-C bonds at the end of the substituents, primary-secondary C-C bonds. This is confirmed by the ratio of secondary-tertiary/primary-secondary is greater than unity for all test molecules. In fact, the former C-C bonds are more inaccessible than the latter ones. This might be in the same line with the higher possibility of breaking tertiary-tertiary C-C bonds observed above. It is the metallocycle intermediate that are likely to be the cause of these

observations. Breaking of both tertiary-tertiary C- C bond of the ring and secondary-tertiary C-C bond of the alkyl group are originated from the same metallocycle intermediate species. Additionally since iridium is a C2-C2 hydrogenolysis catalyst, the secondary-secondary C-C bond of alkyl chain is more prone to be ruptured than the primary-secondary C-C bond. This leads to the high ratio of secondary-secondary/primary-secondary observed some of the tested naphthenic compounds

3. Ring Opening of Dimethylcyclohexanes on Supported Iridium Catalysts in the Presence of Aromatics

Selective ring opening of the naphthenic compounds has been proposed as one of the strategies to improve the cetane number and other fuel properties.[2] However, different cuts from fractionation of crude oils always contain a certain portion of aromatics. For example, light cycle oil fraction contains up to 30% aromatics by volume.[3] Thus, the ring opening reactions of naphthenic compounds need to occur in the presence of aromatics. Since the aromatics usually bear higher heat of adsorption on metal catalysts compared to the hydrogenated naphthenic compound, they might affect the activity and selectivity of the ring opening reaction of the latter. To explore the effect of aromatics in the ring opening reactions, m-xylene was co-fed with 1,2-dimethylcyclohexane over 0.9%Ir/Al_2O_3 catalyst. The reaction was carried at 623 K and 2.1 M Pa. Figure B-4.3 shows the overall activity of 1,2-dimethylcyclohexane in pure feed versus mixed feed containing 10 wt% of m-xylene. Under the reaction conditions, it is clearly seen that the activity of the naphthenic compound remains unchanged regardless of the presence of m-xylene. Hydrogenation activity of the benzene ring was observed with m-xylene. As shown in figure B-4.4, the equilibrium between m-xylene and 1,3-dimethylcyclohexane

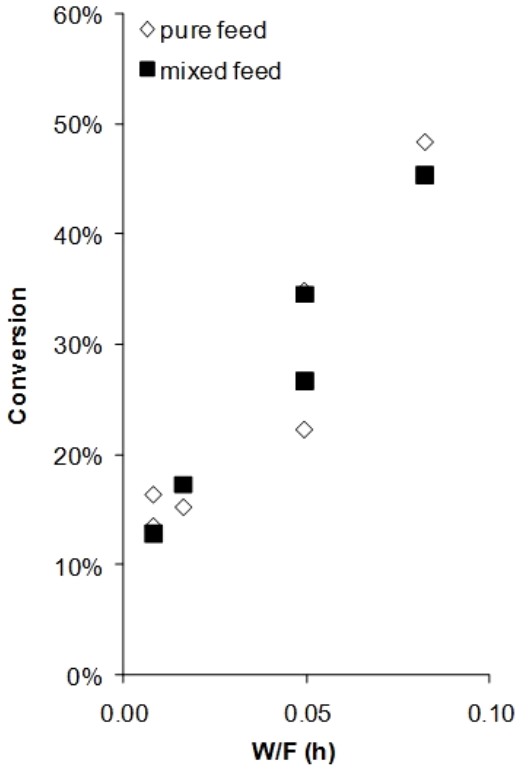

Figure B-4.3: Total activity of 1,2-dimethylcyclohexane in pure and mixed feed with m-xylene on 0.9% Ir/Al_2O_3 catalyst. The reaction was carried at 623 K and 2.1 M Pa.

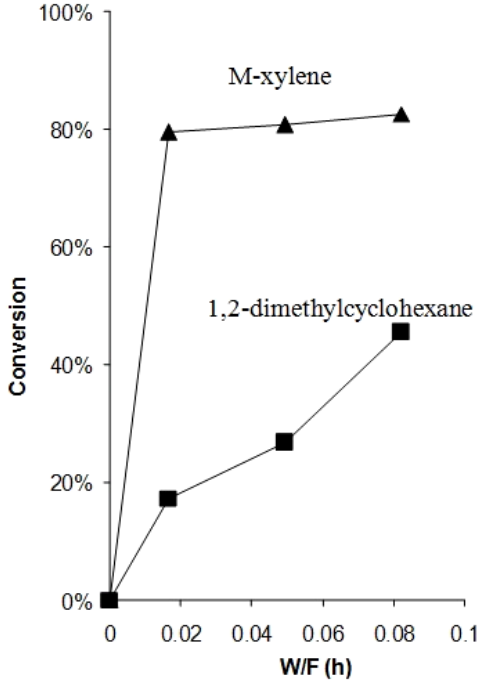

Figure B-4.4: Conversion of m-xylene and 1,2-dimethylcyclohexane on 0.9%Ir/Al_2O_3 catalyst. The reaction was carried at 623 K and 2.1 M Pa.

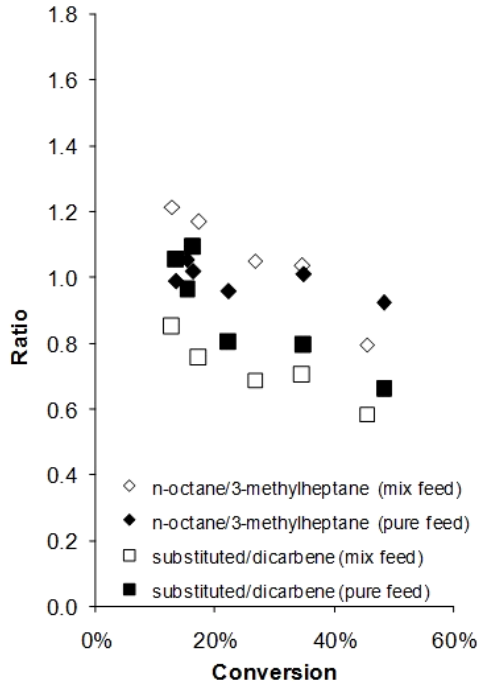

Figure B-4.5: Selectivity of ring opening reaction of 1,2-dimethylcyclohexane in pure and mixed feed with m-xylene on 0.9% Ir/Al_2O_3 catalyst. The reaction was carried at 623 K and 2.1 M Pa.

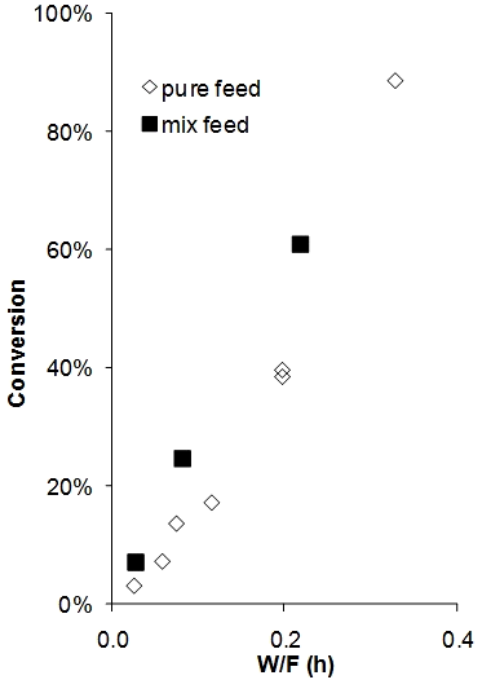

Figure B-4.6: Total activity of 1,3-dimethylcyclohexane in the pure and mix feed with toluene on 0.9% Ir/Al_2O_3 catalyst. The reaction was carried at 603 K and 3.4 M Pa.

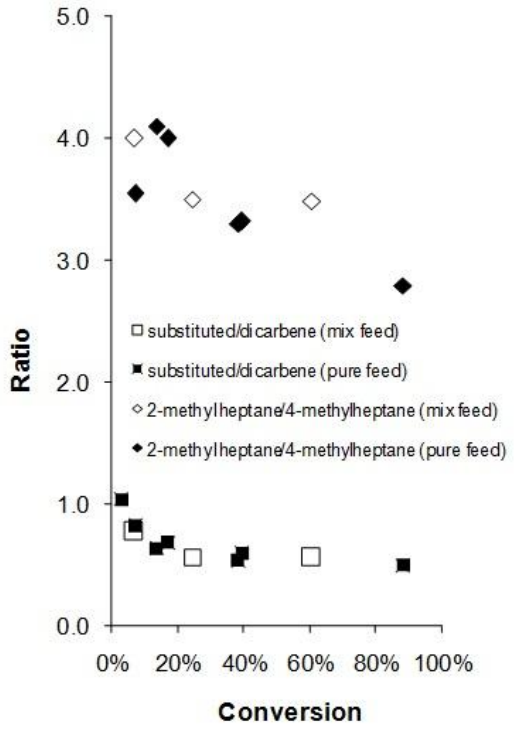

Figure B-4.7: Selectivity of ring opening products from reactions of 1,3-dimethylcyclohexane in pure and mixed feed with toluene on 0.9% Ir/Al_2O_3 catalyst. The reaction was carried at 603 K and 3.4 M Pa.

is quickly reached at low W/F. Not only the overall activity but also the ring opening selectivity of 1,2-dimethylcyclohexane is not heavily affected by the presence of m-xylene. This is confirmed by the data shown in figure B-4.5, in which the substituted/dicarbene and n-octane/3-methylheptane ratios for both pure and mixed feeds are plotted. In fact, the substituted/dicarbene ratio is slightly higher for mixed feed compared to pure feed. Since the hydrogenation reaction of aromatics is faster than the ring opening reaction, the ring opening activity is not affected by the presence of small amount of aromatics, which quickly turn into the hydrogenated naphthenic product. Only small portion of aromatic remains unreacted (20% of m-xylene). The same results were obtained when 1,3-dimethylcyclohexane is co-fed with toluene on the alumina-supported

iridium catalyst. The overall activity and product selectivity of 1,3-dimethylcyclohexane reaction are plotted in figure B-4.6 and figure B-4.7.

In summary, since the hydrogenation reaction of aromatics is faster than the ring opening reaction, it is found that the ring opening activity is not affected by the presence of small amount of aromatics, which quickly turn into the hydrogenated naphthenic product. The ring opening product selectivity also remains unchanged with the presence of aromatics. It could be possible that since the conversion of aromatic is high, the surface coverage of these species is low, leading to minor impact on the ring opening reaction.

4. References

[1] Do, P. T., Alvarez, W.E., and Resasco, D.E., *J. Catal.* **238**, 477 (2006)

[2] Santana, R.C., Do, P.T., Alvarez, W.E., Taylor, J.D., Sughrue, E.L., and Resasco., D.E., *Fuel*, **85**, 643 (2006)

[3] In "Regulation of Fuel and Fuel Additives: Extension of California Enforcement Exemptions for Reformulated Gasoline to California Phase 3 Gasoline".
EPA, Federal Register **70**, 75914 (2005)

CHAPTER V: SUMMARY

In the upgrading of conventional petroleum fuels, aromatics are not desirable components of the diesel fuels due to their low cetane numbers. Conversely, they bear high octane number, which makes them good candidates for gasoline. Due to environmental concerns, the United State legislatures have called for the reduction of aromatic contents in both gasoline and diesel fuels. Hydrogenation of the aromatic rings followed by selective ring opening of the corresponding naphthenic compounds has been proposed as one of the strategies to improve the cetane number and other fuel properties. In this work, the ring opening (RO) reactions of various naphthenic compounds on different modified Ir catalysts have been studied. Ring opening of 1-ring naphthenic compounds over iridium catalysts proceeds via three mechanisms: dicarbene, adsorbed olefin or metallocyclobutane. The dicarbene reaction path, which occurs on 0.9%Ir/SiO_2 catalyst, results in unsubstituted C-C bond cleavages. The products resulting from dicarbene pathway often have more branching; therefore, they bear high octane number. In contrast, the other mechanisms prefer to break C-C bond at substituted positions, which are seen more on highly disperse 0.9%Ir/Al_2O_3 catalyst. Rupturing the C-C bond at tertiary carbon center produces more linear hydrocarbons, which become high cetane number molecules. The following findings all concentrate on the use of several pure and modified Ir catalysts in ring opening reactions of different naphthenic molecules.

- Since the activity of 0.9%Ir/Al_2O_3 is high, the primary RO products from reaction of 1,3-dimethylcyclohexane undergo excessively secondary hydrogenolysis to lighter hydrocarbons as conversion increases. To avoid the cracking problem and make 0.9%Ir/Al_2O_3 more selective toward dicarbene mode, second metals (Ni or

K) were added to Ir catalysts. It has been found that the addition of K and Ni alters both activity and selectivity of Ir catalysts. The activities of alumina-supported Ir-Ni and Ir-K catalysts, together with the dispersions, are lower than that of 0.9%Ir/Al_2O_3, however, still higher than that of 0.9%Ir/Al_2O_3. The incorporations of Ni and K to 0.9%Ir/Al_2O_3 catalyst at a certain ratios can suppress the cleavage of C-C bond at substituted positions and excessive secondary hydrogenolysis, which in turn results in the increasing octane numbers of product mixtures. This might be due to the fact that the introductions of Ni and K block the strong interaction of iridium with alumina. Therefore, both dispersion and the number of active sites responsible for formation of adsorbed olefin or metallocyclobutane intermediates decrease. On the other hand, the dispersion of Ir-K/SiO_2 is higher than that of Ir/SiO_2. Potassium probably helps to create small particle sizes of Ir. Consequently, the addition of K into silica catalyst facilitates the rupture of more sterically hindered C-C bonds, which causes a decrease in octane number.

- Besides the reaction of 1,3-dimethylcylohexane, the study of a class of naphthenic compounds shows that increase in the carbon chain length of substituent has several effects in the ring opening reactions of substituted cyclohexane molecules on iridium catalysts. The presence of ethyl group enhances the ring opening at substituted C-C bonds compared to methyl group. This could be due to the ease of forming 5-membered intermediate ring in respect with 4-membered ring. In addition, the presence of the bulkier ethyl group limits the formation of dicarbene intermediates between secondary-secondary carbons or primary-secondary

carbons. This substituent effects are hold true for both alumina and silica supported catalysts. Increasing both quantity and chain length of the substituents of the naphthenic rings enhances the possibility of rupturing the sterically hindered C-C bonds. However, the long alkyl groups also cause undesirable dealkylation reactions, in which the number of carbons is not preserved.

- Different cuts from fractionation of crude oils always contain a certain portion of aromatics. Thus, the ring opening reactions of naphthenic compounds need to occur in the presence of aromatics. Since the hydrogenation reaction of aromatics is faster than the ring opening reaction, it is found that the ring opening activity is not affected by the presence of small amount of aromatics, which quickly turn into the hydrogenated naphthenic product. The same conclusion is held true with the ring opening product selectivity. It could be possible that since the conversion of aromatic is high, the surface coverage of these species is low, leading to minor impact on the ring opening reaction.